NASA/CR-20205001889

Characterization of the NASA Glenn Research Center 8- by 6-Foot Supersonic Wind Tunnel Supersonic Test Section (2020 Test)

Aaron M. Johnson
Jacobs Technology, Cleveland, Ohio

David A. Rinehart
HX5 Sierra, LLC, Brook Park, Ohio

December 2020

NASA STI Program . . . in Profile

Since its founding, NASA has been dedicated to the advancement of aeronautics and space science. The NASA Scientific and Technical Information (STI) Program plays a key part in helping NASA maintain this important role.

The NASA STI Program operates under the auspices of the Agency Chief Information Officer. It collects, organizes, provides for archiving, and disseminates NASA's STI. The NASA STI Program provides access to the NASA Technical Report Server—Registered (NTRS Reg) and NASA Technical Report Server—Public (NTRS) thus providing one of the largest collections of aeronautical and space science STI in the world. Results are published in both non-NASA channels and by NASA in the NASA STI Report Series, which includes the following report types:

- TECHNICAL PUBLICATION. Reports of completed research or a major significant phase of research that present the results of NASA programs and include extensive data or theoretical analysis. Includes compilations of significant scientific and technical data and information deemed to be of continuing reference value. NASA counter-part of peer-reviewed formal professional papers, but has less stringent limitations on manuscript length and extent of graphic presentations.

- TECHNICAL MEMORANDUM. Scientific and technical findings that are preliminary or of specialized interest, e.g., "quick-release" reports, working papers, and bibliographies that contain minimal annotation. Does not contain extensive analysis.

- CONTRACTOR REPORT. Scientific and technical findings by NASA-sponsored contractors and grantees.

- CONFERENCE PUBLICATION. Collected papers from scientific and technical conferences, symposia, seminars, or other meetings sponsored or co-sponsored by NASA.

- SPECIAL PUBLICATION. Scientific, technical, or historical information from NASA programs, projects, and missions, often concerned with subjects having substantial public interest.

- TECHNICAL TRANSLATION. English-language translations of foreign scientific and technical material pertinent to NASA's mission.

For more information about the NASA STI program, see the following:

- Access the NASA STI program home page at http://www.sti.nasa.gov

- E-mail your question to help@sti.nasa.gov

- Fax your question to the NASA STI Information Desk at 757-864-6500

- Telephone the NASA STI Information Desk at 757-864-9658

- Write to:
  NASA STI Program
  Mail Stop 148
  NASA Langley Research Center
  Hampton, VA 23681-2199

NASA/CR-20205001889

Characterization of the NASA Glenn Research Center 8- by 6-Foot Supersonic Wind Tunnel Supersonic Test Section (2020 Test)

Aaron M. Johnson
Jacobs Technology, Cleveland, Ohio

David A. Rinehart
HX5 Sierra, LLC, Brook Park, Ohio

Prepared under Contract NNC15BA02B

National Aeronautics and
Space Administration

Glenn Research Center
Cleveland, Ohio 44135

December 2020

Level of Review: This material has been technically reviewed by NASA technical management.

Available from

NASA STI Program
Mail Stop 148
NASA Langley Research Center
Hampton, VA 23681-2199

National Technical Information Service
5285 Port Royal Road
Springfield, VA 22161
703-605-6000

This report is available in electronic form at http://www.sti.nasa.gov/ and http://ntrs.nasa.gov/

Characterization of the NASA Glenn Research Center 8- by 6-Foot Supersonic Wind Tunnel Supersonic Test Section (2020 Test)

Aaron M. Johnson
Jacobs Technology
Cleveland, Ohio 44135

David A. Rinehart
HX5 Sierra, LLC
Brook Park, Ohio 44142

Summary

Recent customer requirements for improved Mach number stability for sonic boom signature measurements has piqued interest in the use of the solid-wall supersonic test section in the NASA Glenn Research Center 8- by 6-Foot Supersonic Wind Tunnel. To supply customers with understanding of the operating conditions and flow quality in this region of the tunnel, characterization tests were performed in the solid-wall supersonic test section in January 2020. The test entry covered the operating range of the facility for three-drive-motor operation. Calibration models were generated along with an improved understanding of operational considerations for this region of the tunnel. The data set acquired included centerline axial and planar flow-field distributions to quantify test section flow quality. The collected data provided an improved understanding of operational considerations for this region of the tunnel as well as allowed for the development of detailed calibration models for the solid-wall supersonic test section.

Nomenclature

Symbols

i	index used to denote an item in an array of values (i.e., variable(i), i = 1 to 10)
x	generic variable used to abbreviate equation, value of x defined near equation
A_0 to A_3	coefficient for computing test section static pressure (subsonic)
$A_{S,0}$ to $A_{S,2}$	coefficient for computing test section static pressure (supersonic)
B_0 to B_2	coefficient for computing test section total pressure (subsonic)
$B_{S,0}$ to $B_{S,4}$	coefficient for computing test section total pressure behind a normal shock (supersonic)
C_0 to C_2	coefficient for computing test section total temperature (subsonic)
$C_{S,0}$ to $C_{S,2}$	coefficient for computing test section total temperature (supersonic)
M	Mach number
P	pressure
R	gas constant of air, R = 1,716.59 ft·lbf/slug/R
$R_{S,\mathrm{row1},bm}$	ratio of average row 1 static to bellmouth total pressure
T	temperature
α	pitch flow angle
β	yaw flow angle

Subscripts

2	flow downstream of a normal shock

array	related to a flow parameter measured on the transonic array (i.e., $P_{T,\text{array}}$)
avg	average value
bm	bellmouth rake parameter (i.e., bellmouth total pressure, $P_{T,bm}$)
corr	corrected value, referring to pitch and yaw flow angles
cyl	related to measurements from the cylinder portion of the cone cylinder model
lookup	value obtained from a lookup table
model	measurements on the surface of the cone cylinder model
row1	measurements from the ceiling static pressure ports at test section station 17.0, referred to as "row 1"
S	static condition of a flow parameter (i.e., static pressure, P_S)
T	stagnation condition of a flow parameter (i.e., total or stagnation pressure, P_T)
ts	test section condition (i.e., M_{ts})

1.0 Introduction

In 2012, interest from the research community in Mach number stability for sonic boom signature measurements resulted in flow surveys in the 8- by 6-Foot Supersonic Wind Tunnel (8×6 SWT) porous test section. Following the 2012 surveys, a similar survey of the solid-wall, supersonic test section was conducted. A review of the flow surveys indicated the solid-wall test section was the more favorable option of the two test sections for boom signature research. As a result, it became necessary to characterize the supersonic test section, which includes flow parameter calibration, determination of optimal operating conditions, and assessment of flow quality in this region of the tunnel. A preliminary characterization entry investigated the supersonic test section flow field in 2015, however, a large tunnel loop modification project, the 9- by 15-Foot Low-Speed Wind Tunnel (9×15 LSWT) Acoustic Improvement Modifications, occurred from 2016 to 2018, which necessitated recharacterization of both the 8×6 SWT and 9×15 LSWT test sections. A characterization test entry was performed in January 2020 in the supersonic test section. Details of this 2020 test entry including facility and hardware descriptions, test procedures, data reduction, and results are documented in this report.

1.1 Test Objectives

The objectives of the test were to provide a calibration of the solid-wall, supersonic test section in the 8×6 SWT, as well as characterize the flow quality and investigate any operational considerations in this region of the test section. Specific objectives of the test entry were as follows:

1. Produce an empty test section calibration model for the 8×6 SWT supersonic test section across the operating range of the facility for three-drive-motor operation.
2. Document the flow quality at a cross section in the supersonic test section, specifically total and static pressure, total temperature, and flow angularity.
3. Characterize the axial pressure distribution in the supersonic test section.
4. Investigate the effect of balance chamber pressure on the centerline static pressure profile and planar flow quality in the supersonic test section.
5. Assess the repeatability and test section flow quality effects of operating the 8×6 SWT flexible-wall nozzle at off-nominal settings to achieve average freestream conditions of Mach 1.40 and 1.50 in the supersonic test section.
6. Investigate strut blockage effects on supersonic test section pressures.

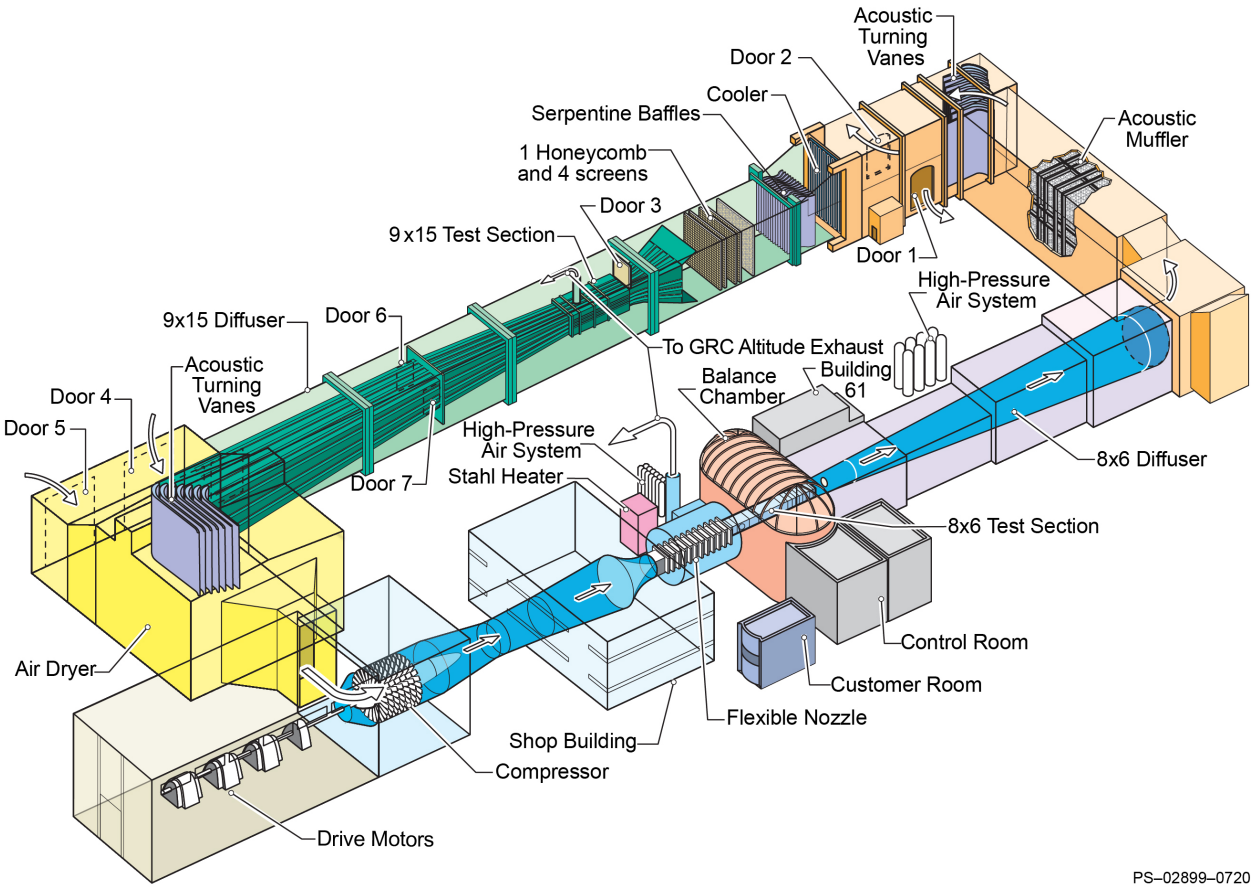

Figure 1.—Overview of 8- by 6-Foot Supersonic (8×6) and 9- by 15-Foot Low-Speed (9×15) Wind Tunnel complex following the 9- by 15-Foot Low-Speed Wind Tunnel Acoustic Improvement Modifications.

2.0 Description of Facility[1]

The 8- by 6-Foot Supersonic and 9- by 15-Foot Low-Speed Wind Tunnel complex, shown in Figure 1, is an atmospheric pressure, continuous flow propulsion wind tunnel. The airflow is driven through the facility by a seven-stage axial compressor (18-ft diam. inlet), which is powered by three 29,000-hp electric motors. The 8- by 6-ft test section is a porous-wall, transonic test section with a Mach number range of 0.25 to 2.0. By using all three drive motors, the Mach number range in the transonic test section is 0.36 to 2.0; one drive motor operation is required to reach the lowest Mach numbers. The 9- by 15-ft test section is located in the return leg of the 8- by 6-ft wind tunnel loop. The 8- by 6-ft test section walls, floor, and ceiling have no divergence over the 23-ft 6-in. length of the test section. The test section consists of a solid-wall supersonic flow region (9-ft 1-in. length) followed by a porous wall transonic region (14-ft 5-in. length). There are six configurations for the transonic test section based on the length of the porous area used and the open area of the test section surfaces; a seventh configuration exists for testing within the solid-wall, supersonic test section with the transonic test section porosity configured as defined below:

1. 14-ft, 5.8-percent porosity
2. 8-ft, 6.2-percent porosity

[1]Adapted from Reference 1.

3. 8-ft, 3.1-percent porosity
4. 8-ft, 6.2-percent porosity modified
5. 8-ft, 3.1-percent porosity modified
6. 14-ft, schlieren windows installed
7. Supersonic test section (transonic test section configured to 8-ft, 6.2-percent porosity)

The 14-ft transonic test section uses the entire length of the porous area; the 8-ft test section is the aft 8 ft of the porous test section with the first 6 ft of 14 ft of porosity plugged (Figure 2). The tunnel can be operated in either an aerodynamic (closed loop) or propulsion (open loop) cycle (for propulsion cycle, flow control doors 1 and 2 are open so that the airflow is exhausted from the tunnel).

The conditions in the 8- by 6-ft test section are set by controlling compressor speed, flexible-wall position, balance chamber pressure (test section bleed), and shock door (second throat) position. For standard operation of the drive system, the test section Mach number range is 0.36 to 2.0. In order to reduce the test section Mach number below 0.36, it is necessary to slow the compressor speed. This is done by powering the compressor using only one of the three electric drive motors. By operating in this mode, it is possible to expand the operational envelop of the facility by reducing the low-end Mach number to 0.25. Very low speed conditions (below Mach 0.1) can be achieved in the 8- by 6-ft test section by using only the air dryer building air circulation fans (the eight fans are used to pull air through the air dryer building to cool the desiccant beds; by properly configuring the tunnel and air dryer flow control doors, the fans will push air through the 8- by 6-ft test section).

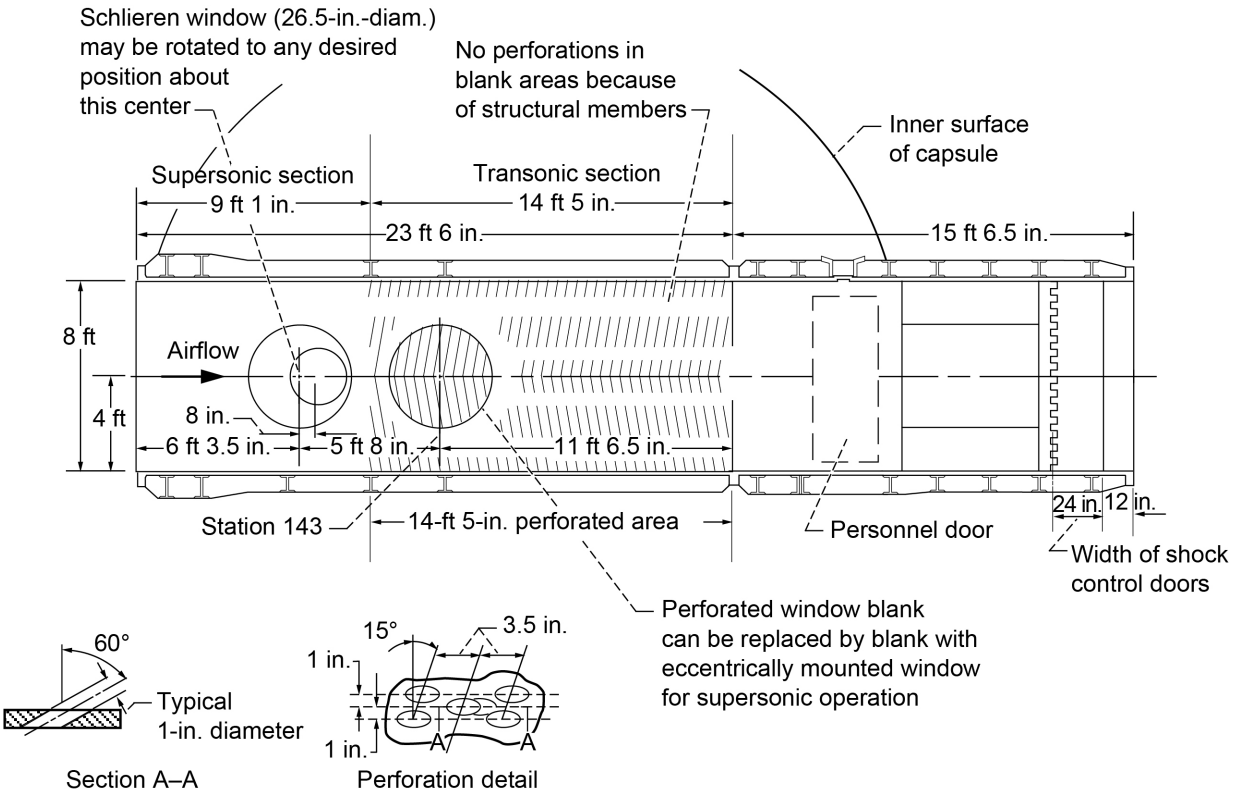

Figure 2.—8- by 6-ft test section elevation view.

Flow quality improvements were installed in the facility in 1992. The improvements that affect the 8- by 6-ft test section are a flow straightening honeycomb and three 10-mesh turbulence reduction screens in the settling chamber upstream of the test section and an aerodynamically contoured compressor exit tailcone fairing. Major tunnel loop modifications were made between 2016 and 2018 as part of the 9×15 LSWT Acoustic Improvement Modifications project. The height, width, and divergence of the 9- by 15-ft test section were maintained, but the following are noteworthy changes to the tunnel loop:

- Acoustically treated turning vanes installed in turn 2 (upstream of the 9- by 15-ft test section).
- Acoustically treated serpentine baffles installed downstream of the tunnel loop heat exchanger (cooler) and upstream of the flow straightening honeycomb.
- An ogive-shaped fairing installed around the inlet of the 9- by 15-ft test section's flow straightening honeycomb.
- Lengthened 9- by 15-ft test section.
- Installed lower-diffusion angle, acoustically treated diffuser downstream of the 9- by 15-ft test section.
- Acoustically treated turning vane structure installed in turn 3 (downstream of the 9- by 15-ft test section) with exit contours designed to spread the flow evenly across the facility air dryer inlet.[2]

A further description of the tunnel loop modifications is documented in Reference 2 and more complete description of the 8×6 SWT is found in Reference 3.

3.0 Instrumentation and Test Hardware[3]

Existing test hardware and instrumentation were used in the 2020 test entry. New facility instrumentation and data systems implemented during the 9×15 LSWT Acoustic Improvement Modifications were also used for this entry. The 4-inch-diameter cone cylinder and transonic array models have been used in previous 8×6 SWT characterization test entries (Refs. 1 and 2). Each of the instruments, their associated support systems, and their locations are described in the following information.

3.1 4-Inch-Diameter Cone Cylinder

The 4-inch-diameter cone cylinder was used to measure the axial static pressure in the test section for each Mach number setting. The 4-in. cone cylinder was chosen for this test entry from the family of cone cylinder models available for use in the 8×6 SWT. The family of cone cylinder models consists of 4-, 8-, 12-, 16-, and 20-in.-diameter models. The 4-in.-diameter model is typically used to provide empty test section calibration data; the larger diameter models provide blockage effect data. The 4-in. model (0.18 percent blockage) is approximately 86 in. long and has a total of 132 static pressure taps. See Figure 3 for details on the 4-in. cone cylinder and instrumentation layout.

[2]For details of the air dryer bed inlet flow field, see Reference 2.
[3]Section and subsections adapted from Reference 1.

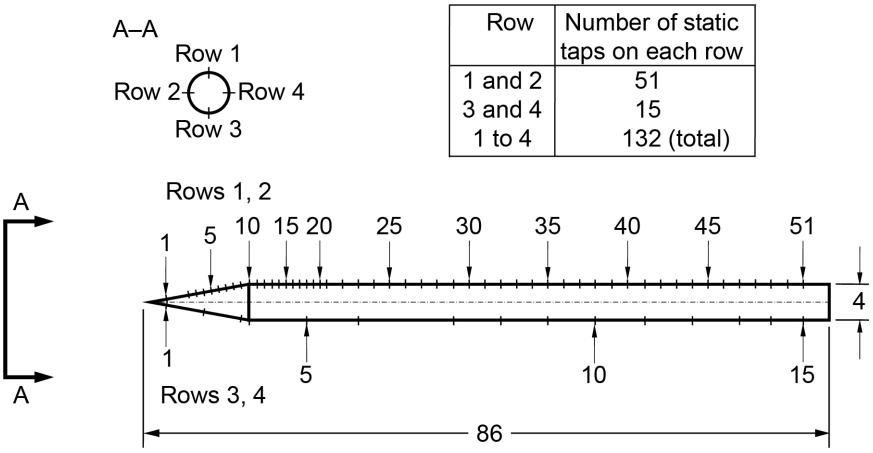

Figure 3.—Instrumentation layout of the 4-inch-diameter cone cylinder. All dimensions in inches.

Each cone cylinder model consists of a 10° half-angle cone with base diameter as listed in the model names above which extends into a constant diameter cylinder. Each model is instrumented with static taps arranged in four axial rows spaced 90° apart. The cone cylinder models are typically sting mounted into the 8×6 SWT transonic strut. Axial position changes of the model in the tunnel are accomplished by means of a split sting section which can be added to or removed from the model assembly without disconnecting the instrumentation lines. The split sting section allows for an axial position change of 34 in. The tip of the cone cylinders can be positioned at either the inlet of the 8-ft test section or at the centerline of the schlieren window blanks in the 14-ft test section.

The 4-inch-diameter cone cylinder was sting mounted to the facility supersonic strut during the 2020 characterization test entry. An adapter sleeve was used with a 4.75-in. inner diameter and 6.5-in. outer diameter to allow the model's sting to fit the supersonic strut's cradle. The facility supersonic strut can be moved to 11 different axial locations in 7 in. increments, allowing the tip of the 4-inch-diameter cone cylinder to be placed as far upstream as test section station (TSTA) –18.0 with the split sting installed or as far downstream as TSTA 86.0 without the split sting. Figure 4 shows the 4-inch-diameter cone cylinder installed during the 2020 test entry with the cone tip at TSTA –4.0 and 29.8.

3.2 Transonic Array

The transonic array was used to survey the test section flow field to provide information on the total and static pressure, total temperature, and flow angle distributions within a cross-sectional plane. The array layout is shown in Figure 5. The standard array instrumentation comprises five flow angularity probes, six pitot-static pressure probes, and 11 thermocouples. Two offset probe supports at rake centerline can be used to hold two hot-film anemometry probes, however, these were not used for the 2020 test entry. The array is typically sting mounted in the transonic strut and further supported by wall plates attached to both ends of the array body and by a vertical support downstream of the array body. As the supersonic test section is historically not the typical mounting location for the transonic array, a unique configuration of the hardware was used. The array wall plates were mounted near the center of the

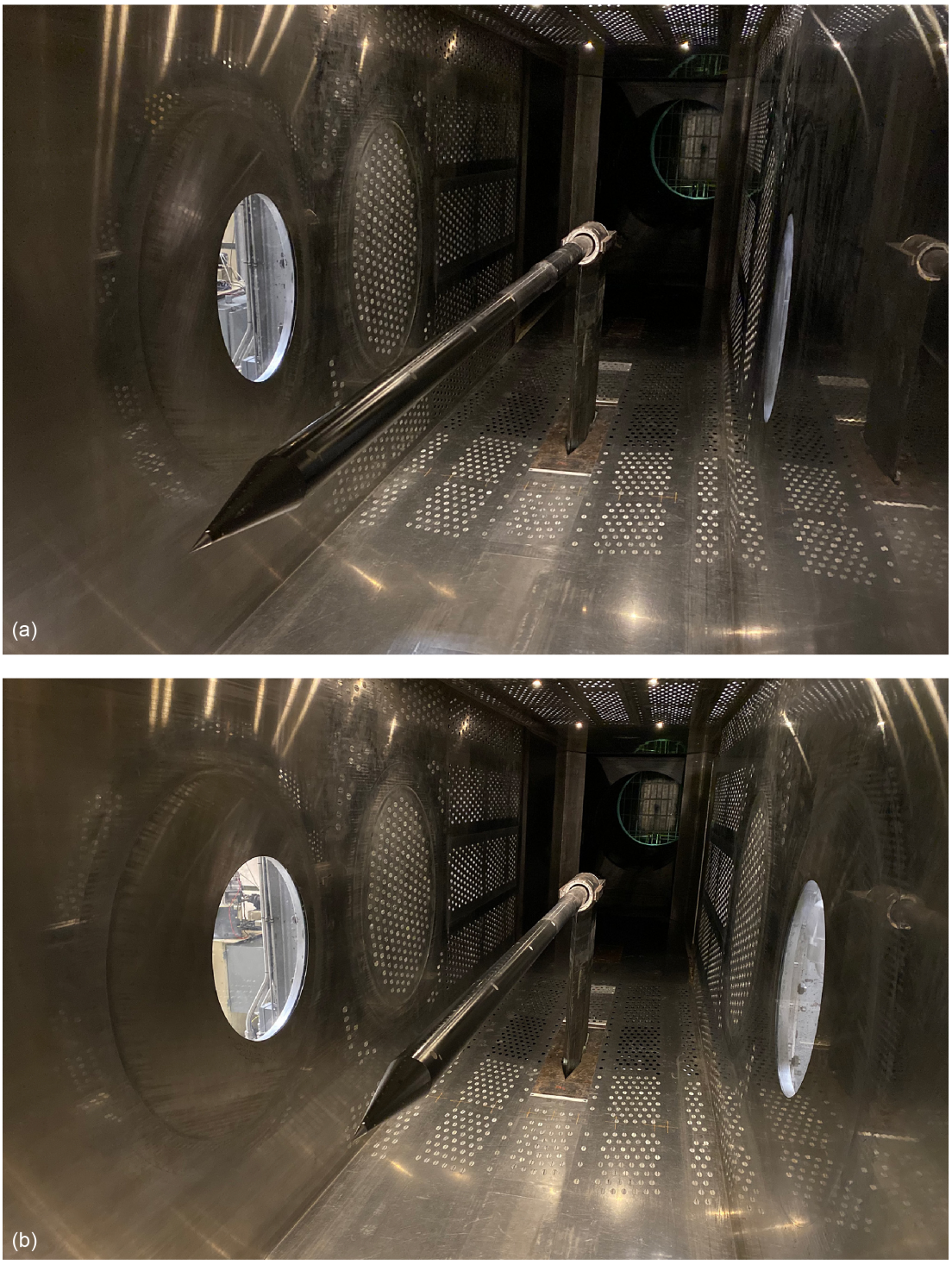

Figure 4.—Installation of the 4-inch-diameter cone cylinder in the 8- by 6-ft test section during the 2020 supersonic test section characterization test entry. Model is shown with the tip of the cone at (a) test section station (TSTA) –4.0 and (b) TSTA 29.8.

upstream-mounted porous window blanks,[4] the vertical support was mounted to a modified test section floor plate, and no sting was used. All the surfaces of the array have a 10° taper to minimize aerodynamic interference. The array body is made of 304 stainless steel and the wall plates of 6061-T6 aluminum. For 2020 test entry, the array was positioned axially such that the tips of the flow angle probes were at approximately TSTA 44.25. The array was tested at three vertical positions at this station (tunnel centerline and 1 ft above and below tunnel centerline). Figure 6 shows a typical installation of the array in the supersonic test section, and Figure 7 shows the array installed at centerline during the 2020 test entry. The wall plates (which are not shown in Figure 6) are attached to the tunnel walls by bolts that pass through the test section porosity holes. The floor plate for the vertical support is attached to the tunnel using T-nuts through holes in the modified test section floor plate in the supersonic test section or through the porosity holes in the transonic test section (same as the wall plates). There are five vertical supports (one for each potential vertical position of the array: centerline and 1 and 2 ft above and below centerline). The vertical support is bolted to the floor plate and to a collar that clamps around the sting just aft of the array body. The sting, through which the instrumentation lines typically pass, was not used during the 2020 test entry. The instrumentation was instead wrapped in Teflon™ tape, clamped down the north side of the vertical support, and routed through the closest three porosity holes in the test section floor. The transonic strut was not present in the test section during the 2020 test entry. Figure 8 shows the measurement locations of the transonic array (and 4-inch-diameter cone cylinder) within the 8- by 6-ft supersonic test section during the 2020 test entry.

The flow angle probes are five-hole, hemispherical-head design, which allow resolution of two flow angle components (pitch and yaw). The flow angle probes were calibrated for a Mach number range of 0.5 to 2.0. The Mach number range of the 8×6 SWT is 0.36 to 2.0 for three-motor operation while the operating range of the probe calibration facility at Sandia National Laboratories (Albuquerque, New Mexico) was 0.5 to 4.0 so probe calibration data were extrapolated at the low Mach number conditions in the 8×6 SWT. These probes extend 21.5 in. from the leading edge of the array. The pitot-static probes also extend 21.5 in. from the array leading edge.

The thermocouple probes (type-E “special-limit-of-error” wire) are mounted to the bottom of the array body, with the heads of the thermocouples about even with the array leading edge and 2.25 in. below rake centerline. All thermocouples are terminated to the temperature reference junctions without any intermediate connections (commonly referred to as “home-run-length” thermocouples). Except for the thermocouple at centerline, the wires exit the array through notches in the instrumentation cover plates in the top of the array body, are nichrom-strapped to the top of the array body to its aft end, and are routed alongside the centerline thermocouple and pressure tubing out of the test section. The thermocouple probes on the transonic array were modified prior to a customer-specific characterization test entry in 2016. Due to space constraints within the array body and the size of the thermocouple wire chosen, 10 of the 11 wires were routed on the exterior of the model.

[4]All holes in the upstream-mounted porous window blanks were plugged except for those used for attaching the array wall plates to the tunnel walls.

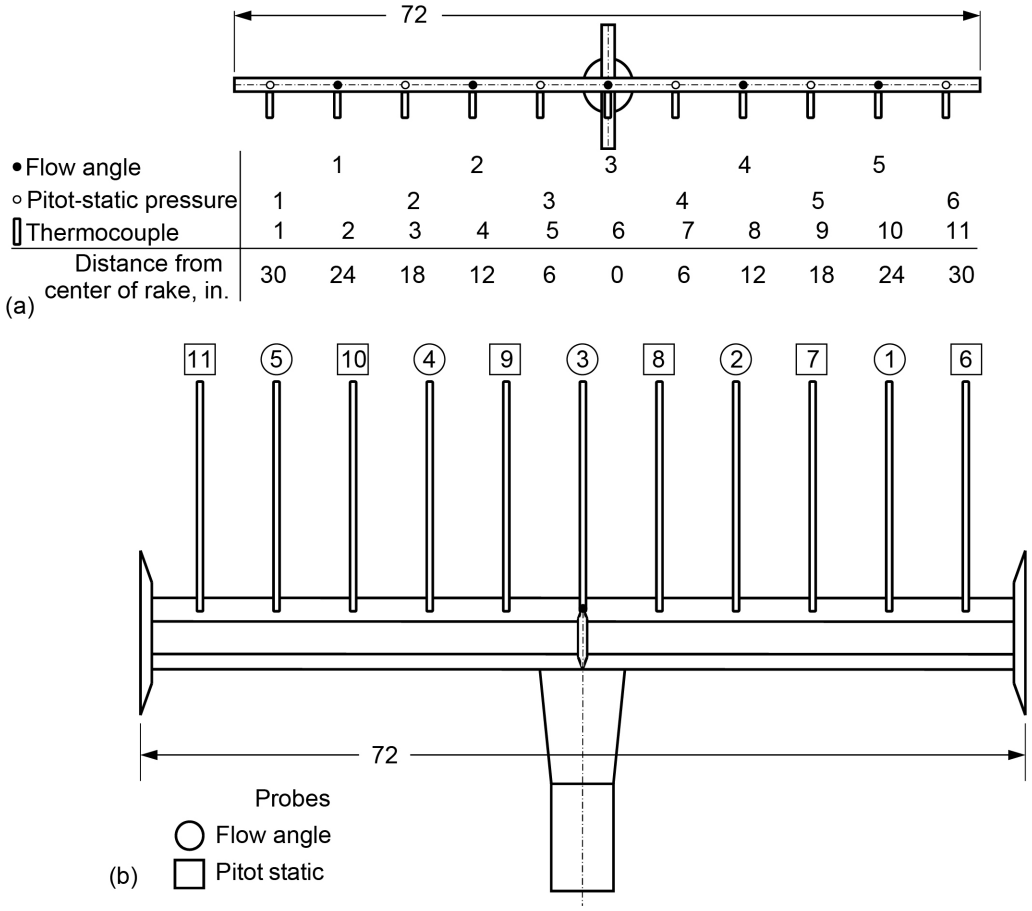

Figure 5.—Instrumentation layout of transonic array. (a) Upstream looking aft view. (b) Top-down view. All dimensions are in inches.

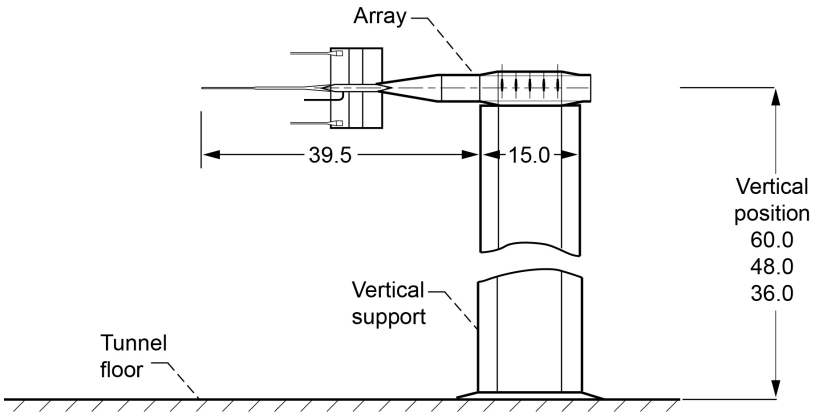

Figure 6.—Typical installation of the transonic array in 8- by 6-ft solid-wall, supersonic test section (elevation view). The array can be stationed at one axial position and three vertical heights in the supersonic test section. All dimensions are in inches.

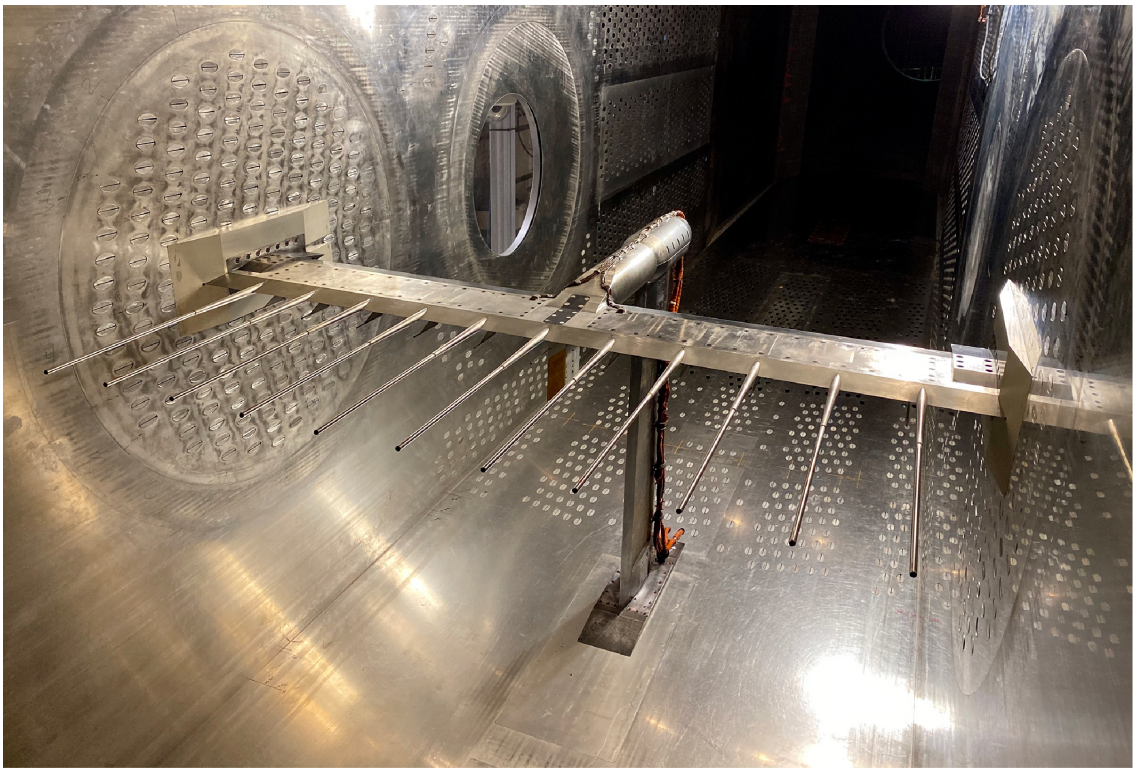

Figure 7.—Transonic array installed at centerline in the 8- by 6-ft supersonic test section during the 2020 test entry with pressure probe tips near test section station 44.25.

Test section station (TSTA) of hardware locations in the 8x6 SWT (2020 test)		
Model		TSTA
4-in.-diam. cone cylinder		−4.0
		29.8
Transonic array	Centerline (CL)	44.34
	CL + 1 ft	44.26
	CL − 1 ft	44.29

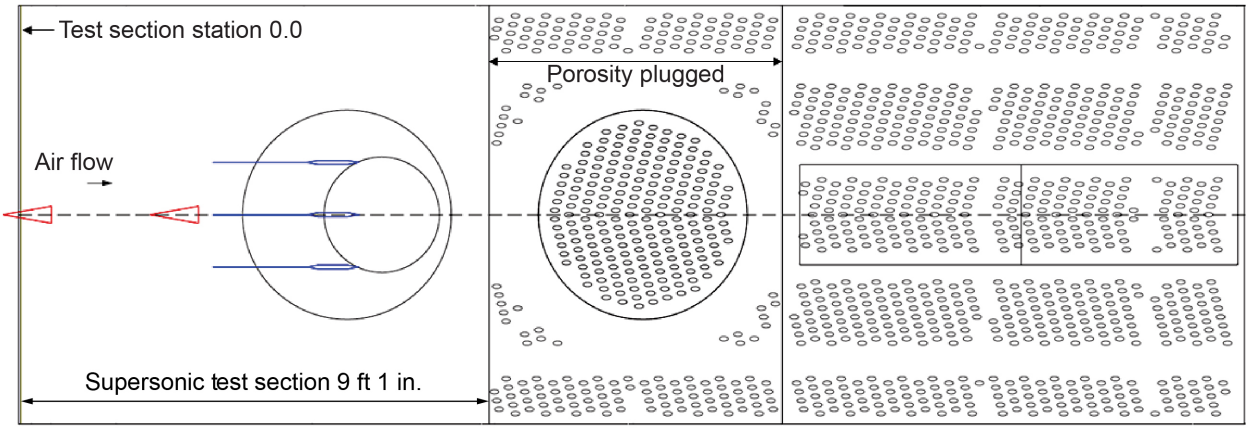

Figure 8.—Measurement locations of the 4-inch-diameter cone cylinder and transonic array during the supersonic test section characterization (2020 test). Air flows from left to right. Measurement locations are defined as cone tip for cone cylinder models and pressure probe tips for transonic array. SWT is Supersonic Wind Tunnel.

3.3 Facility Instrumentation

The following permanent instrumentation was used during the supersonic test section characterization 2020 test entry:

- Bellmouth rakes—two wall-mounted rakes are located near the exit of the bellmouth upstream of the test section. One rake is mounted to the north tunnel wall and the other to the south tunnel wall at approximately the tunnel centerline (the rakes are designated "north" and "south," see Figure 9). The instrumentation mounted on each rake consists of four total pressure and two total temperature probes. Each rake has a fifth pitot tube devoted to the tunnel control system, and one of the four total temperature probes is devoted to the tunnel control system. Similar to the transonic array, the total temperature thermocouples on the bellmouth rakes were modified in 2016. The thermocouples are the same type-E special-limit-of-error wire as used on the transonic array with aspirated probe tips. Thermal recovery corrections are not implemented on the bellmouth rake thermocouple measurements.
- Balance chamber pressure—four pressures are measured within the balance chamber. These pressure taps are distributed around the balance chamber.
- Facility Static Pressures—Figure 10 shows the location of all static pressure taps located on the ceiling of the 8- by 6-ft test section and high-speed diffuser section.
- Flexible-wall nozzle camshaft encoder—an encoder on the flexible-wall nozzle's camshaft measures the rotational angle of the shaft. There are known orientations of the camshaft to achieve the appropriate contour for Mach 1.1 to 2.0 in 0.1 Mach increments. Calibrations of the walls' contours have been performed to verify this relationship.[5]

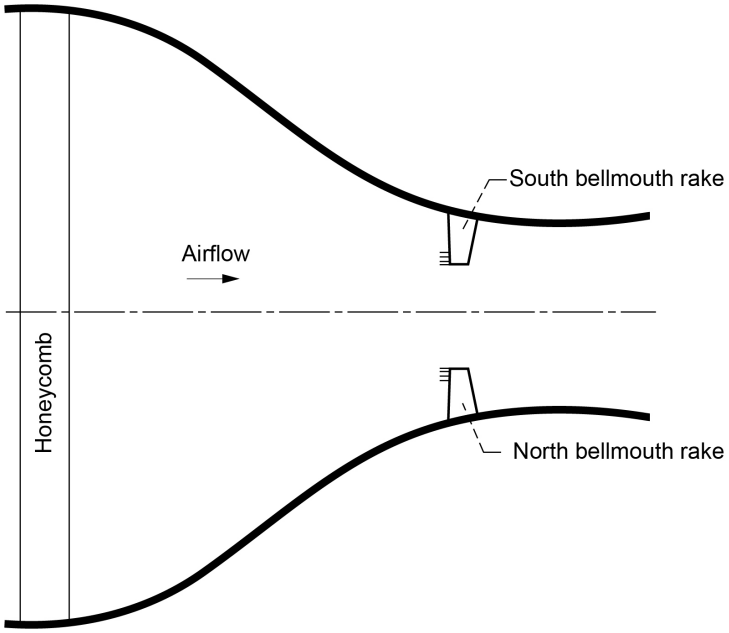

Figure 9.—Installation of bellmouth rakes upstream of 8- by 6-ft test section. Rakes measure both total pressure and temperature.

[5]The most recent flexwall calibration was performed prior to the 2019 test entry at flexwall settings of Mach 1.0, 1.4, and 2.0. Typical variations from contour measurements taken in 2005 were less than 0.015 in. at each of the 14 measurement locations along the walls length.

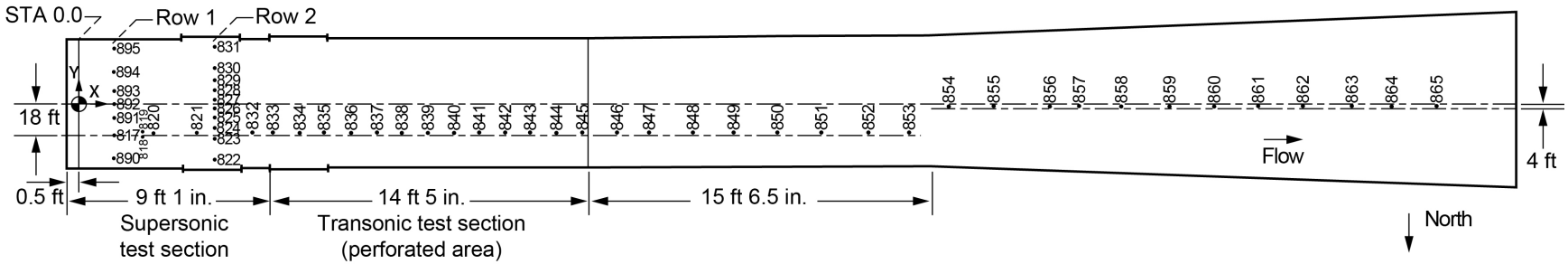

Static tap location	Axial station, X, in.	Distance from centerline, Y, in.	Static tap location	Axial station, X, in.	Distance from centerline, Y, in.
817	17.00	–18.00	838	169.25	–18.00
890	17.00	–30.63	839	183.25	–18.00
891	17.00	–7.50	840	197.50	–18.00
892	17.00	0.00	841	211.50	–18.00
893	17.00	7.56	842	225.50	–18.00
894	17.00	18.06	843	239.50	–18.00
895	17.00	25.78	844	253.38	–18.00
818	32.88	–19.56	845	267.63	–18.00
819	32.88	–16.56	846	286.50	–18.00
820	39.31	–18.00	847	303.75	–18.00
821	63.31	–18.00	848	327.50	–18.00
822	72.25	–31.50	849	350.50	–18.00
823	72.25	–19.50	850	374.06	–18.00
824	72.25	–13.50	851	398.75	–18.00
825	72.25	–7.50	852	422.63	–18.00
826	72.25	–2.50	853	446.00	–18.00
827	72.25	2.50	854	473.38	–4.00
828	72.25	7.50	855	497.44	–4.00
829	72.25	13.50	856	528.19	–4.00
830	72.25	19.50	857	543.31	–4.00
831	72.25	31.50	858	567.19	–4.00
832	87.50	–18.00	859	593.25	–4.00
833	99.25	–18.00	860	617.31	–4.00
834	113.25	–18.00	861	641.25	–4.00
835	127.25	–18.00	862	665.25	–4.00
836	141.38	–18.00	863	692.31	–4.00
837	155.75	–18.00	864	713.25	–4.00

Figure 10.—Facility static tap locations in 8- by 6-ft test section ceiling and diffuser.

3.4 Data Systems

The tunnel data system used during this test entry in the 8×6 SWT was COBRA (Collect, Observe, Broadcast, Record, and Analyze), which was implemented during the 9×15 LSWT Acoustic Improvement Modifications project construction period (2016 to 2018). Real-time data acquisition and display was provided by COBRA, the standard data system being implemented in the large test facilities at the NASA Glenn Research Center to replace the Escort data acquisition system. The COBRA data system accommodates the electronically scanned pressure (ESP) inputs, plus all steady-state analog and digital signals used including thermocouples and pertinent tunnel control parameters such as compressor speed, shock door positions, and positions of flow control doors 1 and 2. Data acquisition, engineering unit conversions, and calculations are performed by the data system at selected frequencies. All data during the 2020 test entry were acquired at 12.5 Hz.[6] For this test, unless noted otherwise, each collected data reading was 30 s in length. Data can be filtered and batched several ways following data collection through the COBRA data system. All data shown in this report, unless otherwise noted, is averaged across the length of the reading.

Steady-state pressure data were acquired with the Optimus Data System (TE Connectivity) and 32-channel, 15-psid electronic pressure scanners (ESP–32HD DTC Gen–1 and Gen–2). The pressure scanners are miniature electronic differential pressure measurement units with an individual piezoresistive pressure sensor for each channel. This model of pressure scanner allows for digital temperature compensation and in situ calibrations. An in situ calibration consists of setting five pressures, as measured by a high-accuracy 30-psia pressure calibration unit across the span of the pressure scanner then making a span and zero adjustment for each channel. In situ calibrations are typically performed every 2 hr or more frequently per data engineer and test conductor judgement. The reference pressure for the differential pressures sensed by the pressure scanner are measured by a 15-psia Mensor pressure transducer (Model CPT6180).

The thermocouples on the transonic array and bellmouth rakes were terminated to the same Kaye Uniform Temperature Reference (UTR) where the thermocouples were junctioned to copper. Two resistance temperature detectors (RTDs) in each reference measured the temperature of the junction using a Fluke 2562 module (Fluke Corporation). Copper wires connect the Kaye UTR to COBRA.

4.0 Operational Considerations[7]

Descriptions of test setup, operational procedures, and test matrices used during the 2020 test entry is contained in this section. In general, the test setup and operational procedures are similar to those used in previous entries (Refs. 1 and 2).

4.1 Test Setup and Procedures

The test procedures specific to each piece of characterization hardware are described in the following sections.

[6]The Mensor LP pressure transducer used for the ESP reference pressure provided samples to the data system at 10 Hz.

[7]Section and subsections adapted from Reference 1.

4.1.1 4-Inch-Diameter Cone Cylinder

End-to-end checks of all instrumentation lines were conducted following installation of the cone cylinder model in the test section. Any issues were resolved prior to testing and noted in the test log. Prior to each run, the cone cylinder was positioned such that the tip of the cone was at the test section centerline and leveled in pitch using a digital inclinometer placed just downstream of the shoulder of the cone cylinder. During a typical tunnel run, the highest Mach number conditions were set first to preserve air dryer capacity. The model pitch angle was monitored during the run by an electrolytic inclinometer in the forward portion of the cylinder. If required, the model was adjusted back to 0° during the test using the supersonic strut pitch controls.

4.1.2 Transonic Array

Following the initial installation of the array in the test section, the flow angle probe pitch and yaw alignment offsets were measured using a portable FaroArm® coordinate measuring machine (CMM) (Faro® Technologies, Inc.) and the baseline rake pitch and yaw angles were measured using a digital inclinometer and tape measure. The CMM used the tunnel floor for a reference plane in the pitch axis and a plane created from both tunnel walls for a reference in the yaw axis. For each rake height change, the rake pitch and yaw angles were measured and compared to the baseline values. The differences from the baseline values were used to correct the measured flow angles for rake misalignment. End-to-end instrumentation checks were also made following the array installation. Similar to the cone cylinder procedures, the highest Mach number conditions were set first during the array surveys. Vertical position changes for the array were made manually, so there was no translation of the hardware while the tunnel was running.

4.2 Test Matrix

The test matrix for the supersonic conditions surveyed in the 2020 test entry is shown in Table I. Subsonic flow conditions were surveyed between approximately Mach 0.84 and 0.40. All testing during this entry was performed in closed loop (aerodynamic cycle). In this mode of operation, air is recirculated through the tunnel loop with makeup air entering the loop through vents in turn 3 (upstream of the air dryer building). The porosity holes in the transonic test section were plugged for the first 6 ft, resulting in an 8-ft, 6.2-percent porosity transonic test section for the duration of this test entry. While testing in the supersonic test section with this porosity configuration, the test section is considered to be in test section configuration 7. During the test entry, the 4-inch-diameter cone cylinder surveyed the supersonic test section first with its cone tip at TSTA –4.0 and then at TSTA 29.8 by removing the split sting. The transonic array surveys followed with pressure probe tips of the array positioned near TSTA 44.25. The transonic array surveyed the supersonic test section flow field at centerline and 1 ft above and below centerline.

In addition to the nominal flexwall settings of Mach 1.1 to 2.0 in 0.1 Mach increments, off-nominal flexwall settings were surveyed per requests from a future 8×6 SWT customer. These off-nominal flexwall settings were an attempt to achieve an average freestream Mach number as near to Mach 1.40 and 1.50 as possible with 0.01 increments of the flexwall Mach number setting. Off-nominal flexwall settings surveyed include the following: 1.42 to 1.44 and 1.52 to 1.55 in 0.01 Mach increments. With the 4-inch-diameter cone cylinder in its upstream position and the transonic array at centerline, three data points were acquired at each supersonic condition surveyed.[8] Subsonic three-motor operation conditions

[8]Only one reading was acquired at flexwall setting of Mach 1.53 with the 4-inch-diameter cone cylinder in its upstream position, as indicated in Table I.

TABLE I.—TEST MATRIX OF SUPERSONIC CONDITIONS SURVEYED WITH 4-INCH-DIAMETER CONE CYLINDER AND TRANSONIC ARRAY DURING 8- BY 6-FOOT SUPERSONIC WIND TUNNEL SUPERSONIC TEST SECTION CHARACTERIZATION (2020 TEST)

Flexwall Mach number	4-inch-diameter cone cylinder[a]		Transonic array		
	Cone tip test section station		Vertical position		
	–4	29.8	Centerline	1 ft below centerline	1 ft above centerline
2.00	R	B	R		
1.90	R	B	R		
1.80	R	B	R		
1.70	R, B	B	R		
1.60	R, B	B	R		
1.55	R	R	R		
1.54	R	R	R		
1.53		R	R		
1.52	R	R	R		
1.50	R, B, S	R, B, S	R		
1.44	R	R	R		
1.43	R	R	R		
1.42	R	R	R		
1.40	R, B, S	R, B, S	R		
1.30	R, B	B	R		----
1.20	R, B	B	----	----	----
1.10	----	----	----	----	----

[a]R = repeats acquired (total of three data points). B = balance chamber pressure variation investigated. S = strut height variation investigated. ---- = subsonic in solid-wall test section. Blank cells = supersonic data without additional investigations.

were surveyed at facility settings (compressor speed, balance chamber pressure, and shock door positions), which typically produce the following conditions in the transonic test section: Mach 0.95 and 0.90 to 0.40 in 0.10 Mach increments.

Balance chamber pressure influences were investigated in the supersonic test section with the 4-inch-diameter cone cylinder model. The balance chamber pressure has been used to raise and lower the average Mach number of the flow in the transonic test section at a given flexwall setting (Ref. 2). Similar balance chamber variation levels previously used in transonic test section characterizations were used for the supersonic test section characterization.

Customers intending to use the supersonic test section require condition stability during test points as well as across test points when the supersonic strut has moved. The supersonic strut, when raised or lowered, typically results in increased or decreased balance chamber pressure, respectively, thus altering the calibrated transonic test section static pressure. During the 2020 test entry, the supersonic strut was raised and lowered between centerline and 1 ft below centerline to investigate the impact, or lack thereof, on the supersonic test section pressures with the 4-inch-diameter cone cylinder. This study was conducted at flexwall settings of Mach 1.4 and 1.5 due to the interest of the upcoming customer near these facility settings.

For all testing, a detailed log was maintained to track reading number, test conditions, problems, etc. On-line data monitoring was used to ensure data quality.

5.0 Data Reduction[9]

The data analysis methodology used for each part of the calibration tests is described in the following sections. The information presented here applies to the general treatment of the data; for some specific applications, details of the data reduction are included in the discussion section.

The first step of the data reduction and analysis was a thorough review of the data to ensure data quality. While most instrumentation and data problems were detected and resolved either prior to or during the testing, there were instances where bad or questionable data was collected and further investigation was required (i.e., bad data points were flagged and therefore not used in subsequent steps of the analysis). Notes taken during the testing as part of the test engineers' log were used to troubleshoot problems with data channels.

At the completion of the test entry, the data were reprocessed using programs that mimicked the on-line data reduction. This step corrected any errors in data from instrumentation problems or test setup errors. All posttest analyses were performed by custom scripts in MATLAB® (The MathWorks, Inc.).

5.1 4-Inch-Diameter Cone Cylinder

A detailed description of the development of the cone cylinder data analysis methodology is contained in Reference 4, but an abbreviated explanation is included here. The average static pressure on the cone portion of the model can be used to estimate the local freestream Mach number and static pressure for supersonic conditions; a theoretical relationship between a cone cylinder model's cone surface static pressure and the freestream Mach number exists for supersonic conditions (see Ref. 4 for details). The average static pressure over the aft portion of the cylinder, $P_{S,cyl,avg}$, provides a direct measurement of the freestream static pressure for all Mach number settings. The static pressure measurements on the model are first averaged circumferentially at each axial station before averaging in the streamwise direction.

5.2 Transonic Array

A detailed description of the transonic array data reduction methodology is contained in Reference 1 with some high-level descriptions included in this section. The local freestream total pressure at the pitot-static and five-hole hemispherical head flow angularity probes is measured at subsonic test section conditions. The local total pressure downstream of a normal shock ($P_{T,2}$) is measured by each of these probes at supersonic test section conditions. The calibrated test section static pressure generated from the aft portion of the 4-inch-diameter cone cylinder was used to compute local Mach numbers at each pressure probe on the transonic array. It is believed that the cone cylinder is a more accurate measurement of freestream static pressure, particularly at supersonic conditions between Mach 1.0 and 1.5 where probe-to-probe interference is apparent in the array data. Two components of flow angle are computed at each of the five-hole flow angularity probes per data reduction method in Reference 1. Data acquired in the Sandia National Laboratory Trisonic Wind Tunnel were used to calibrate the flow angle probes (Refs. 8 and 9 from Ref. 1).

[9]Adapted from Reference 1.

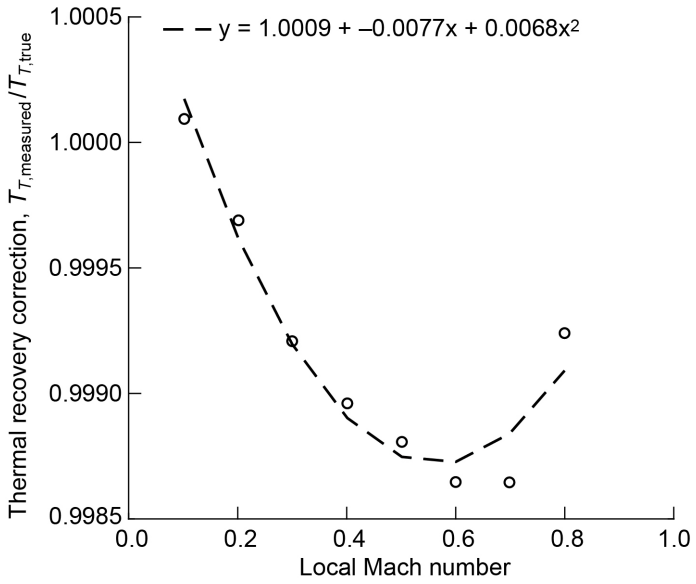

Figure 11.—Thermal recovery correction data and regression model for transonic array thermocouple design. Data acquired in NASA Glenn Research Center Engine Research Building free-jet calibration facility (CE-12).

In 2016, a model of the centerline thermocouple probe used on the transonic array was created, instrumented using the same type and length of wire used in the array, and the thermal recovery characteristics of the probe determined (Ref. 2). The transonic array's thermocouple probes are corrected for thermal recovery at Mach numbers between Mach 0.1 and 0.8 per results obtained from a characterization test conducted in a 3.5-inch-diameter free-jet calibration facility in the NASA Glenn Engine Research Building (ERB). The measured thermocouple temperature (in Rankine) is divided by a correction factor to yield the corrected freestream total temperature (in Rankine). The correction factor was found to be a second-order polynomial function of local Mach number. Figure 11 shows the thermal recovery correction data acquired from the free-jet characterization test and the regression model fit through the data. On the transonic array, the local Mach number at each pressure probe is used to correct the thermocouple at the same lateral location along the array. If the local Mach number is greater than Mach 0.8 or less than Mach 0.1, no correction is applied.

6.0 Discussion of Results

All results discussed and data presented in the following sections are from the 2020 supersonic test section characterization test entry unless otherwise noted.

6.1 Flow Quality Goals[10]

Flow quality goals for the NASA Glenn wind tunnels have been defined and are listed in Table II. These flow quality goals are based on information and recommendations from the Wind Tunnel Calibration Workshop held at NASA Langley Research Center (Ref. 10 from Ref. 1) and modified for the specific missions of the propulsion wind tunnel facilities at NASA Glenn.

[10]Adapted from Reference 1.

TABLE II.—TEST SECTION FLOW QUALITY GOALS FOR NASA GLENN RESEARCH CENTER WIND TUNNELS

Flow quality parameter	Aeropropulsion tunnels[a]	Icing Research Tunnel
Mach number variation	0.005	0.005
Flow angularity, degree	±0.25	±0.25
Turbulence intensity, percent	0.25	0.50
Total temperature variation, °F	4	2

[a]The aeropropulsion tunnels at NASA Glenn are the 9- by 15-Foot Low-Speed, the 8- by 6-Foot Supersonic, and the 10- by 10-Foot Supersonic Wind Tunnels.

6.2 Supersonic Test Section Starting Conditions

The solid-wall supersonic test section in the 8×6 SWT has more stringent model blockage requirements when compared to the porous transonic test section located downstream. For both models used during this test entry, bringing the flexwalls in to a setting of Mach 1.1 to start the test section resulted in subsonic flow in the supersonic test section and supersonic flow in the transonic test section. With the 4-inch-diameter cone cylinder model (0.18 percent blockage), the supersonic test section did not produce supersonic flow until the flexwalls were set to Mach 1.2 or greater. The transonic array at centerline and at 1 ft below centerline (approximately 2.37 and 2.19 percent blockage, respectively) produced supersonic flow at a flexwall setting of Mach 1.3 or greater. With the transonic array at 1 ft above centerline (approximately 2.54 percent blockage), the supersonic test section was started at a flexwall setting of Mach 1.4. Some of this information is also summarized in the test matrix (Table I). Due to the lack of transient data during condition changes between the nominal flexwall settings of Mach 1.1 to 1.4, only visual observations recorded in the test run log can give closer approximations of the point at which the flow started in the supersonic test section. It should be noted that the flow through the transonic test section was supersonic from flexwall settings of Mach 1.1 to 2.0 with each piece of hardware installed during the test entry, as observed from ceiling static pressure measurements in the porous test section.

Historical blockage criteria for the 8×6 SWT transonic and supersonic test sections are shown in Figure 12 (Ref. 5). This figure does not show that the supersonic test section is started at test section Mach number less than 1.5 (with a blockage of about 4.5 percent). The blockage levels in this figure are the projected frontal area of the model and the support strut. If the supersonic strut blockage were included in the 4-in. cone cylinder's blockage estimate, the projected frontal area blockage was 3.65 percent. In Reference 6, a simple area-Mach-number relation is used to illustrate that a model of 2.8 percent blockage is theoretically able to operate at Mach 1.20 and no slower without choking the flow in the test section. As stated in Reference 5, the model shape and other factors influence the limiting starting Mach number of a model in the wind tunnel. The supersonic strut leading edge and 4-inch-diameter cone cylinder cone tip were approximately 11-ft 7-in. apart with the cone cylinder in its aft position during this test entry. Additionally, the supersonic strut leading edge was located at about TSTA 169 and the 8-ft porous test section begins about 1 ft downstream of this station. The proximity of the blockage sources to one another and the location of the support strut relative to the test section porosity likely influences the starting ability of the supersonic test section.

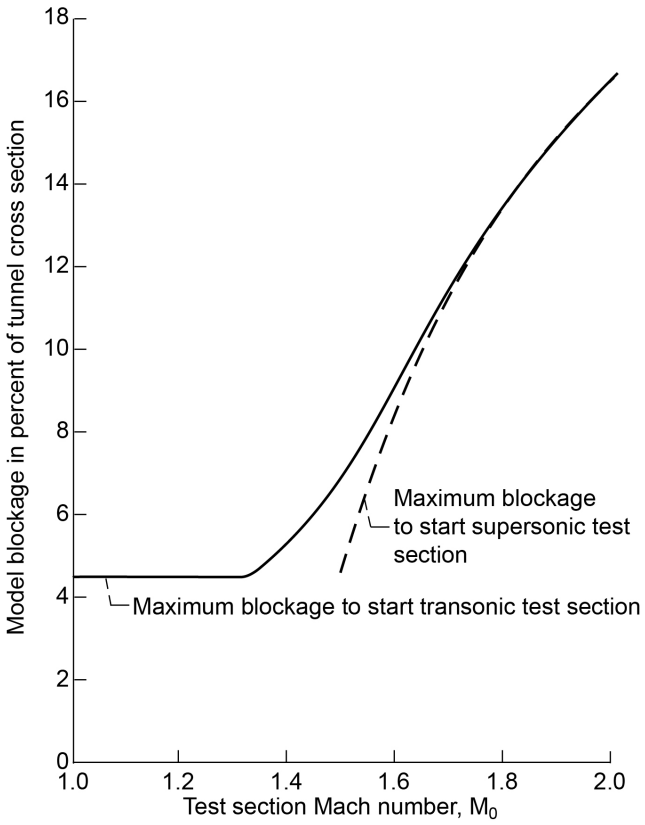

Figure 12.—Legacy figure describing model blockage limits as a function of test section Mach number for the 8- by 6-Foot Supersonic Wind Tunnel from Reference 5 (NASA TM X–71542).

6.3 4-Inch-Diameter Cone Cylinder

The static pressure distributions along the 4-inch-diameter cone cylinder model at both of the axial positions surveyed in the supersonic test section are shown in Figure 13 to Figure 30. The model static pressure, $P_{S,\text{model}}$, data shown are normalized by the average bellmouth total pressure, $P_{T,bm}$, to remove potential temporal variation between the two static pressure data sets. Each data point in the cone cylinder model's data set is an average of either two or four static pressure measurements around the circumference of the model at that axial station. If repeat points were acquired with the cone cylinder at a given condition, the data displayed in the figure are an average of the repeat readings. The data are overlaid upon an image of the cone cylinder model in the supersonic test section. The upstream position of the cone, with the cone tip at TSTA –4.0, is upstream of the flexwall seam (vertical solid line) and TSTA 0.0 (vertical dashed line), whereas the downstream position of the cone cylinder is shown as a dashed outline of the model with the cone tip at TSTA 29.8. Note that the flare of the cone cylinder sting for the downstream position of the model is not shown in these figures and is approximately 34 in. aft of where it is shown for the upstream position of the model. The large circle centered about TSTA 75 is the upstream schlieren window in the 8- by 6-ft test section. For reference, the supersonic test section length is 9-ft 1-in., in other words, the plugged porosity holes begin at approximately TSTA 109. The average static pressure along the cylinder is displayed downstream of the cone cylinder data for both the upstream and downstream data sets in Figure 13 to Figure 30. Also plotted is the theoretical pressure ratio along a 10° half-angle cone cylinder model at the average cylinder Mach number for supersonic conditions (Ref. 4).

The theoretical freestream Mach number and static pressure estimates from cone surface pressures were not used in these figures or further analyses of the test entry's data set. The average cylinder static pressure is a more direct measurement of freestream flow and was therefore chosen to be the primary representation of freestream static pressure in the 8×6 SWT supersonic test section.

After review of the combined static pressure distributions from both cone cylinder positions at flexwall settings of Mach 1.8 through 1.5, a weak oblique shock wave generated near the end of the flexwall is present on both data sets at the same axial station. At a flexwall setting of Mach 1.8, there is a rise in static pressure on both pressure distributions peaking at about TSTA 80. At Mach 1.7, the wave impacts the cylinder near TSTA 72, at Mach 1.6: TSTA 66, and at Mach 1.5: TSTA 58. This pressure wave observation along the cylinder was corroborated with schlieren images taken in the 8- by 6-ft supersonic test section in 2012.

In References 1 and 2, the static pressure on the cylinder is an average of all static pressure stations 40 in. downstream from the cone tip (10 diam. for a 4-in.-diam. model). During the supersonic test section characterization, the conical oblique shock generated by the tip of the cone is noticeable in the cylinder static pressure distribution as it is reflected off the test section surfaces. To prevent a biasing of the freestream static pressure measurements, the static pressure port stations selected for averaging needed to be limited further. For this reason, Table III was created based upon observed static pressure rises on the cylinder at each flexwall setting, which produced supersonic flow over the model. At flexwall settings of Mach 1.7 and greater, the reflected shock impacted the model aft of all instrumentation. On the other extreme, at a flexwall setting of Mach 1.2, only three axial stations of pressure ports are available for each position of the 4-inch-diameter cone cylinder model.

TABLE III.—UPSTREAM AND DOWNSTREAM STATIC PRESSURE PORT LIMITS

[For determining the average cylinder static pressure on the 4-inch-diam. cone cylinder during the supersonic test section characterization in the 8- by 6-Foot Supersonic Wind Tunnel (2020 test).]

Flexwall Mach number	Upstream limit (start)		Downstream limit (end)	
	Port station from cone tip	Distance from cone tip, in.	Port station from cone tip	Distance from cone tip, in.
2.00	29	40.34	51	84.34
1.90	29	40.34	51	84.34
1.80	29	40.34	51	84.34
1.70	29	40.34	51	84.34
1.60	29	40.34	48	78.34
1.55	29	40.34	46	74.34
1.54	29	40.34	45	72.34
1.53	29	40.34	45	72.34
1.52	29	40.34	44	70.34
1.50	29	40.34	44	70.34
1.44	29	40.34	40	62.34
1.43	29	40.34	39	60.34
1.42	29	40.34	38	58.34
1.40	29	40.34	38	58.34
1.30	29	40.34	32	46.34
1.20	29	40.34	31	44.34

The static pressures within the ranges described in Table III from both the upstream and downstream positions of the cone cylinder model were combined to quantitatively assess the pressure gradient seen in this region of the 8- by 6-ft test section. This information is tabulated in Table IV; static pressure gradients are documented for each flexwall setting and subsonic test section Mach number surveyed during the test entry with the corresponding TSTA range over which the static pressure data were collected. For conditions at which repeat data points were collected, data were averaged across the repeats to prevent uneven weighting of the first-order curve fit through the cylinder static pressure data. To prevent temporal biases from affecting the pressure gradient value, the ratio of model static pressure to bellmouth total pressure was used in the curve fit and the resulting slope was multiplied by the average bellmouth total pressure across the 4-inch-diameter cone cylinder tests conducted at that condition.

TABLE IV.—PRESSURE AND MACH NUMBER GRADIENTS IN 8- BY 6-FT SUPERSONIC TEST SECTION AT GIVEN FLEXWALL SETTING AND RANGE OF TEST SECTION STATIONS OVER WHICH GRADIENT VALUES APPLY

Flexwall Mach number setting	Axial static pressure gradient, psia/in.	Axial Mach number gradient, 1/in.	First port TSTA,[a] in.	Last port TSTA, in.	Average TSTA of ports used, in.	Number of data points used
2.00	0.0024	–0.0005	36.34	114.14	75.24	46
1.90	.0016	–.0003	36.34	114.14	75.24	46
1.80	.0005	–.0001	36.34	114.14	75.24	46
1.70	0	0	36.34	114.14	75.24	46
1.60	0	0	36.34	108.14	72.24	40
1.55	–.0006	.0001	36.34	104.14	70.24	36
1.54	0	0	36.34	102.14	69.24	34
1.53	0	0	36.34	102.14	69.24	34
1.52	0	0	36.34	100.14	68.24	32
1.50	0	0	36.34	100.14	68.24	32
1.44	0	0	36.34	92.14	64.24	24
1.43	0	0	36.34	90.14	63.24	22
1.42	0	0	36.34	88.14	62.24	20
1.40	.0014	–.0002	36.34	88.14	62.24	20
1.30	.0049	–.0005	36.34	76.14	56.24	8
1.20	.0035	–.0004	36.34	74.14	55.24	6
Subsonic operating conditions						
M_{ts}[b]						
0.840	–0.0012	0.0001	36.34	114.14	75.24	46
0.817	–.0013	.0001	36.34	114.14	75.24	46
0.758	–.0018	.0002	36.34	114.14	75.24	46
0.670	–.0006	.0001	36.34	114.14	75.24	46
0.584	–.0007	.0001	36.34	114.14	75.24	46
0.487	.0004	.0000	36.34	114.14	75.24	46
0.395	–.0004	.0001	36.34	114.14	75.24	46

[a]Test section station (TSTA) is defined as distance downstream of the 8- by 6-ft test section datum line (datum line is 0.5 in. downstream of flexwall floor seam).

[b]For subsonic operating conditions, calibrated test section Mach number (M_{ts}) is given instead of flexwall setting.

Pressure gradient data are shown in Table IV only at flexwall settings, which had a significant linear correlation (p-value ≤0.05) between static pressure and test section station. Similarly, the Mach number gradient per inch is shown in Table IV using cylinder static pressure and calibrated test section total pressure. Subsonic operating condition Mach number gradients are typically 0.0002 per inch or less. About half of the supersonic operating conditions surveyed had an insignificant linear fit when computing these gradients, and the other half had gradients between 0.0001 and –0.0005 Mach per inch. As the boundary layer grows in the streamwise direction in the solid-wall, nondiverging 8- by 6-ft test section, the supersonic flow's Mach number decreases with decreasing test section area, whereas the subsonic flow Mach number increases slightly with the decreasing area.

To predict the approximate local Mach number within the TSTA ranges specified in Table IV, the calibrated test section Mach number, M_{ts}, can be adjusted by adding the product of the distance in inches downstream of the average TSTA (see Table IV) and the Mach number gradient value (see Table IV) for the corresponding flexwall setting. If the region of interest is upstream of the average TSTA from Table IV, the distance value would be negative when estimating local Mach number. For example, the Mach number at TSTA 65.24, 10 in. upstream of the average TSTA from Table IV, is approximately 0.005 Mach greater than the calibrated Mach number for a flexwall Mach number of 2.0.

6.3.1 Balance Chamber Pressure and Supersonic Strut Height Variation Investigations

Balance chamber pressure is one of the primary controls for transonic test section testing in the 8×6 SWT and can be used to slightly alter the average flow conditions in the porous test section. When models or model support hardware change orientation or blockage levels in the porous test section balance chamber pressure and thus average flow conditions can be affected. For these reasons, the sensitivity of supersonic test section conditions to balance chamber pressure fluctuations needed to be investigated, whether through adjustment of the exhaust control valve in the lower balance chamber or varying supersonic strut height.

With the 4-inch-diameter cone cylinder in its aft positon, the balance chamber pressure was varied at each nominal flexwall setting by varying the lower balance chamber exhaust control valve position. In the porous test section, variations in the balance chamber exhaust valve caused obvious and significant changes to the pressure measurements along the cone cylinder model (Ref. 2). Little to no effect from the balance chamber was sensed by even the aft-most cylinder static taps (TSTA 114.14) during the supersonic test section characterization.

The supersonic strut, upon which the 4-inch-diameter cone cylinder was mounted, was moved from 1 ft below centerline back to centerline and vice versa to assess the effects of this movement on facility measurements, particularly balance chamber and supersonic test section ceiling static pressures. This strut movement was completed at flexwall settings of Mach 1.4 and 1.5. Figure 31 and Figure 32 show the effect of strut height increase on the balance chamber and the average static pressure across the six ceiling static pressures at TSTA 17, also referred to as "row 1." The rise in balance chamber pressure seen around 5 to 15 s in these figures results in no significant static pressure change at row 1. Based on results of these two investigations, there is little to no effect on the supersonic test section conditions from balance chamber pressure fluctuations, whether caused by model or strut blockage changes or balance chamber exhaust control valve movement.

6.4 Transonic Array

The total pressure ratio distributions across the 8- by 6-ft supersonic test section at the pressure probe tips (near TSTA 44.25) at centerline and 1 ft above and below centerline are shown in Figure 33 to Figure 54. The freestream total pressure at each pressure probe, $P_{T,\text{array}}$, is normalized by the calibrated test section total pressure, $P_{T,ts}$, to remove temporal variation. The freestream local Mach number at each pressure probe on the array is calculated using the Rayleigh pitot formula, the measured total pressure

behind a normal shock at each probe, $P_{T,2}$, and the calibrated test section static pressure, $P_{S,ts}$, as discussed in the data reduction section. The freestream total pressure at each probe is calculated using isentropic relations, the local Mach number, and $P_{S,ts}$ (Ref. 7). The total pressure ratio data at a flexwall setting of Mach 1.3 at 1 ft above centerline was omitted because the supersonic test section was subsonic at that data point (see Subsection 6.2). Total pressure data are not shown for a flexwall setting of Mach 1.1 or 1.2 for the same reason. Subsonic total pressure ratio data are shown in Figure 48 to Figure 54, however, the local array total pressure is simply the measured pitot pressure.

Similarly, the freestream Mach number ratio distributions across the 8- by 6-ft supersonic test section are shown in Figure 55 to Figure 76 where the local freestream Mach number at each probe, M_{array}, is normalized by the calibrated test section Mach number, M_{ts}. For the same reasons as those listed previously, Mach number data at a flexwall setting of Mach 1.3 at 1 ft above centerline and flexwall settings of Mach 1.2 and 1.1 were omitted. For subsonic Mach number ratio data in Figure 70 to Figure 76, the local array Mach number is computed using isentropic relations, measured pitot pressure, and calibrated test section static pressure, $P_{S,ts}$ (Ref. 7). Because a constant static pressure is used to compute the local freestream total pressure and Mach number at the array probes, the profiles are very similar between the total pressure ratio and Mach number ratio distributions. The Mach number spatial variation in the core of the test section[11] at a flexwall setting of Mach 2.0 is about 0.012 and shows the deficit at centerline from the flow separation off the compressor exit tailcone as seen in previous entries (Ref. 1). Other flexwall settings exhibited smaller spatial Mach number variation; typical variation at other supersonic operating conditions was between 0.003 and 0.010 Mach, even at the off-nominal flexwall settings where nonuniformities were suspected. Subsonic operating condition Mach number spatial variations were less than 0.001.

As there was no significant influence from balance chamber pressure fluctuations on the static pressure along the cone cylinder model, this type of investigation was not conducted with the transonic array. In hindsight, the supersonic strut height variation (i.e., blockage change) investigations should have been conducted near Mach 1.3 and/or 1.4 with the transonic array installed to better understand this effect on supersonic test section starting characteristics.

The total temperature ratio distributions across the 8- by 6-ft supersonic test section are shown in Figure 77 to Figure 98 where the local total temperature, $T_{T,array}$, is normalized by the calibrated test section total temperature, $T_{T,ts}$. The array thermocouple measurements at local array Mach numbers, M_{array}, less than Mach 0.8 are corrected for thermal recovery. Total temperature ratio data at 1 ft above centerline were counterintuitively lower than that at the other two array heights at many of the Mach numbers surveyed. At flexwall settings of Mach 1.9 and 2.0, this counterintuitive trend applies to the data acquired at 1 ft below centerline as well; the temperature data at Mach 1.9 and 2.0 appears to have a trend with relatively colder flow being above centerline and warmer below. Thermocouple wires for the bellmouth rake and array total temperature measurement were not disconnected from the reference junction between vertical height changes of the array. In Reference 2, data from the 2019 characterization test entry show similar temperature trends, thus removing the uniqueness of the array installation in the supersonic test section from the potential causes for this gradient. The cause of this temperature gradient measured by the array is unknown at this time and the cause of this flow feature would be purely speculation by the test engineer.[12]

[11]The core of the test section is considered the area surveyed by the center seven array probes, whether pressure or temperature probes, during the 2020 test entry.

[12]Investigations were conducted related to thermal-soaking differences prior to data acquisition across run days and ambient temperature differences on run days, however, no trends matching the total temperature distribution were observed.

The lateral gradient in total temperature observed at high supersonic Mach numbers (Mach 1.9 and 2.0) in past characterization tests (Ref. 1) was much less pronounced during this test entry, likely due to some of the changes to the tunnel loop from the Acoustic Improvement Modifications project. At all other Mach numbers, supersonic (Mach 1.8 and less) and subsonic, the flow at the center of the test section appeared relatively warmer than the flow near the tunnel walls. When considering the data from 1 ft above centerline, the typical temperature variation across the core of the test section is on the order of 2.5 to 4.0 °F, however, when the suspect data at 1 ft above centerline is neglected, that spatial variation is reduced to 1.5 °F or less in most cases.

The flow angle distributions in the 8- by 6-ft supersonic test section are shown in Figure 99 to Figure 120. The corrected pitch, α_{corr}, and yaw, β_{corr}, flow angles at the array five-hole flow angle probes are corrected by prerun measurements of the array and pretest probe misalignment measurements, as discussed in the Section 4.1. Nearly all corrected flow angles were less than 0.50° at all Mach numbers surveyed and, in some cases, flow angles were much less than 0.50°. These are very similar levels of flow angularity as those observed in previous transonic test section characterization test entries and are attributed to the presence of the compressor upstream of the test section (Ref. 1).

6.5 Calibration Models for Determining Test Section Operating Conditions

One of the primary objectives of the supersonic test section characterization entry was to provide calibration relationships for determining test section operating conditions in this region of the tunnel. These calibration relationships relate measured test section flow parameters during the characterization test entry to facility instrumentation measurements. Only calibration relationships for the supersonic test section, referred to as "test section configuration (TSCFG) 7", are discussed in the following information. The supersonic test section calibration relationships, generated only from 2020 test entry data, cover three-drive-motor operation (Mach 0.40 to 2.0) in the 8×6 SWT. This section will describe the required inputs, outputs, calibration routines, and additional test section flow parameter calculations. The information in this section was used to modify the facility data system's subroutine (CAL8X6) used in all data collection programs to compute test section conditions.

The inputs to the calibration relationships are listed as follows:

- Bellmouth total pressure (psia), $P_{T,bm}$: average of eight bellmouth total pressure measurements, $P_{T,bm}$(i), i = 1 to 8; there are four pressures on the north and four on the south bellmouth rake.
- Bellmouth total temperature (R), $T_{T,bm}$: average of four bellmouth total temperature measurements, $T_{T,bm}$(i), i = 1 to 4; there are two thermocouple probes (type-E special-limit-of-error wire) per bellmouth rake.[13]
- Row 1 static pressure (psia), $P_{S,\text{row1},avg}$: average of six ceiling static pressures at row 1, $P_{S,\text{row1}}$(i), i = 1 to 6; row 1 is a lateral row of ceiling static pressure taps in the 8- by 6-ft supersonic test section at TSTA 17.0.
- Flexwall camshaft angle (degrees), FLEX: rotational angle of the camshaft, which controls the flexible-wall nozzle contour upstream of the 8- by 6-ft test section.
- Test section configuration, TSCFG:
  - TSCFG = 1 for the 14-ft, 5.8-percent porosity
  - TSCFG = 2 for the 8-ft, 6.2-percent porosity
  - TSCFG = 3 for the 8-ft, 3.1-percent porosity

[13]One of the four thermocouple measurements on the bellmouth rakes is used for the facility control system and is "coded out" in the facility data system.

- TSCFG = 4 for the 8-ft, 6.2-percent modified porosity
- TSCFG = 5 for the 8-ft, 3.1-percent modified porosity
- TSCFG = 6 for the 14-ft schlieren porosity
- TSCFG = 7 for the supersonic test section with the transonic test section configured for an 8-ft, 6.2-percent porosity

The calibration relationships were based on data collected with the 4-inch-diameter cone cylinder and transonic array. To avoid a bias between the cone cylinder's upstream (TSTA –4.0) and downstream (TSTA 29.8) data sets, the average cylinder pressure data from the cone cylinder were averaged across repeats of conditions at a given position of the model and then data from both model positions were averaged. The average cylinder static pressure on the 4-inch-diameter cone cylinder was chosen to represent $P_{S,ts}$. Data acquired at tunnel centerline with the transonic array were used to create the test section total pressure ($P_{T,ts}$ or $P_{T,2}$) and total temperature ($T_{T,ts}$) calibration relationships. Stagnation pressure and temperature data were averaged across the center seven probe locations on the array to obtain average test section conditions, $P_{T,avg}$ and $T_{T,avg}$, respectively, for use in the regression models. At supersonic conditions, the array produces the average total pressure behind a normal shock, $P_{T,2,avg}$.

In the transonic test section, a ratio of balance chamber to bellmouth total pressure is used as a key parameter in determining test section conditions (Refs. 1 and 2). In the supersonic test section, however, the balance chamber was shown to have little to no effect on flow conditions. The key parameter used in each of the calibration relationships for the supersonic test section is the ratio of average row 1 static to bellmouth total pressure:

$$R_{S,\mathrm{row1},bm} = P_{S,\mathrm{row1},avg} \,/\, P_{T,bm}$$

For supersonic conditions, regression models for both $P_{S,ts}$ and $P_{T,2}$ normalized by $P_{T,bm}$, were generated as a function of $R_{S,\mathrm{row1},bm}$ (Figure 121 and Figure 122).[14] The residuals produced for the $P_{T,2}$ regression model were typically larger than the scatter between repeat points at a given flexwall Mach number setting. Additionally, it was decided to communicate the average static pressure within the supersonic test section rather than a local value dependent upon axial station. The streamwise pressure gradient information in this report should be consulted for further refinement of local Mach number estimates. The observation of the $P_{T,2}$ residuals, the decision regarding reporting of $P_{S,ts}$, and the discrete manner in which supersonic conditions are obtained in the 8×6 SWT suggested that a lookup table approach for the surveyed flexwall settings be utilized for the two flow parameters. The regression models are still necessary as operators of the wind tunnel need flow condition feedback between the calibrated flexwall settings. The lookup tables for computing test section static pressure, $P_{S,ts}$, and total pressure behind a normal shock, $P_{T,2}$, in the supersonic test section are shown in Table V. Subsonic regression models are also shown in these figures (Figure 121 and Figure 122). In generating all the supersonic regression models, only data acquired at nominal flexwall settings (i.e., Mach 2.0, 1.9, 1.8, etc.) were used to ensure the models were evenly weighted; data from off-nominal flexwall settings were used as confirmation points in the residual analyses.

[14]The residuals in the supersonic static pressure regression only show two data points per flexwall setting as the repeats were averaged out prior to performing the regression to avoid biasing the model, as previously discussed.

TABLE V.—SUPERSONIC TEST SECTION STATIC PRESSURE AND TOTAL PRESSURE BEHIND NORMAL SHOCK WHEN OPERATING NEAR CALIBRATED FLEXWALL SETTINGS WITH SUPERSONIC FLOW IN SUPERSONIC TEST SECTION

[Test section static pressure data represented by data acquired on the cylinder of the 4-inch-diameter cone cylinder. Total pressure behind the normal shock represented by data acquired by the pressure probes on the transonic array at test section centerline. These values are related to Revision 7 of the computing requirements for the CAL8X6 subroutine dated August 4, 2020.]

Flexwall Mach number setting	Static pressure[a]		Total pressure[b]	
	Flexwall camshaft angle, FLEX, degree	$\frac{P_{S,ts}}{P_{T,bm}}$	Flexwall camshaft angle, FLEX, degree	$\frac{P_{T,2}}{P_{T,bm}}$
2.00	190.40	0.13274	190.39	0.72614
1.90	179.97	.15554	180.04	.77181
1.80	167.69	.18103	167.47	.81901
1.70	154.11	.21033	154.10	.86222
1.60	138.79	.24418	138.78	.90114
1.55	129.51	.26520	129.52	.92129
1.54	127.75	.26955	127.75	.92481
1.53	126.03	.27412	126.03	.92847
1.52	124.23	.27864	124.25	.93238
1.50	121.29	.28355	121.28	.93605
1.44	108.72	.31388	108.71	.95595
1.43	106.70	.31922	106.71	.95825
1.42	104.72	.32457	104.71	.96055
1.40	101.31	.32891	101.33	.96282
1.30	80.14	.37832	80.02	.98298
1.20	67.54	.39382	NA	NA

[a]$P_{S,ts}$ = test section static pressure. $P_{T,bm}$ = bellmouth total pressure.

[b]$P_{T,2}$ = total pressure behind a normal shock. $P_{T,bm}$ = bellmouth total pressure.

When (1) the flexwall camshaft angle is within a certain tolerance of a nominal flexwall camshaft angle shown in Table V[15] and (2) the supersonic test section is supersonic, as determined by $R_{S,\text{row1},bm} < 0.5283$, the following calculations are performed to compute $P_{S,ts}$ and $P_{T,2}$:

$$P_{S,ts} = P_{T,bm}\left(P_{S,ts} / P_{T,bm}\right)_{\text{lookup}}$$

$$P_{T,2} = P_{T,bm}\left(P_{T,2} / P_{T,bm}\right)_{\text{lookup}}$$

For supersonic conditions when the camshaft angle is not one of the calibrated flexwall settings in Table V, the following regression models are used to compute $P_{S,ts}$ and $P_{T,2}$:

[15]The flexwall camshaft angle tolerance is currently suggested to be ±0.75° from the nominal values in Table V, however, future operational considerations could cause this value to change.

$$P_{S,ts} = P_{T,bm}\left(A_{S,0} + A_{S,1}x + A_{S,2}x^2\right), \text{ where } x = R_{S,\text{row1},bm}$$

$$P_{T,2} = P_{T,bm}\left(B_{S,0} + B_{S,1}x + B_{S,2}x^2 + B_{S,3}x^3 + B_{S,4}x^4\right), \text{ where } x = R_{S,\text{row1},bm}$$

All coefficients for computing calibrated test section flow conditions are shown in Table VI. For the subsonic regression models shown in Figure 121 and Figure 122, use the following equations to compute the test section static and total pressure, $P_{S,ts}$ and $P_{T,ts}$, respectively:

$$P_{S,ts} = P_{T,bm}\left(A_0 + A_1x + A_2x^2 + A_3x^3\right), \text{ where } x = R_{S,\text{row1},bm}$$

$$P_{T,ts} = P_{T,bm}\left(B_0 + B_1x + B_2x^2\right), \text{ where } x = R_{S,\text{row1},bm}$$

TABLE VI.—SUPERSONIC TEST SECTION (TSCFG = 7) REGRESSION MODEL COEFFICIENTS FOR TEST SECTION STATIC ($P_{S,ts}$) AND TOTAL PRESSURE ($P_{T,ts}$), TOTAL PRESSURE BEHIND NORMAL SHOCK ($P_{T,2}$), AND TOTAL TEMPERATURE ($T_{T,ts}$) IN 8- BY 6-FOOT SUPERSONIC WIND TUNNEL

[Coefficients associated with regression models in Figure 121, Figure 122, and Figure 123. These coefficients are related to Revision 7 of the computing requirements for the CAL8X6 subroutine dated August 4, 2020.]

Flow parameter (speed regime)	Coefficient	Value
$P_{S,ts}$ (subsonic)	A_0	–0.13762443
	A_1	1.45052840
	A_2	–.49067542
	A_3	.17762299
$P_{S,ts}$ (supersonic)	$A_{S,0}$	–.00005287
	$A_{S,1}$	1.03278523
	$A_{S,2}$	–.03660058
$P_{T,ts}$ (subsonic)	B_0	.99902923
	B_1	.00155542
	B_2	–.00056255
$P_{T,2}$ (supersonic)	$B_{S,0}$	.25967999
	$B_{S,1}$	5.10861063
	$B_{S,2}$	–13.92598837
	$B_{S,3}$	17.98218677
	$B_{S,4}$	–9.14953772
$T_{T,ts}$ (subsonic)	C_0	.96750519
	C_1	.11368582
	C_2	–.08240644
$T_{T,ts}$ (supersonic)	$C_{S,0}$	.99012547
	$C_{S,1}$	.06822755
	$C_{S,2}$	–.07073262

The regression model for test section total temperature, $T_{T,ts}$, normalized by the bellmouth total temperature, $T_{T,bm}$, is shown in Figure 123. Note that the predictor variable is the same pressure ratio as used in the static and total pressure regression models. This formulation of the regression model is believed to account for the lack of a thermal recovery correction on the bellmouth thermocouples; the relationship between true total temperature and the bellmouth measurements is shown to change with the Mach number setting of the facility. Also, the day-to-day differences in ambient temperature are thought to be accounted for through the presence of bellmouth total temperature in the normalized response variable. Test section total temperature is computed for supersonic ($R_{S,\text{row1},bm} < 0.5283$) and subsonic ($R_{S,\text{row1},bm} > 0.5283$) conditions in the supersonic test section using the following equations:

$$T_{T,ts} = T_{T,bm}\left(C_{S,0} + C_{S,1}x + C_{S,2}x^2\right), \text{ where } x = R_{S,\text{row1},bm}$$

$$T_{T,ts} = T_{T,bm}\left(C_0 + C_1x + C_2x^2\right), \text{ where } x = R_{S,\text{row1},bm}$$

The calculation of test section Mach number (at subsonic and supersonic condition) total pressure at supersonic conditions are shown in Reference 1 as well as other flow parameters of interest (i.e., test section dynamic pressure, Reynolds number, etc.). A summary of the inputs and outputs for the computing requirements described in this section are shown in Table VII (other inputs and outputs are used for transonic test section configurations but not listed in Table VII, see Ref. 2 for omitted variables). A table of the typical operating conditions in the 8- by 6-ft supersonic test section, as computed using the data reduction process discussed in this section, is included in Table VIII.

As mentioned in previous sections, the flow in the supersonic test section was subsonic at a flexwall setting of Mach 1.1 with the 4-inch-diameter cone cylinder installed at a flexwall setting of Mach 1.1 and 1.2 with the transonic array at centerline. When the flexwall is set to Mach 1.2 in future tests, the subroutine will extrapolate the supersonic regression models for $P_{T,2}$ and $T_{T,ts}$. Similarly, at Mach 1.1, all three supersonic regression models will be extrapolated. Therefore, the supersonic test section is considered uncalibrated at flexwall settings of Mach 1.1 and 1.2. It has been a typical practice for the 8×6 SWT to calibrate only at the nominal flexwall settings (Mach 2.0 to 1.0 in 0.1 Mach increments) (Refs. 1 and 2). The test section flow field at off-nominal flexwall settings of Mach 1.42, 1.43, 1.44, 1.52, 1.53, 1.54, and 1.55 have been surveyed as thoroughly as each of the calibrated nominal flexwall positions in the supersonic test section. The repeatability of the off-nominal flexwall settings' flow conditions, as observed in the residual plots in Figure 121 to Figure 123, are near the same level as that of nominal flexwall settings.[16] Therefore, this subset of off-nominal flexwall settings are considered calibrated operational settings in the 8×6 SWT supersonic test section when in TSCFG 7.

[16]This note is an operational consideration for future testing at the set of off-nominal flexwall settings described in this report. The off-nominal flexwall settings were always performed moving the flexwall inward from the nearest, lower nominal flexwall setting. This practice is suggested by future tunnel users to attempt to maintain the same level of repeatability observed in this report at these off-nominal flexwall settings.

TABLE VII.—PARAMETERS USED TO DETERMINE TEST SECTION AEROTHERMAL CONDITIONS IN 8- BY 6-FOOT SUPERSONIC WIND TUNNEL SUPERSONIC TEST SECTION

Parameter	Data system program name	Description	Units	Source
Inputs—Facility measurements and operational settings				
$P_{T,bm}$	APTBM	Bellmouth total pressure	psia	Input
$P_{S,\mathrm{row1},avg}$	APSROW1	Average row 1 ceiling static pressure	psia	Input
$T_{T.bm}$	ATTBM	Bellmouth total temperature	°R	Input
FLEX	FLEX	Flexwall camshaft angle	Degree	Input
TSCFG	TSCFG	Test Section Configuration	None	Input
Test section conditions—calculated prior to calibrated flow parameters				
$R_{S,\mathrm{row1},bm}$	RSROW1BM	Ratio of average row 1 static to bellmouth total pressure	Dimensionless	Calculation
Test section conditions—calibrated flow parameters—subsonic (RSROW1BM > 0.5283)				
$P_{S,ts}$	PSTS	Test section static pressure	psia	Calibration
$P_{T,ts}$	PTTS	Test section total pressure	psia	Calibration
$T_{T,ts}$	TTTS	Test section total temperature	°R	Calibration
Test section conditions—calibrated flow parameters—supersonic (RSROW1BM < 0.5283)				
$P_{S,ts}$	PSTS	Test section static pressure	psia	Calibration
$P_{T,2}$	PTTS	Test section total pressure downstream of a normal shock	psia	Calibration
$T_{T,ts}$	TTTS	Test section total temperature	°R	Calibration
Test section conditions—calculations for supersonic flow only (RSROW1BM < 0.5283)				
$P_{T,ts}$	PTTS	Test section total pressure	psia	Calculation
Test section condition—calculated flow parameters				
M_{ts}	MTS	Test section Mach number	Dimensionless	Calculation
$T_{S,ts}$	TSTS	Test section static temperature	°R	Calculation
V_{ts}	VTS	Test section airspeed	ft/s	Calculation
ρ_{ts}	RHOTS	Test section air density	slugs/ft^3	Calculation
μ_{ts}	MUTS	Test section air viscosity	slugs/(ft s)	Calculation
Re_{ts}	REFT	Test section Reynolds number per foot	10^6/ft	Calculation
q_{ts}	QTS	Test section dynamic pressure	psia	Calculation
Constants and coefficients				
γ	GAMMA	Ratio of specific heats = 1.4	Dimensionless	Constant
R	R	Gas constant = 1716.49	lbf-ft/(slug°R)	Constant
	A0-A3	Subsonic static pressure calibration	Dimensionless	Calibration coefficients (Table VI)
	AS0-AS2	Supersonic static pressure calibration		
	B0-B2	Subsonic total pressure calibration		
	BS0-BS4	Supersonic total pressure calibration		
	C0-C2	Subsonic total temperature calibration		
	CS0-CS2	Supersonic total temperature calibration		

TABLE VIII.—TYPICAL SUPERSONIC TEST SECTION CONDITIONS IN 8- BY 6-FOOT SUPERSONIC WIND TUNNEL FOR TEST SECTION CONFIGURATION 7

[Three drive motors were used for all conditions; all values computed from facility measurements acquired during 4-inch-diameter cone cylinder runs during the January 2020 test entry.]

Nominal Mach number (wall setting)	Test section Mach number, M_{ts}	Test section total pressure, $P_{T,ts}$		Test section static pressure, $P_{S,ts}$		Test section dynamic pressure, q_{ts}		Test section total temperature, $T_{T,ts}$, R	Test section static temperature, $T_{S,ts}$, R	Reynolds number per unit length, 10^6/ft
		psia	psfa	psia	psfa	psia	psfa			
2.00	1.967	24.203	3,485.3	3.259	469.2	8.821	1,270.2	653.3	368.4	4.850
1.90	1.863	23.574	3,394.7	3.727	536.7	9.051	1,303.4	652.7	385.3	4.947
1.80	1.768	22.280	3,208.3	4.071	586.3	8.909	1,282.9	644.6	396.6	4.935
1.70	1.671	21.165	3,047.8	4.480	645.1	8.755	1,260.7	631.9	405.5	4.983
1.60	1.571	20.059	2,888.5	4.922	708.8	8.509	1,225.3	623.8	417.5	4.953
1.55	1.516	19.616	2,824.7	5.221	751.8	8.399	1,209.5	620.1	424.8	4.953
1.54	1.505	19.478	2,804.9	5.270	758.9	8.352	1,202.7	619.1	426.1	4.942
1.53	1.493	19.400	2,793.6	5.338	768.7	8.330	1,199.5	618.2	427.6	4.945
1.52	1.482	19.241	2,770.7	5.378	774.5	8.270	1,190.9	617.3	428.8	4.927
1.50	1.470	19.075	2,746.8	5.426	781.3	8.207	1,181.9	616.8	430.7	4.902
1.44	1.399	18.578	2,675.2	5.847	841.9	8.010	1,153.4	609.1XX	437.8	4.921
1.43	1.386	18.453	2,657.3	5.911	851.1	7.953	1,145.2	608.5	439.5	4.904
1.42	1.374	18.331	2,639.7	5.974	860.2	7.895	1,136.9	607.9	441.3	4.887
1.40	1.365	18.235	2,625.8	6.021	867.0	7.849	1,130.2	610.0	444.5	4.846
1.30	1.263	17.867	2,572.8	6.774	975.5	7.570	1,090.1	602.9	457.0	4.868
1.20[a]	1.234	17.653	2,542.0	6.957	1,001.9	7.421	1,068.7	601.4	460.9	4.830
1.10[a]	.875	17.345	2,497.7	10.534	1,517.0	5.646	813.0	598.2	518.8	4.451
1.00	.840	17.346	2,497.8	10.930	1,574.0	5.396	777.0	598.8	524.8	4.368
1.00	.817	17.382	2,502.9	11.208	1,614.0	5.239	754.5	598.6	528.1	4.324
1.00	.758	17.634	2,539.3	12.049	1,735.0	4.848	698.1	599.6	537.7	4.214
1.00	.670	17.860	2,571.9	13.217	1,903.2	4.156	598.4	598.1	548.8	3.983
1.00	.584	17.818	2,565.8	14.146	2,037.0	3.375	486.0	593.8	555.9	3.653
1.00	.487	16.824	2,422.6	14.302	2,059.5	2.377	342.4	579.2	552.9	3.103
1.00	.395	16.712	2,406.5	15.005	2,160.7	1.641	236.4	571.9	554.6	2.632

[a]Not considered calibrated due to calibration regression model extrapolation of total pressure and temperature at Mach 1.2 and of total and static pressure and total temperature at Mach 1.1.

7.0 Summary of Results

The following is a summary of the primary results from this test entry specifically related to the objectives stated in this report:

1. The 8×6 SWT solid-wall supersonic test section is calibrated at flexwall settings of Mach 1.3 to 2.0 in 0.1 increments and 1.42 to 1.44 and 1.52 to 1.55 in 0.01 increments. There is a lack of supersonic total pressure and temperature calibration data at a flexwall setting of Mach 1.2 and no supersonic calibration data at a flexwall setting of Mach 1.1. It is suggested that customers only use the flexwall settings listed above for supersonic operation in the supersonic test section. Subsonic three-drive-motor operation is also sufficiently calibrated to determine the average freestream flow conditions in the supersonic test section. The subroutine for calculating test section conditions in the supersonic test section has been modified with the regression models defined in this report.
2. Transonic array data were acquired at centerline and 1 ft above and below centerline to characterize the flow quality in this region of the tunnel, including total pressure, total temperature, and flow angularity.
    a. Total pressure and Mach number variation show very similar trends as static pressure is assumed constant across the array. Mach number variation in the core of the test section is about 0.012 Mach at a flexwall setting of 2.0. Variation levels are between 0.003 and 0.010 Mach at other supersonic operating conditions surveyed, even off-nominal flexwall settings. Subsonic Mach number variation is less than 0.001.
    b. Total temperature variation across the core of the test section is on the order of 1.5 °F (or 2.5 to 4.0 °F if suspect data is included). The temperature at the center of the test section is typically higher than the temperature nearer the tunnel walls at Mach numbers of 1.8 and less, including subsonic conditions. High supersonic Mach numbers displayed a relatively flat lateral temperature profile.
    c. The pitch and yaw flow angles across the test section are typically ±0.50° or less across the three-drive-motor operating range of the facility.
3. The 4-inch-diameter cone cylinder surveyed the supersonic test section with freestream measurements of static pressure over spans as far as TSTA 36.34 to 114.14. Due to shock interference on the aft end of the cylinder between Mach 1.6 and 1.2, the amount of data available to analyze was reduced with decreasing Mach number. Data from the two axial stations of the cone cylinder model were combined to determine average freestream static pressure and gradients, if statistically significant, of static pressure and Mach number. Mach number gradients at supersonic operating conditions were between 0.0001 and –0.0005 per inch and, at subsonic conditions, 0.0002 per inch or less.
4. Balance chamber pressure had a negligible effect on the supersonic test section centerline pressure profile as far aft as TSTA 114.14 between flexwall settings of Mach 1.2 and 2.0. Due to the lack of influence seen during cone cylinder testing, this investigation was not conducted with the transonic array installed. Balance chamber pressure is not included in the regression models for freestream parameters in the supersonic test section.
5. Off-nominal flexwall settings of Mach 1.42, 1.43, 1.44, 1.52, 1.53, 1.54, and 1.55 were surveyed as thoroughly as the nominal flexwall settings (Mach 2.0 to 1.1 in 0.1 Mach increments). The repeatability of freestream conditions at these off-nominal flexwall settings was found to be comparable to that of nominal flexwall settings.
6. Strut blockage changes, which affect balance chamber pressure levels, were found to be inconsequential to the supersonic test section conditions. However, the presence of increased blockage from the transonic array prevented acquisition of supersonic data with the flexwall set to Mach 1.2. Additionally, supersonic Mach 1.3 data could not be obtained with the array at 1 ft above centerline, likely due to increased blockage of the supersonic test section.

8.0 Concluding Remarks

A characterization test entry in the NASA Glenn Research Center 8- by 6-Foot Supersonic Wind Tunnel (8×6 SWT) solid-wall, supersonic test section was completed in January 2020. This entry provided data used to create calibration relationships for facility operation as well as an understanding of the flow field in the supersonic test section. The following are recommendations for future work or operational considerations per results of this test entry:

1. There is a general lack of turbulence data for the 8- by 6-ft test section (porous and solid-wall). The importance of this type of information to future facility customers should be investigated and, if appropriate, this measurement should be an objective and priority of a future characterization test entry of the 8×6 SWT.
2. To more fully understand the starting characteristics of the supersonic test section, supersonic strut height variations should be conducted nearer the limiting Mach numbers. For example, the investigation should be conducted with the 4-inch-diameter cone cylinder at a flexwall setting of Mach 1.2 and with the transonic array at centerline at Mach 1.3.
    a. Additionally, the supersonic strut axial location could be varied (i.e., further out of the porous region) during this investigation. The proximity of the supersonic strut to the porosity, or, in other words, ability of the facility's balance chamber to relieve the blockage of the strut, likely influences the ability of the supersonic test section to start.
3. Gathering axial pressure profile data is plagued by the reflected oblique shock waves generated from the 4-inch-diameter cone cylinder's cone tip. It is suggested that a new static pressure profile characterization tool be designed and fabricated for any future characterization of the 8×6 SWT, especially in the supersonic test section.
4. The aerothermal characterization testing in the 8×6 SWT should be a recurring activity with periodic checks of the calibration to ensure a stable and repeatable flow field for future customer testing.
5. Test customers for the 8×6 SWT should be briefed on tunnel operation and test section flow quality to make them aware of nuances of testing in this facility. For example, a flexwall Mach number setting of Mach 2.0 produces an average supersonic test section Mach number of 1.967. This trend of actual Mach number being less than nominal is present in both the porous and solid-wall test sections and across the supersonic operating range for each test section.

References

1. Arrington, E. Allen: Calibration of the NASA Glenn 8- by 6-Foot Supersonic Wind Tunnel (1996 and 1997 Tests). NASA/CR—2012-217270, 2012. https://ntrs.nasa.gov
2. Johnson, Aaron M.; and Rinehart, David A.: Characterization of the NASA Glenn 8- by 6-Foot Supersonic Wind Tunnel (2019 Test). NASA/CR-20205006102, 2020. https://ntrs.nasa.gov
3. Soeder, Ronald H.: NASA Lewis 8- by 6-Foot Supersonic Wind Tunnel User Manual. NASA TM–105771, 1993. https://ntrs.nasa.gov
4. Arrington, E. Allen; Pickett, Mark T.; and Soeder, Ronald H.: Baseline Calibration of the NASA Lewis Research Center 8- by 6-Foot Supersonic Wind Tunnel (1991 and 1992 Tests). NASA/TM—97-107431, 1998. Available from the NASA STI Program.
5. Swallow, Robert J.; and Aiello, Robert A.: NASA Lewis 8- by 6-Foot Supersonic Wind Tunnel. NASA TM X-71542, 1974. https://ntrs.nasa.gov
6. Pope, Alan: Wind Tunnel Testing. 2nd ed., John Wiley, New York, NY, 1954.
7. Ames Research Staff: Equations, Tables, and Charts for Compressible Flow. NACA–TR–1135, 1953. https://ntrs.nasa.gov

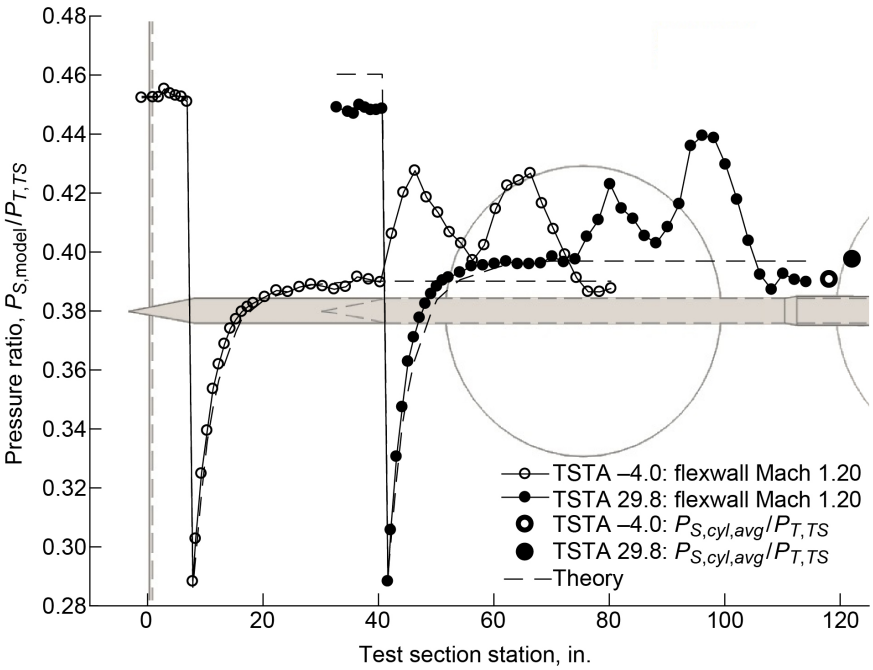

Figure 13.—Combined axial static pressure distributions along 4-inch-diameter cone cylinder with cone tip at both test section station (TSTA) –4.0 and 29.8 in the 8- by 6-ft test section. Data acquired during supersonic test section characterization (2020 test) at flexwall setting of Mach 1.20.

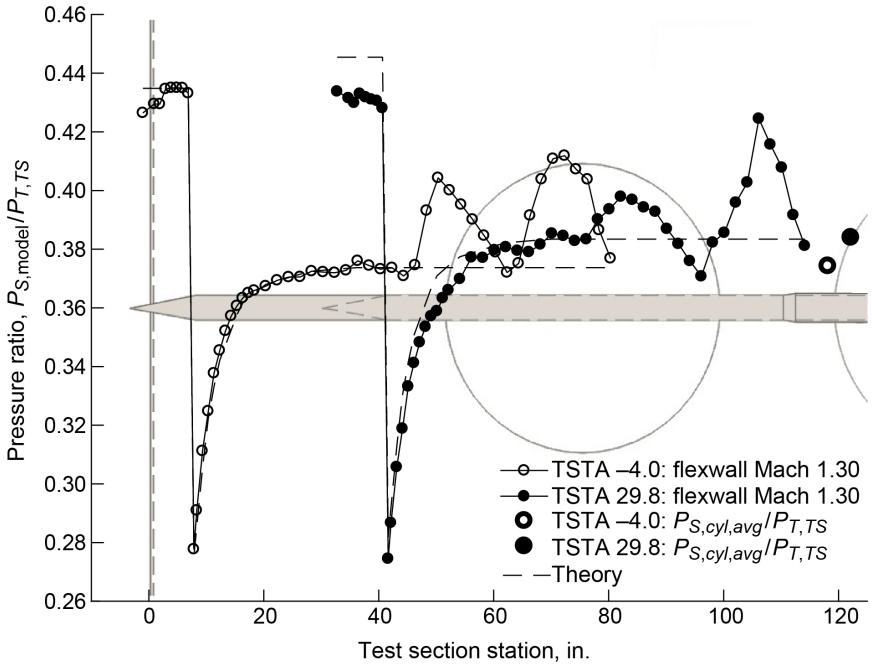

Figure 14.—Combined axial static pressure distributions along 4-inch-diameter cone cylinder with cone tip at both test section station (TSTA) –4.0 and 29.8 in the 8- by 6-ft test section. Data acquired during supersonic test section characterization (2020 test) at flexwall setting of Mach 1.30.

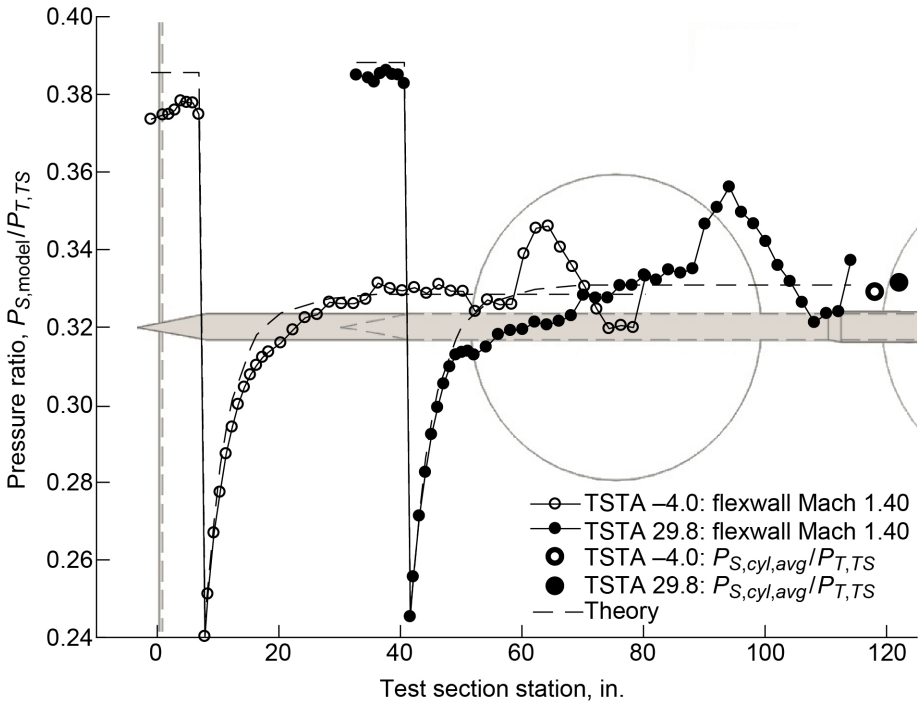

Figure 15.—Combined axial static pressure distributions along 4-inch-diameter cone cylinder with cone tip at both test section station (TSTA) –4.0 and 29.8 in the 8- by 6-ft test section. Data acquired during supersonic test section characterization (2020 test) at flexwall setting of Mach 1.40.

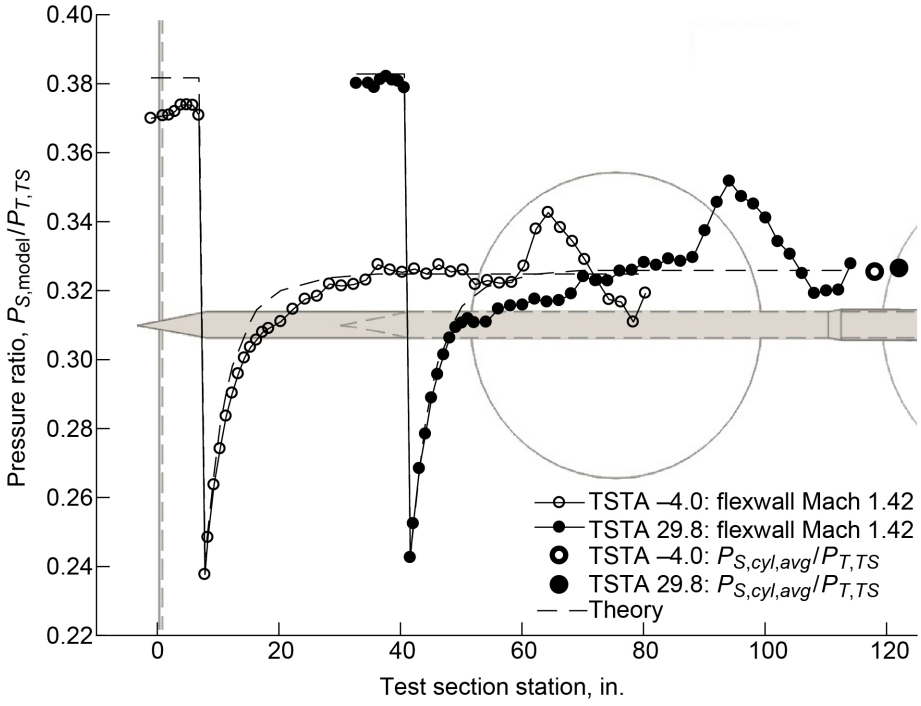

Figure 16.—Combined axial static pressure distributions along 4-inch-diameter cone cylinder with cone tip at both test section station (TSTA) –4.0 and 29.8 in the 8- by 6-ft test section. Data acquired during supersonic test section characterization (2020 test) at flexwall setting of Mach 1.42.

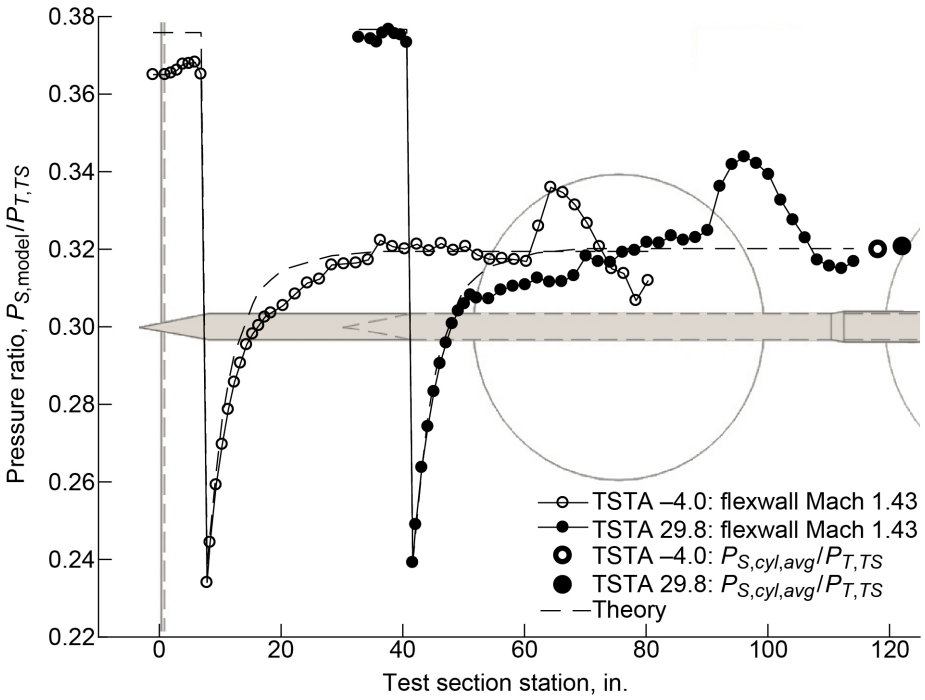

Figure 17.—Combined axial static pressure distributions along 4-inch-diameter cone cylinder with cone tip at both test section station (TSTA) –4.0 and 29.8 in the 8- by 6-ft test section. Data acquired during supersonic test section characterization (2020 test) at flexwall setting of Mach 1.43.

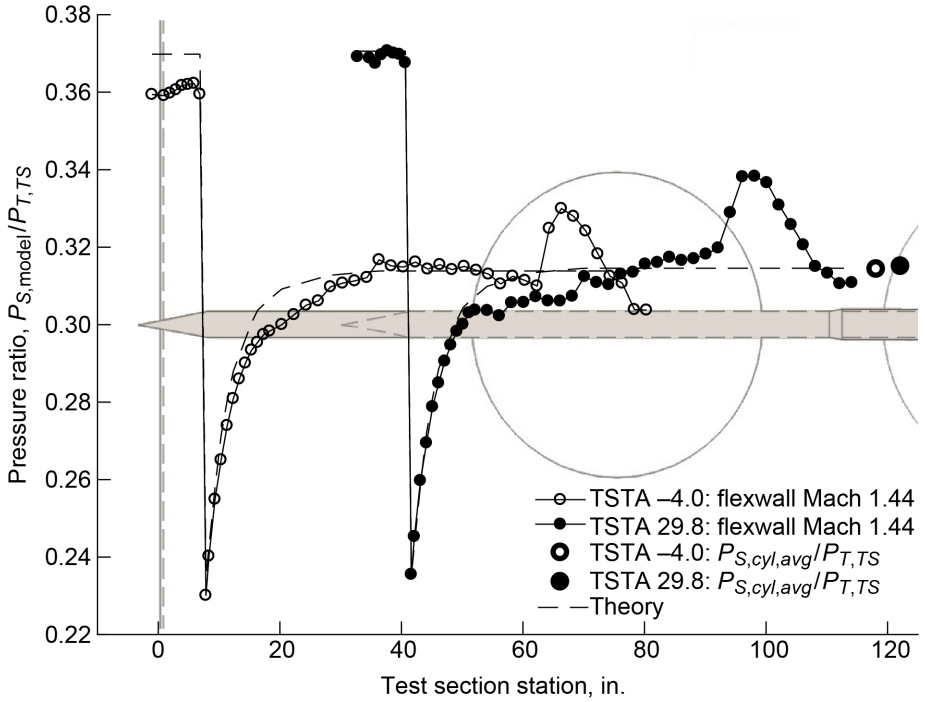

Figure 18.—Combined axial static pressure distributions along 4-inch-diameter cone cylinder with cone tip at both test section station (TSTA) –4.0 and 29.8 in the 8- by 6-ft test section. Data acquired during supersonic test section characterization (2020 test) at flexwall setting of Mach 1.44.

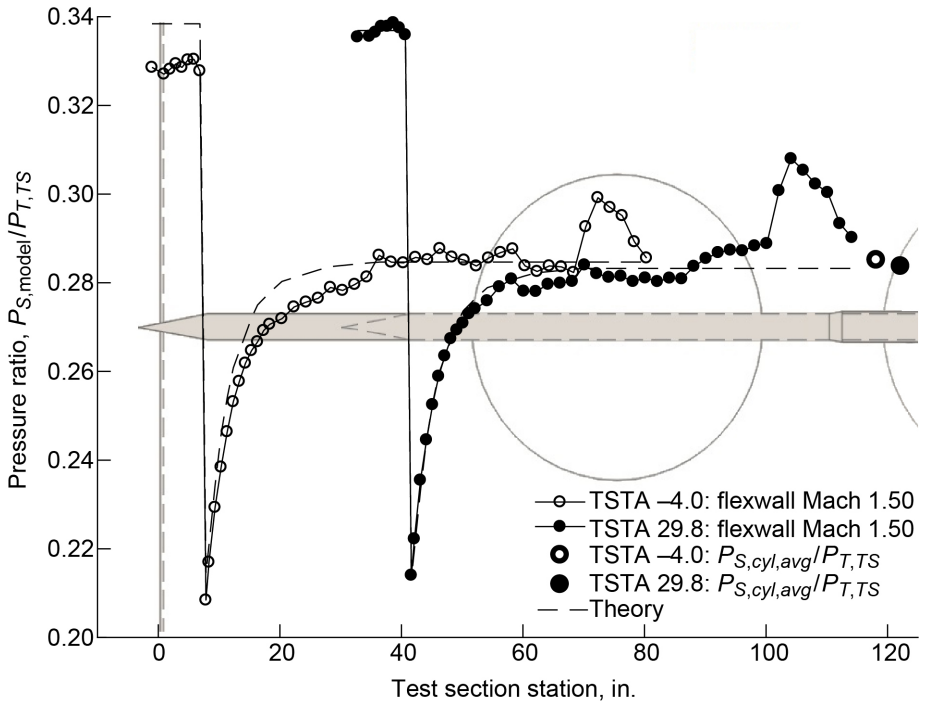

Figure 19.—Combined axial static pressure distributions along 4-inch-diameter cone cylinder with cone tip at both test section station (TSTA) –4.0 and 29.8 in the 8- by 6-ft test section. Data acquired during supersonic test section characterization (2020 test) at flexwall setting of Mach 1.50.

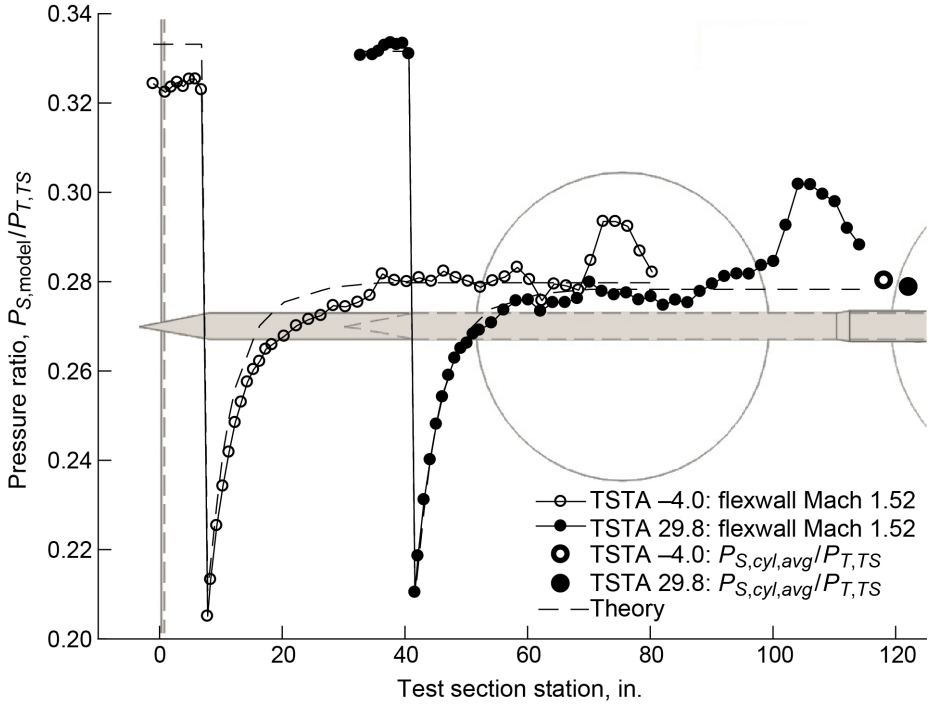

Figure 20.—Combined axial static pressure distributions along 4-inch-diameter cone cylinder with cone tip at both test section station (TSTA) –4.0 and 29.8 in the 8- by 6-ft test section. Data acquired during supersonic test section characterization (2020 test) at flexwall setting of Mach 1.52.

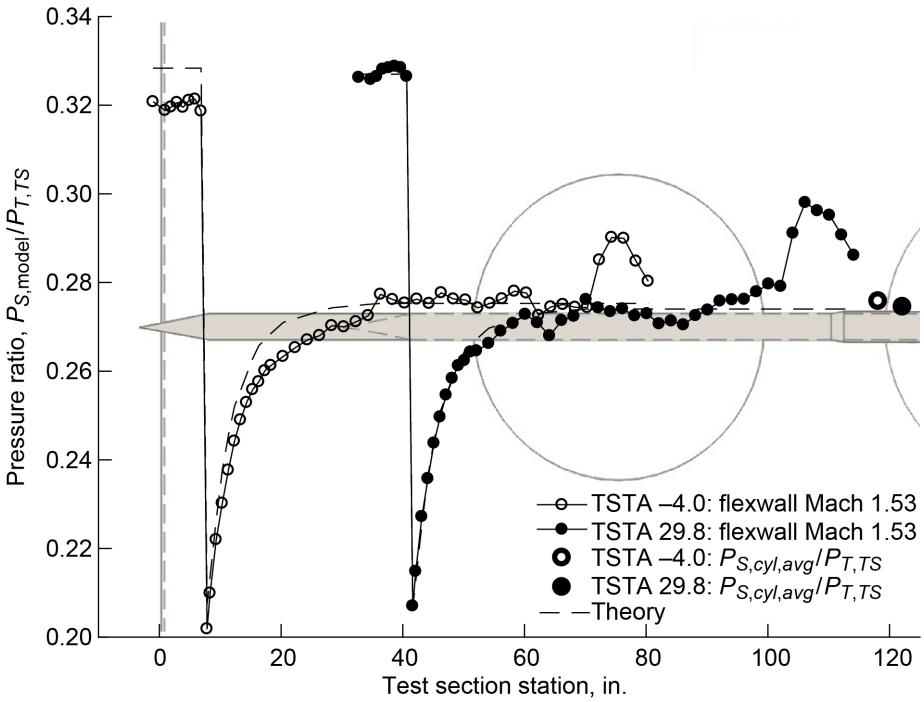

Figure 21.—Combined axial static pressure distributions along 4-inch-diameter cone cylinder with cone tip at both test section station (TSTA) –4.0 and 29.8 in the 8- by 6-ft test section. Data acquired during supersonic test section characterization (2020 test) at flexwall setting of Mach 1.53.

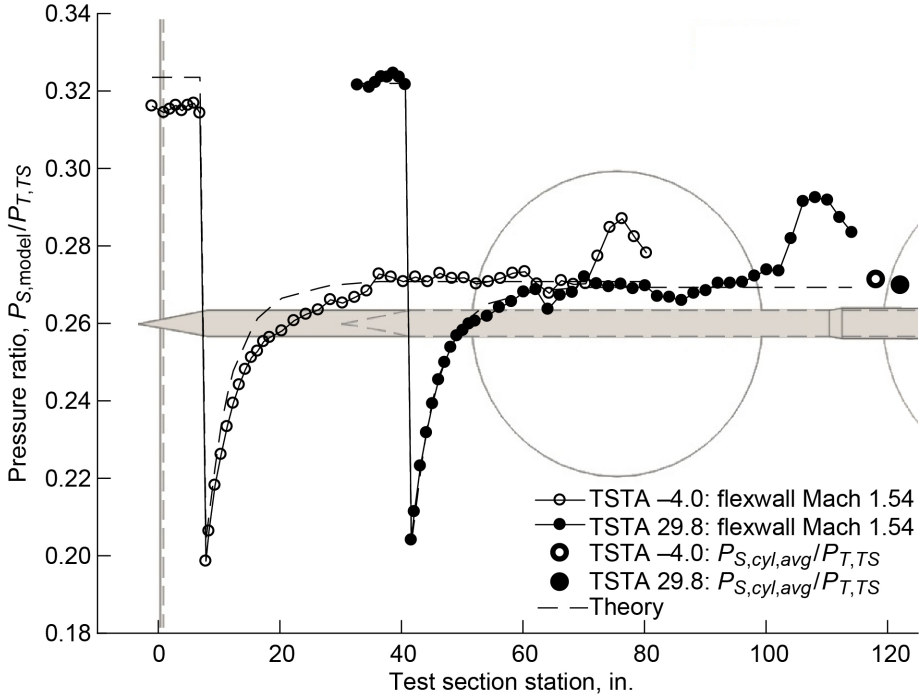

Figure 22.—Combined axial static pressure distributions along 4-inch-diameter cone cylinder with cone tip at both test section station (TSTA) –4.0 and 29.8 in the 8- by 6-ft test section. Data acquired during supersonic test section characterization (2020 test) at flexwall setting of Mach 1.54.

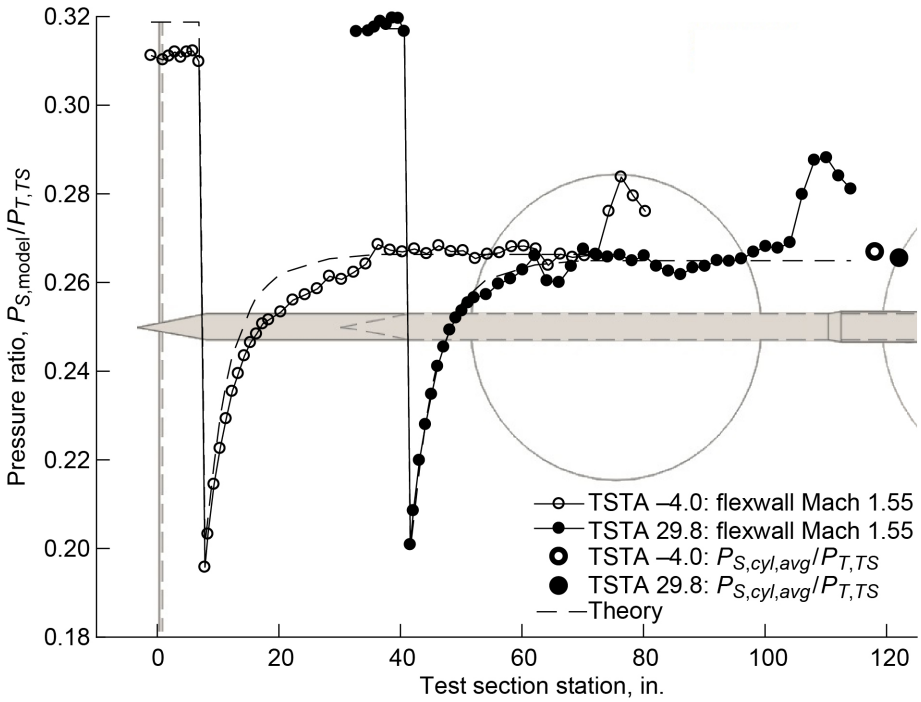

Figure 23.—Combined axial static pressure distributions along 4-inch-diameter cone cylinder with cone tip at both test section station (TSTA) –4.0 and 29.8 in the 8- by 6-ft test section. Data acquired during supersonic test section characterization (2020 test) at flexwall setting of Mach 1.55.

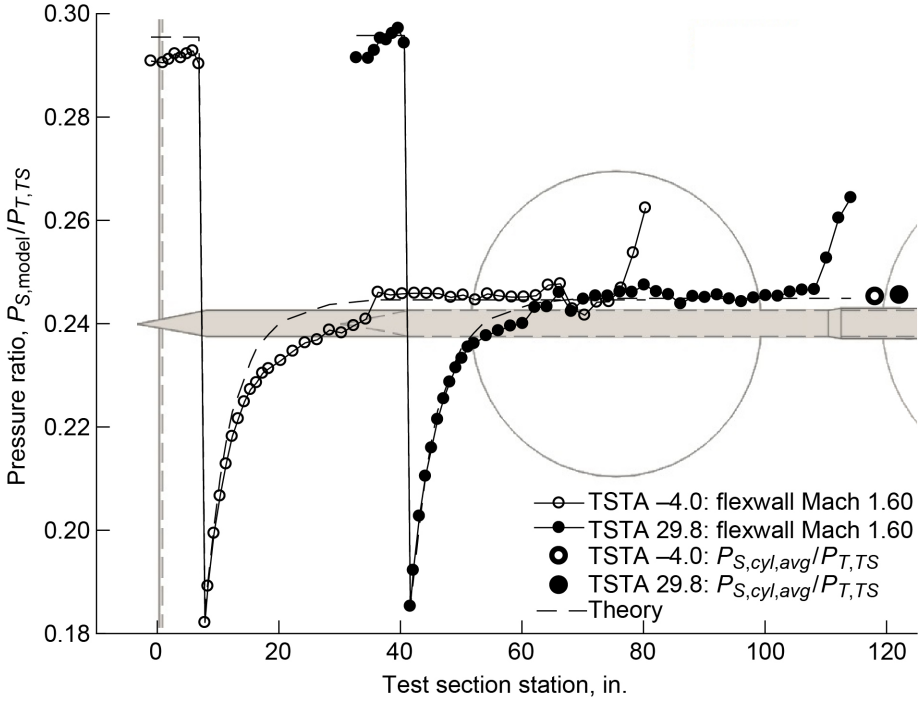

Figure 24.—Combined axial static pressure distributions along 4-inch-diameter cone cylinder with cone tip at both test section station (TSTA) –4.0 and 29.8 in the 8- by 6-ft test section. Data acquired during supersonic test section characterization (2020 test) at flexwall setting of Mach 1.60.

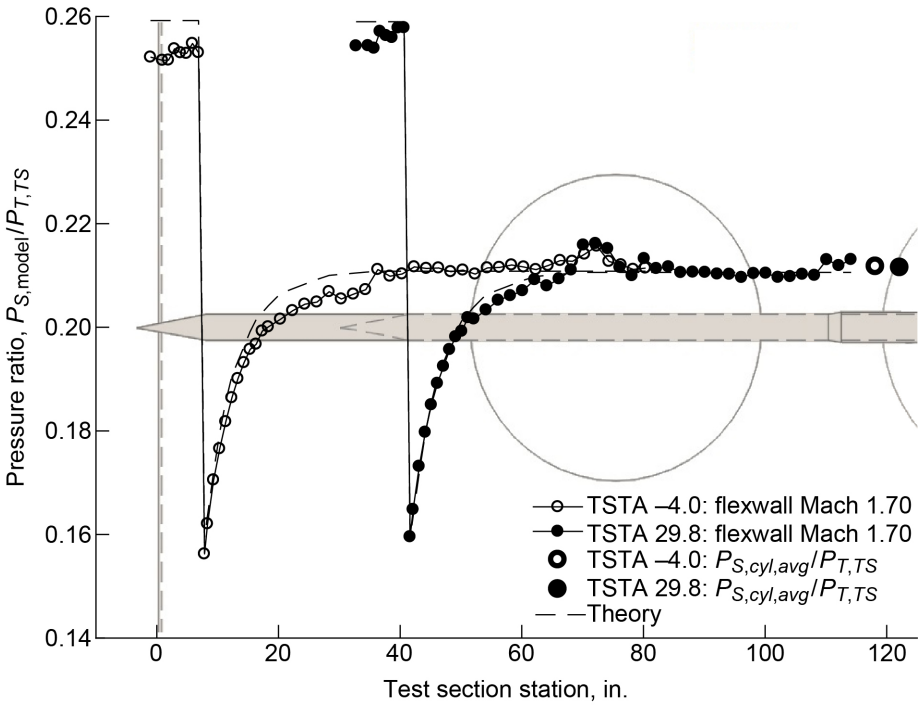

Figure 25.—Combined axial static pressure distributions along 4-inch-diameter cone cylinder with cone tip at both test section station (TSTA) –4.0 and 29.8 in the 8- by 6-ft test section. Data acquired during supersonic test section characterization (2020 test) at flexwall setting of Mach 1.70.

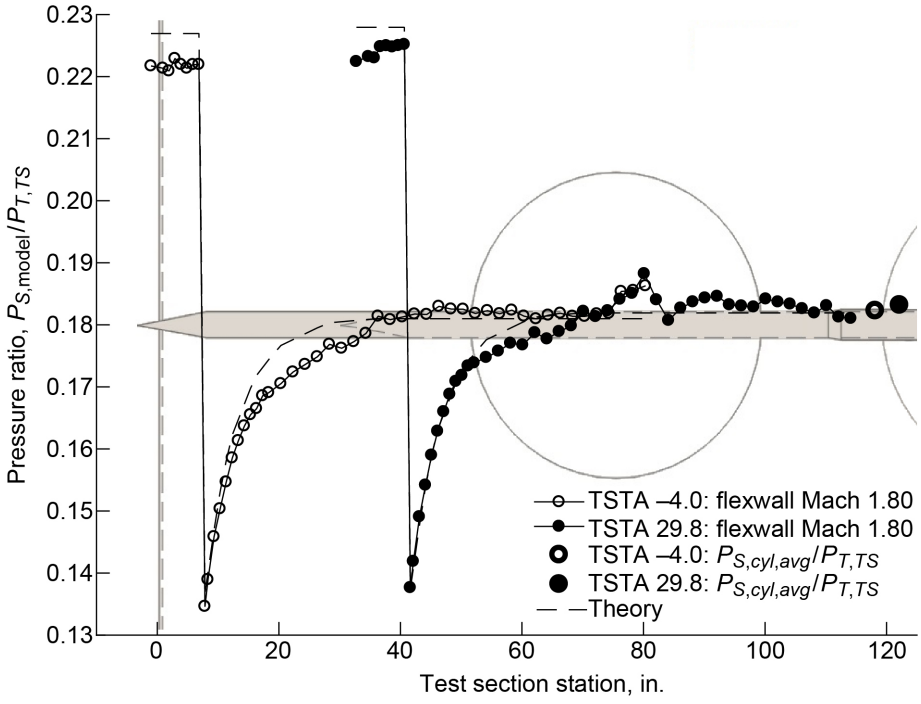

Figure 26.—Combined axial static pressure distributions along 4-inch-diameter cone cylinder with cone tip at both test section station (TSTA) –4.0 and 29.8 in the 8- by 6-ft test section. Data acquired during supersonic test section characterization (2020 test) at flexwall setting of Mach 1.80.

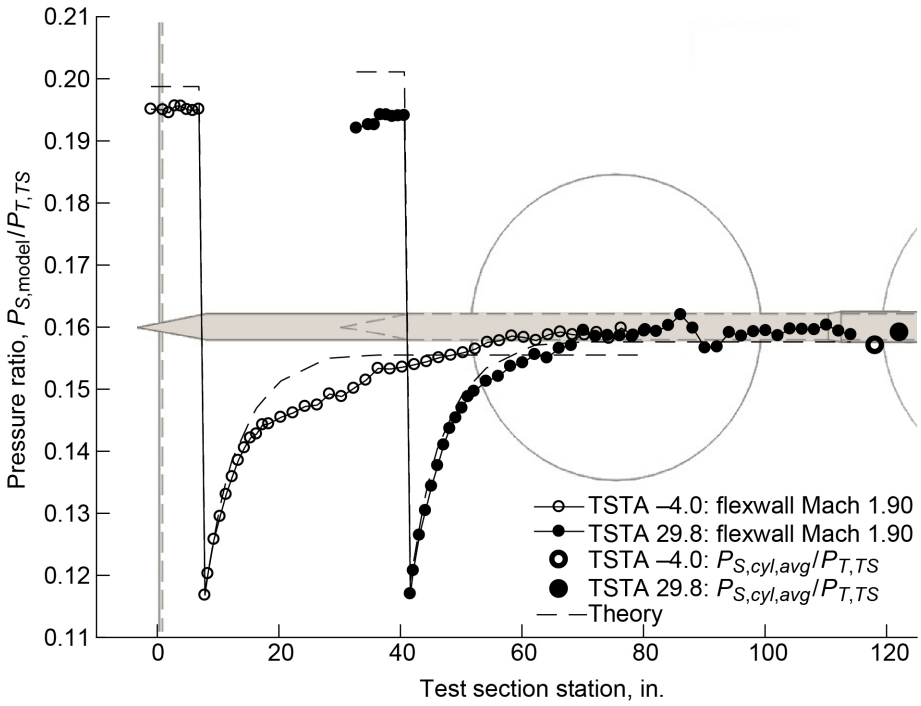

Figure 27.—Combined axial static pressure distributions along 4-inch-diameter cone cylinder with cone tip at both test section station (TSTA) –4.0 and 29.8 in the 8- by 6-ft test section. Data acquired during supersonic test section characterization (2020 test) at flexwall setting of Mach 1.90.

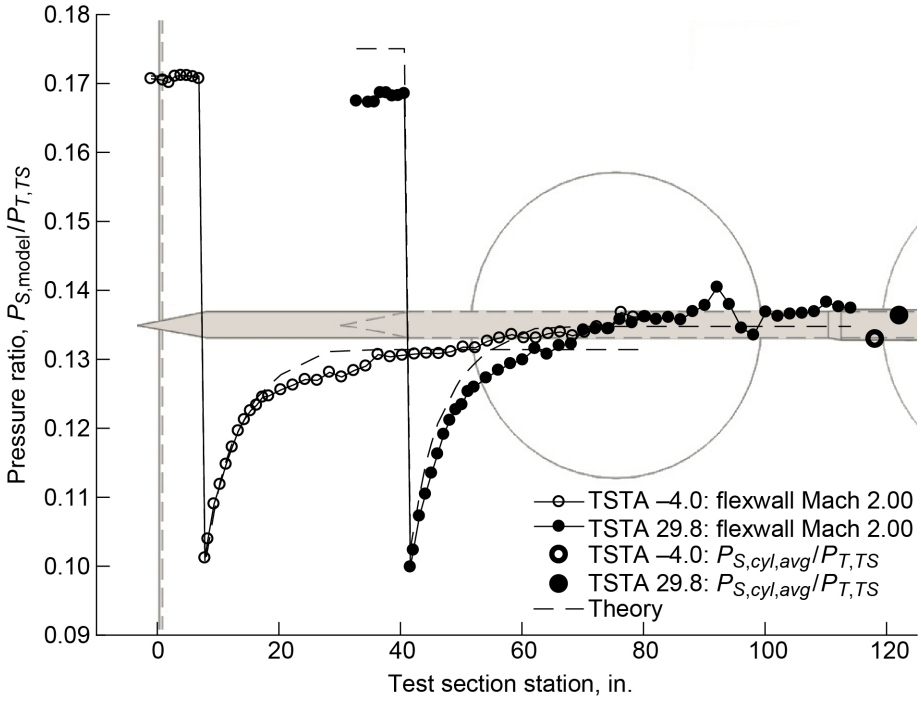

Figure 28.—Combined axial static pressure distributions along 4-inch-diameter cone cylinder with cone tip at both test section station (TSTA) –4.0 and 29.8 in the 8- by 6-ft test section. Data acquired during supersonic test section characterization (2020 test) at flexwall setting of Mach 2.00.

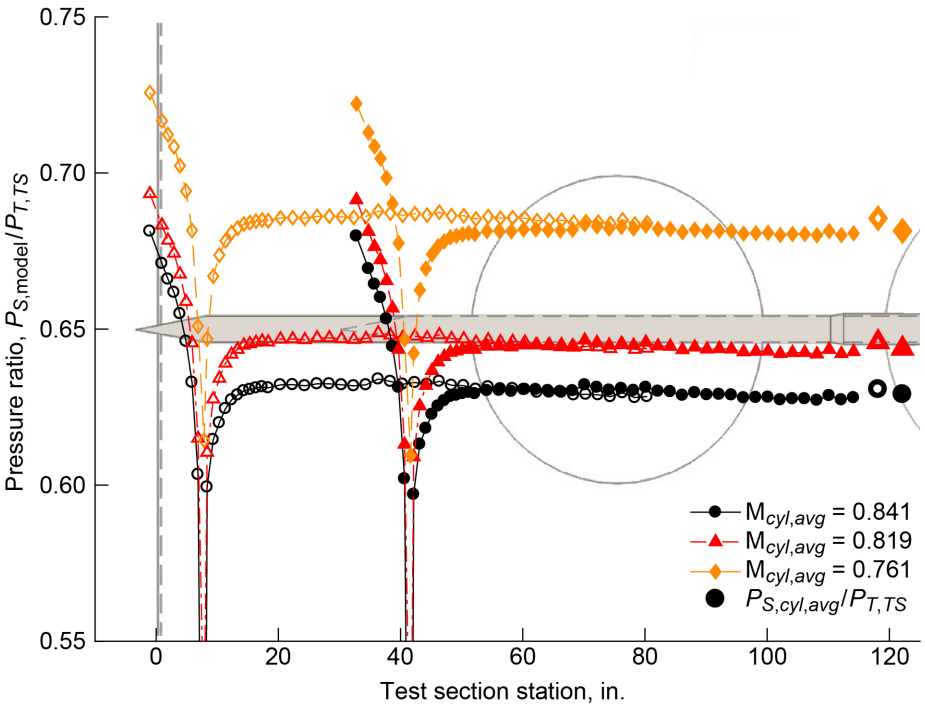

Figure 29.—Combined axial static pressure distributions along 4-inch-diameter cone cylinder with cone tip at both test section station –4.0 and 29.8 in 8- by 6-ft test section. Data acquired during supersonic test section characterization (2020 test) at subsonic conditions.

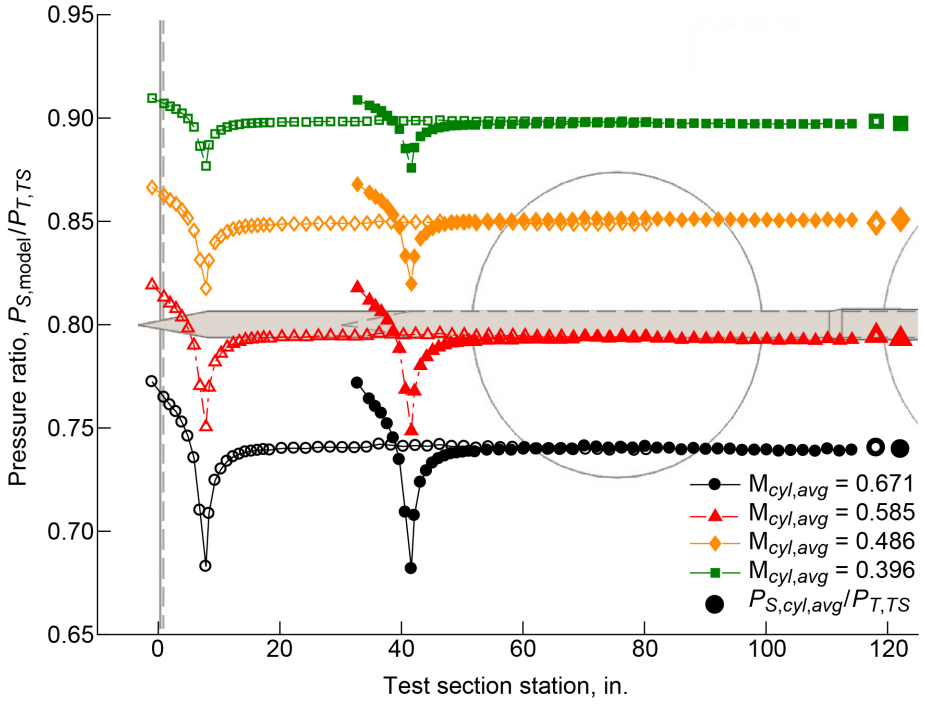

Figure 30.—Combined axial static pressure distributions along 4-inch-diameter cone cylinder with cone tip at both test section station –4.0 and 29.8 in 8- by 6-ft test section. Data acquired during supersonic test section characterization (2020 test) at subsonic conditions.

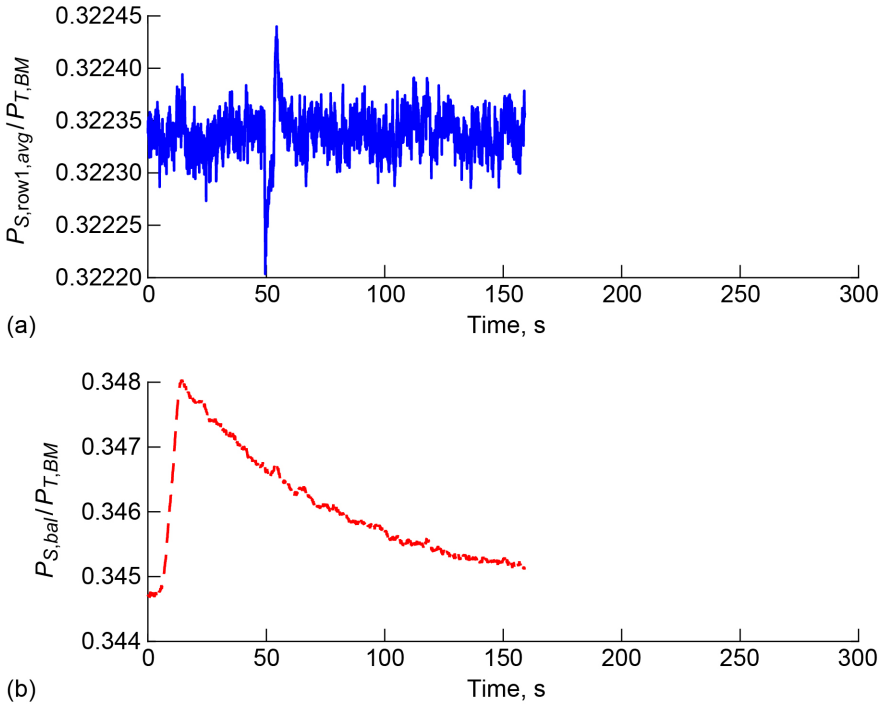

Figure 31.—Transient pressure data acquired from 8- by 6-Foot Supersonic Wind Tunnel balance chamber and average row 1 ceiling static pressure normalized by bellmouth total pressure during movement of the supersonic strut from 1 ft below centerline up to centerline. Strut movement occurs approximately between 5 and 15 s. The six row 1 ceiling static pressures are located at test section station (TSTA) 17.0. Data acquired during the 2020 supersonic test section characterization with the tip of the 4-in.-diameter cone cylinder at TSTA 29.8 at a flexwall setting of Mach 1.4. (a) 0.00005 = $\Delta P_{S,row1,avg}$ of 0.0009 psia. (b) 0.0010 = $\Delta P_{S,bal}$ of 0.0185 psia.

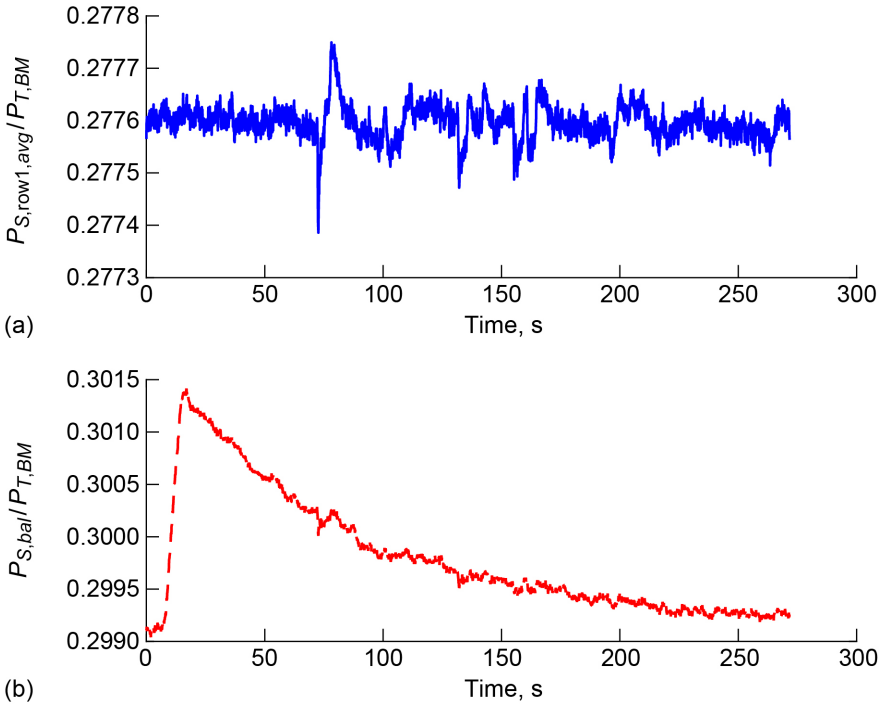

Figure 32.—Transient pressure data acquired from 8- by 6-Foot Supersonic Wind Tunnel balance chamber and average row 1 ceiling static pressure normalized by bellmouth total pressure during movement of supersonic strut from 1 ft below centerline up to centerline. Strut movement occurs approximately between 5 and 15 s. The six row 1 ceiling static pressures are located at test section station (TSTA) 17.0. Data acquired during the 2020 supersonic test section characterization with tip of 4-in.-diameter cone cylinder at TSTA 29.8 at flexwall setting of Mach 1.5. (a) 0.00010 = $\Delta P_{S,row1,avg}$ of 0.0019 psia. (b) 0.0005 = $\Delta P_{S,bal}$ of 0.0096 psia.

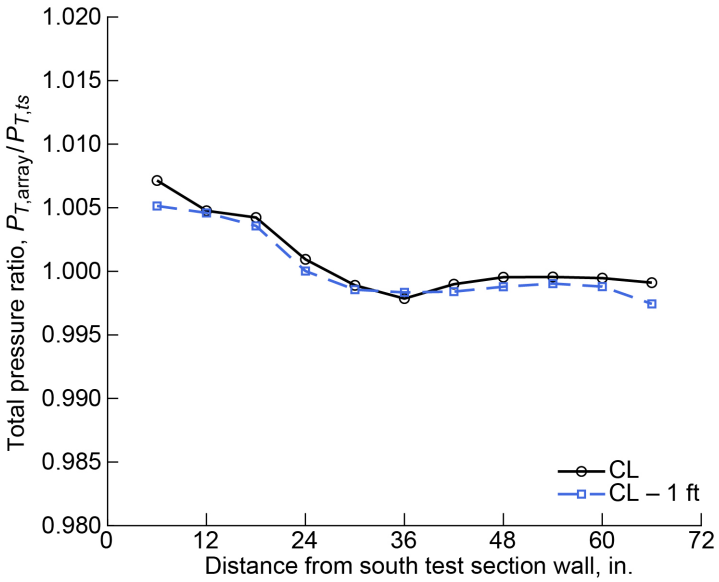

Figure 33.—Total pressure ratio distributions in 8- by 6-ft supersonic test section near test section station 44.25 at centerline (CL) and 1 ft below CL. Data acquired during supersonic test section characterization (2020 test) at flexwall setting of Mach 1.30; 0.005 = ΔP_T of 0.0878 psia.

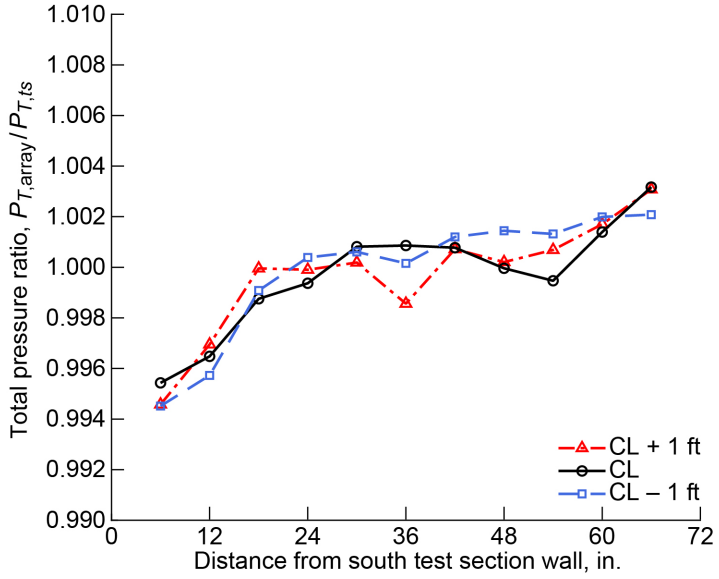

Figure 34.—Total pressure ratio distributions in 8- by 6-ft supersonic test section near test section station 44.25 at centerline (CL) and 1 ft above and below CL. Data acquired during supersonic test section characterization (2020 test) at flexwall setting of Mach 1.40; 0.002 = ΔP_T of 0.0362 psia.

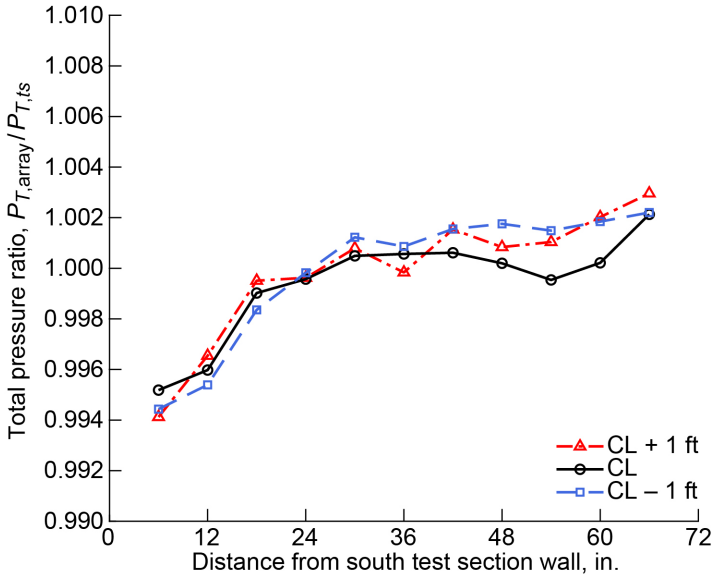

Figure 35.—Total pressure ratio distributions in 8- by 6-ft supersonic test section near test section station 44.25 at centerline (CL) and 1 ft above and below CL. Data acquired during supersonic test section characterization (2020 test) at flexwall setting of Mach 1.42; 0.002 = ΔP_T of 0.0363 psia.

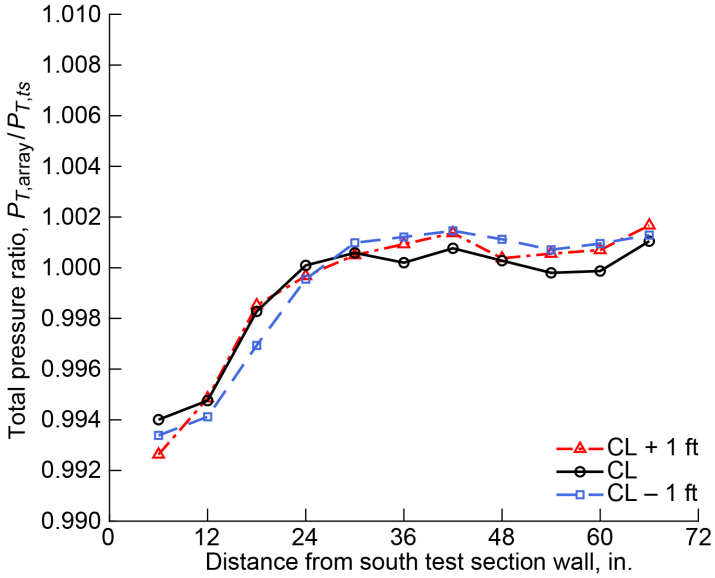

Figure 36.—Total pressure ratio distributions in 8- by 6-ft supersonic test section near test section station 44.25 at centerline (CL) and 1 ft above and below CL. Data acquired during supersonic test section characterization (2020 test) at flexwall setting of Mach 1.43; 0.002 = ΔP_T of 0.0366 psia.

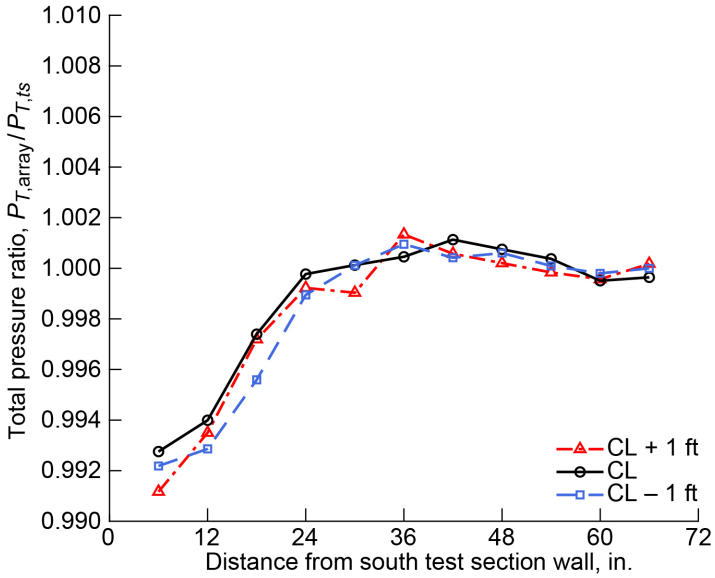

Figure 37.—Total pressure ratio distributions in 8- by 6-ft supersonic test section near test section station 44.25 at centerline (CL) and 1 ft above and below CL. Data acquired during supersonic test section characterization (2020 test) at flexwall setting of Mach 1.44; 0.002 = ΔP_T of 0.0368 psia.

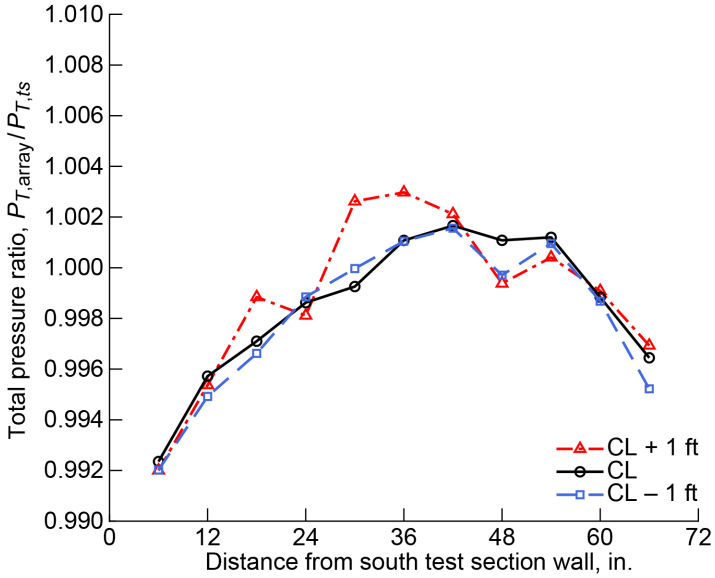

Figure 38.—Total pressure ratio distributions in 8- by 6-ft supersonic test section near test section station 44.25 at centerline (CL) and 1 ft above and below CL. Data acquired during supersonic test section characterization (2020 test) at flexwall setting of Mach 1.50; 0.002 = ΔP_T of 0.0382 psia.

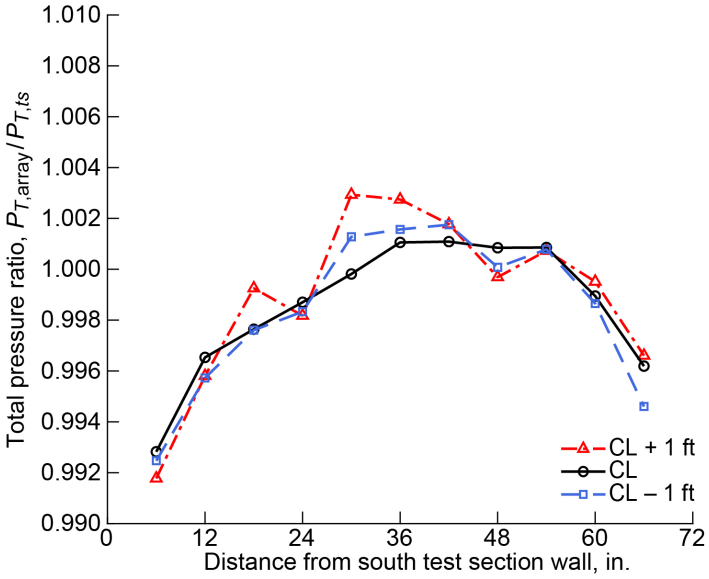

Figure 39.—Total pressure ratio distributions in 8- by 6-ft supersonic test section near test section station 44.25 at centerline (CL) and 1 ft above and below CL. Data acquired during supersonic test section characterization (2020 test) at flexwall setting of Mach 1.52; 0.002 = ΔP_T of 0.0384 psia.

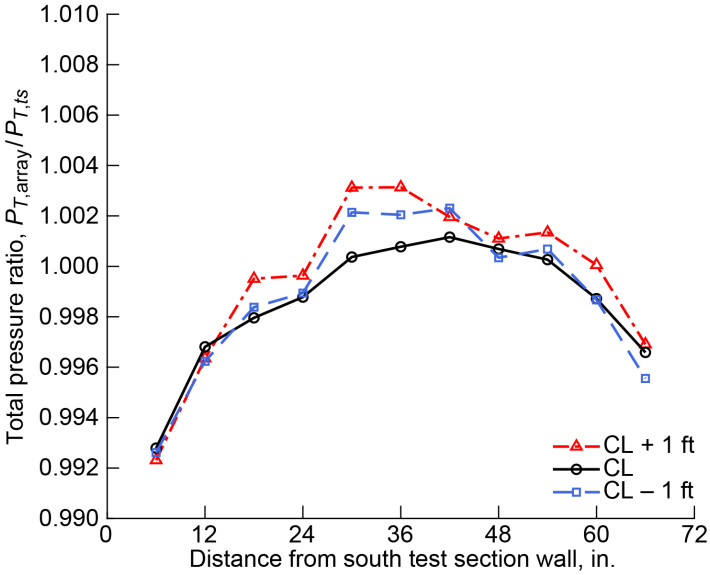

Figure 40.—Total pressure ratio distributions in 8- by 6-ft supersonic test section near test section station 44.25 at centerline (CL) and 1 ft above and below CL. Data acquired during supersonic test section characterization (2020 test) at flexwall setting of Mach 1.53; 0.002 = ΔP_T of 0.0387 psia.

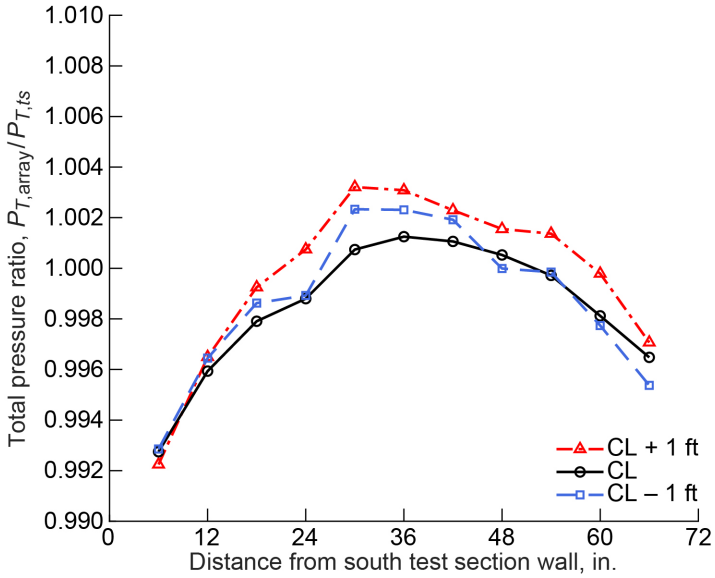

Figure 41.—Total pressure ratio distributions in 8- by 6-ft supersonic test section near test section station 44.25 at centerline (CL) and 1 ft above and below CL. Data acquired during supersonic test section characterization (2020 test) at flexwall setting of Mach 1.54; 0.002 = ΔP_T of 0.0389 psia.

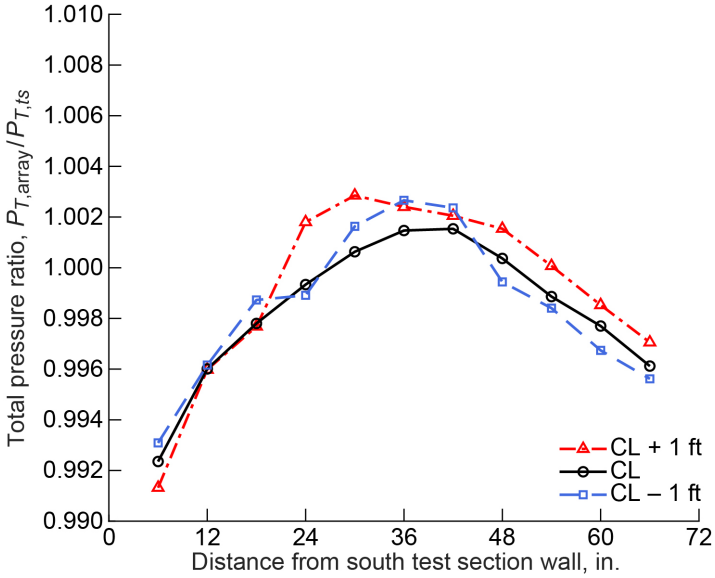

Figure 42.—Total pressure ratio distributions in 8- by 6-ft supersonic test section near test section station 44.25 at centerline (CL) and 1 ft above and below CL. Data acquired during supersonic test section characterization (2020 test) at flexwall setting of Mach 1.55; 0.002 = ΔP_T of 0.0392 psia.

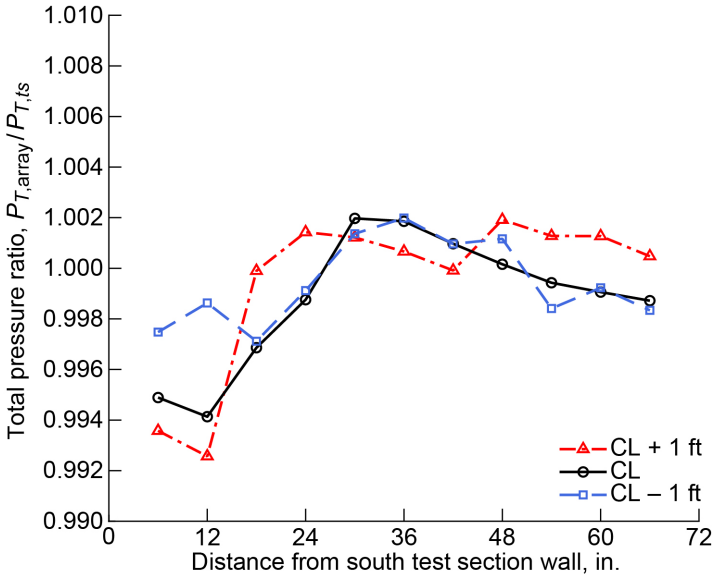

Figure 43.—Total pressure ratio distributions in 8- by 6-ft supersonic test section near test section station 44.25 at centerline (CL) and 1 ft above and below CL. Data acquired during supersonic test section characterization (2020 test) at flexwall setting of Mach 1.60; 0.002 = ΔP_T of 0.0396 psia.

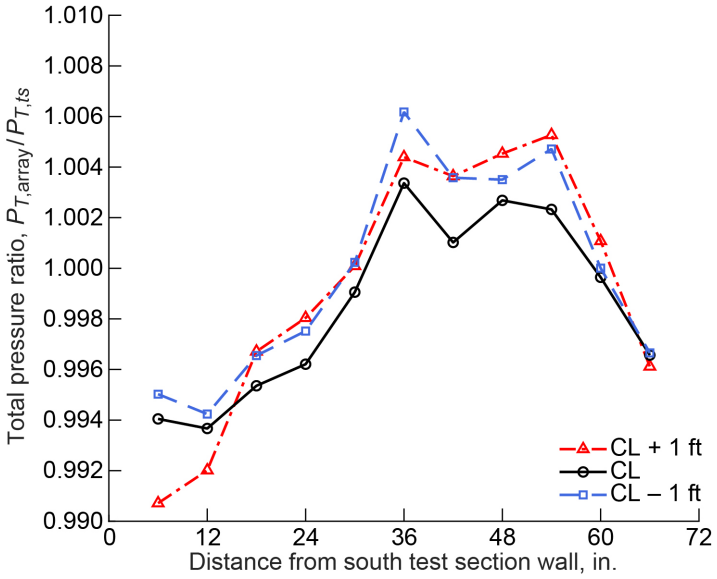

Figure 44.—Total pressure ratio distributions in 8- by 6-ft supersonic test section near test section station 44.25 at centerline (CL) and 1 ft above and below CL. Data acquired during supersonic test section characterization (2020 test) at flexwall setting of Mach 1.70; 0.002 = ΔP_T of 0.0422 psia.

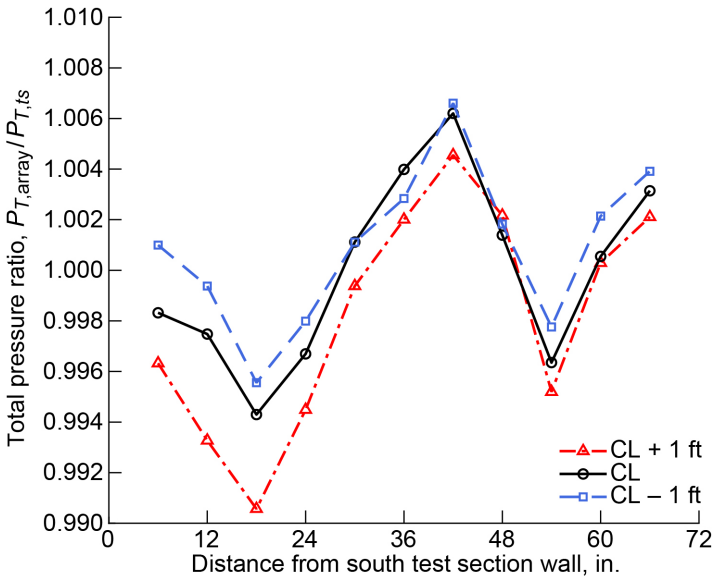

Figure 45.—Total pressure ratio distributions in 8- by 6-ft supersonic test section near test section station 44.25 at centerline (CL) and 1 ft above and below CL. Data acquired during supersonic test section characterization (2020 test) at flexwall setting of Mach 1.80; 0.002 = ΔP_T of 0.0445 psia.

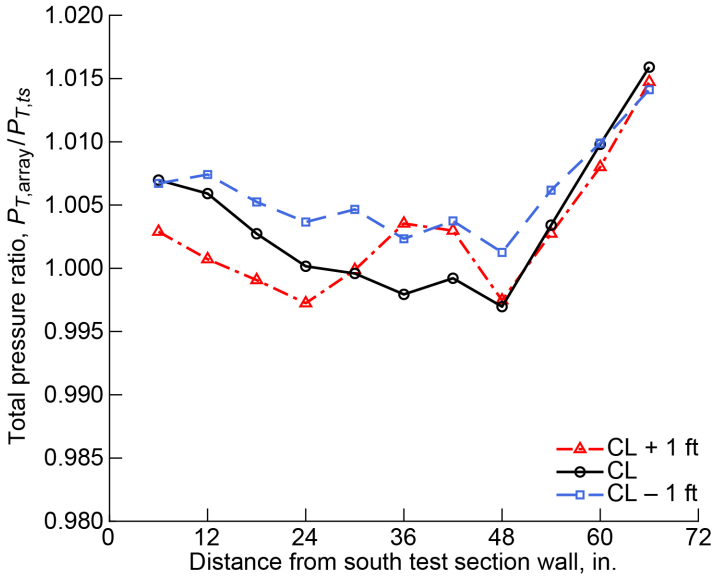

Figure 46.—Total pressure ratio distributions in 8- by 6-ft supersonic test section near test section station 44.25 at centerline (CL) and 1 ft above and below CL. Data acquired during supersonic test section characterization (2020 test) at flexwall setting of Mach 1.90; 0.005 = ΔP_T of 0.1178 psia.

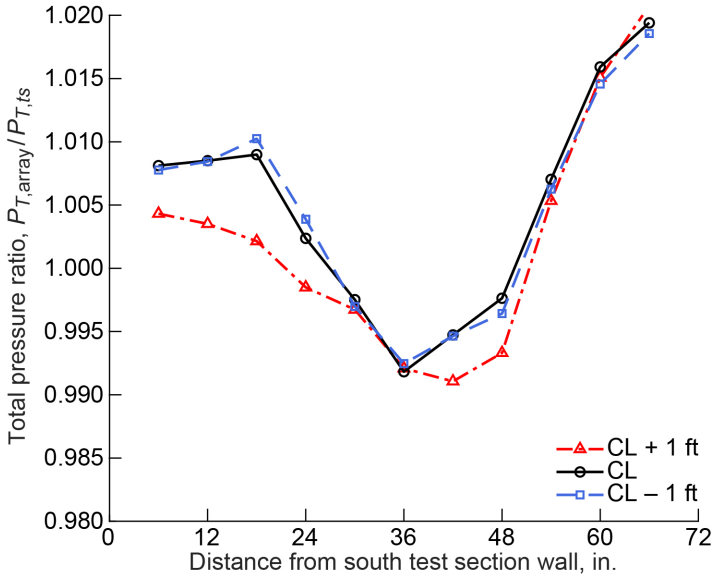

Figure 47.—Total pressure ratio distributions in 8- by 6-ft supersonic test section near test section station 44.25 at centerline (CL) and 1 ft above and below CL. Data acquired during supersonic test section characterization (2020 test) at flexwall setting of Mach 2.00; 0.005 = ΔP_T of 0.1205 psia.

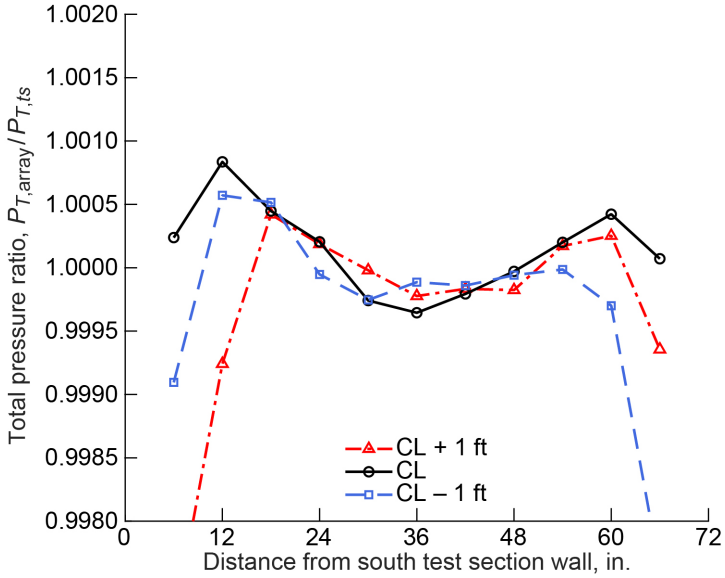

Figure 48.—Total pressure ratio distributions in 8- by 6-ft supersonic test section near test section station 44.25 at centerline (CL) and 1 ft above and below CL. Data acquired during supersonic test section characterization (2020 test) at transonic array Mach number of 0.842; 0.005 = ΔP_T of 0.0085 psia.

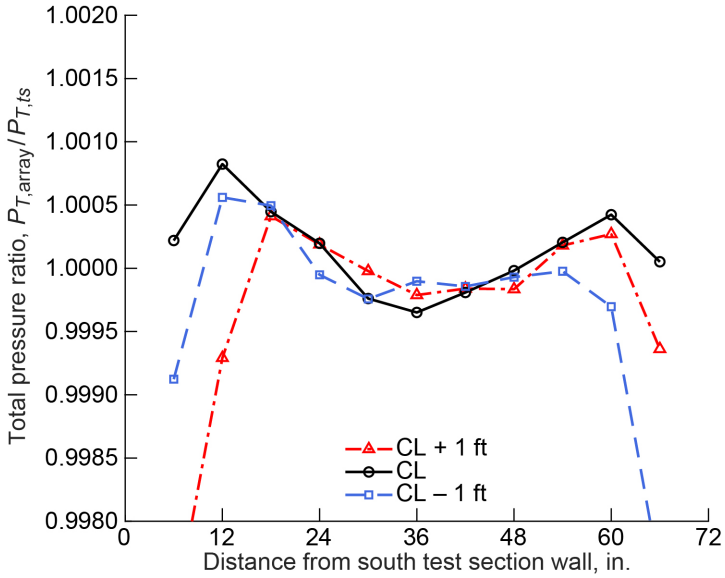

Figure 49.—Total pressure ratio distributions in 8- by 6-ft supersonic test section near test section station 44.25 at centerline (CL) and 1 ft above and below CL. Data acquired during supersonic test section characterization (2020 test) at transonic array Mach number of 0.831; 0.005 = ΔP_T of 0.0085 psia.

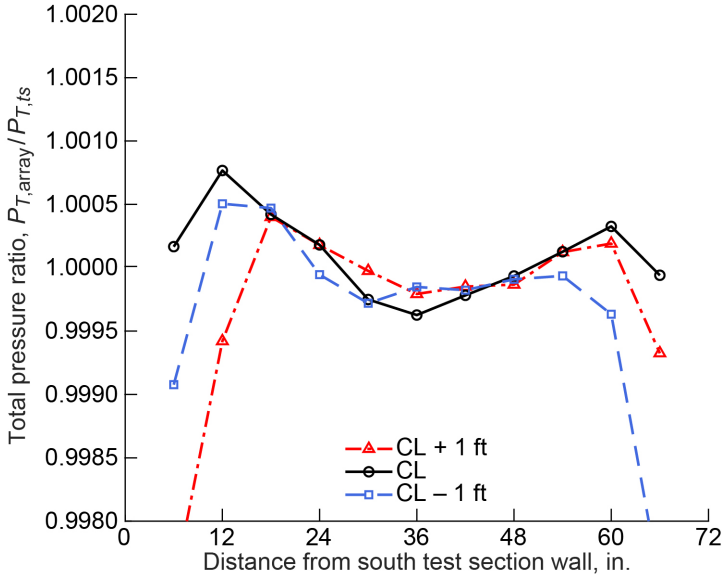

Figure 50.—Total pressure ratio distributions in 8- by 6-ft supersonic test section near test section station 44.25 at centerline (CL) and 1 ft above and below CL. Data acquired during supersonic test section characterization (2020 test) at transonic array Mach number of 0.769; 0.005 = ΔP_T of 0.0087 psia.

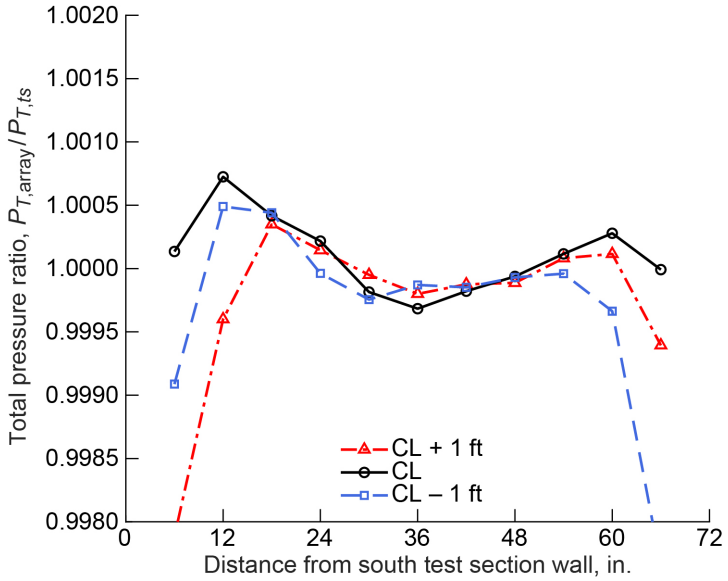

Figure 51.—Total pressure ratio distributions in 8- by 6-ft supersonic test section near test section station 44.25 at centerline (CL) and 1 ft above and below CL. Data acquired during supersonic test section characterization (2020 test) at transonic array Mach number of 0.683; 0.005 = ΔP_T of 0.0088 psia.

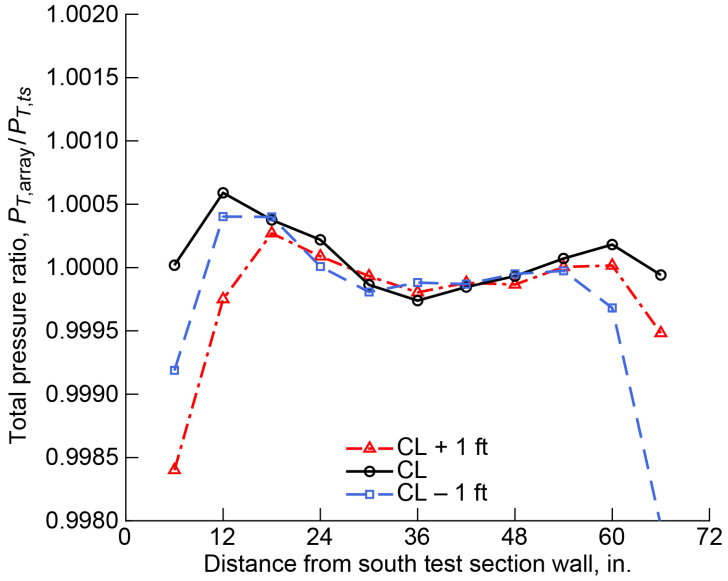

Figure 52.—Total pressure ratio distributions in 8- by 6-ft supersonic test section near test section station 44.25 at centerline (CL) and 1 ft above and below CL. Data acquired during supersonic test section characterization (2020 test) at transonic array Mach number of 0.586; 0.005 = ΔP_T of 0.0087 psia.

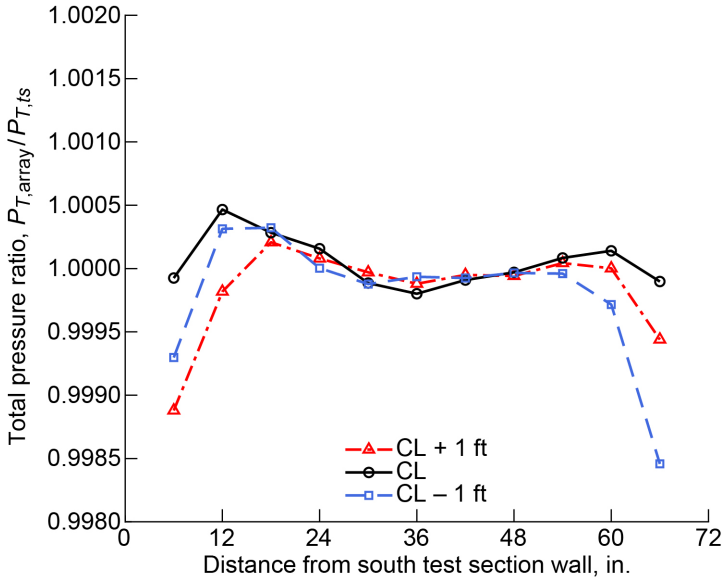

Figure 53.—Total pressure ratio distributions in 8- by 6-ft supersonic test section near test section station 44.25 at centerline (CL) and 1 ft above and below CL. Data acquired during supersonic test section characterization (2020 test) at transonic array Mach number of 0.492; 0.005 = ΔP_T of 0.0081 psia.

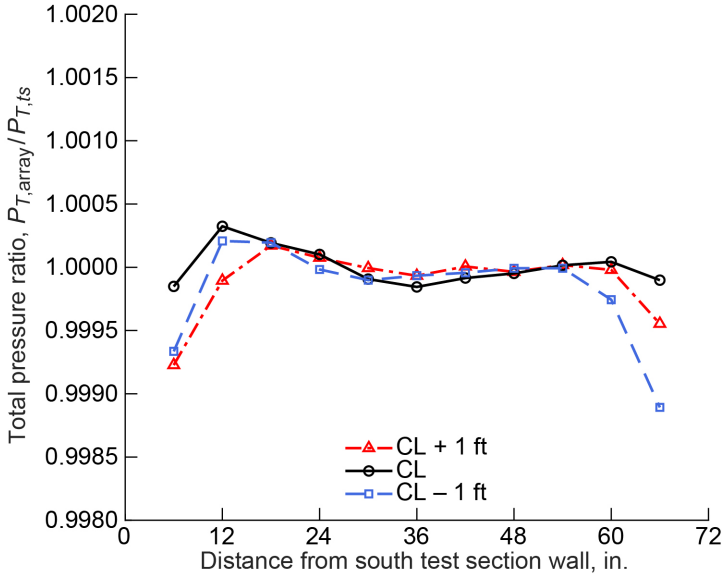

Figure 54.—Total pressure ratio distributions in 8- by 6-ft supersonic test section near test section station 44.25 at centerline (CL) and 1 ft above and below CL. Data acquired during supersonic test section characterization (2020 test) at transonic array Mach number of 0.395; 0.005 = ΔP_T of 0.0083 psia.

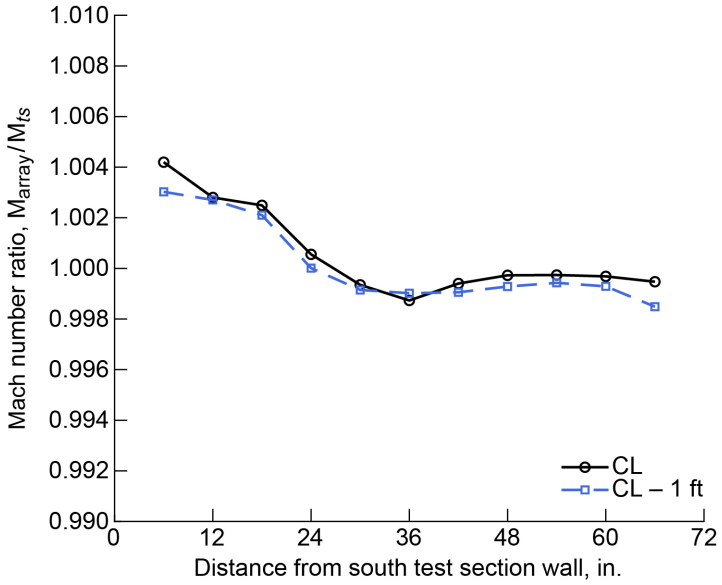

Figure 55.—Mach number ratio distributions in 8- by 6-ft supersonic test section near test section station 44.25 at centerline (CL) and 1 ft below CL. Data acquired during supersonic test section characterization (2020 test) at flexwall setting of Mach 1.30; 0.002 = ΔM of 0.0025.

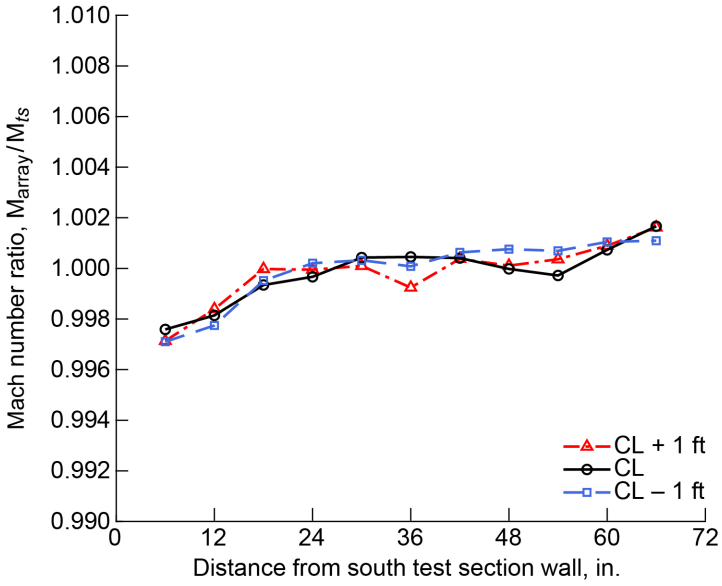

Figure 56.—Mach number ratio distributions in 8- by 6-ft supersonic test section near test section station 44.25 at centerline (CL) and 1 ft above and below CL. Data acquired during supersonic test section characterization (2020 test) at flexwall setting of Mach 1.40; 0.002 = ΔM of 0.0027.

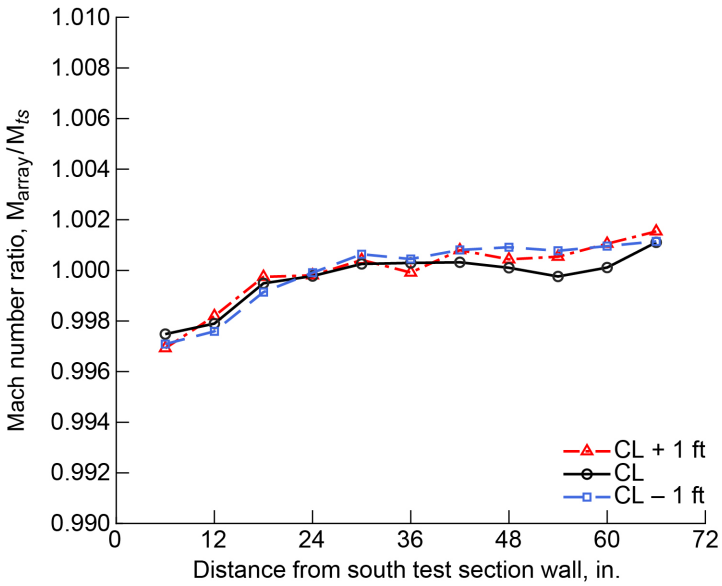

Figure 57.—Mach number ratio distributions in 8- by 6-ft supersonic test section near test section station 44.25 at centerline (CL) and 1 ft above and below CL. Data acquired during supersonic test section characterization (2020 test) at flexwall setting of Mach 1.42; 0.002 = ΔM of 0.0027.

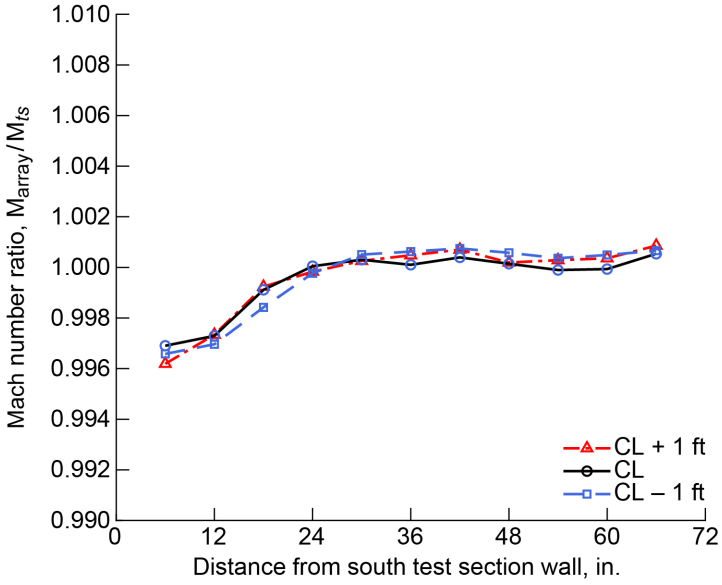

Figure 58.—Mach number ratio distributions in 8- by 6-ft supersonic test section near test section station 44.25 at centerline (CL) and 1 ft above and below CL. Data acquired during supersonic test section characterization (2020 test) at flexwall setting of Mach 1.43; 0.002 = ΔM of 0.0028.

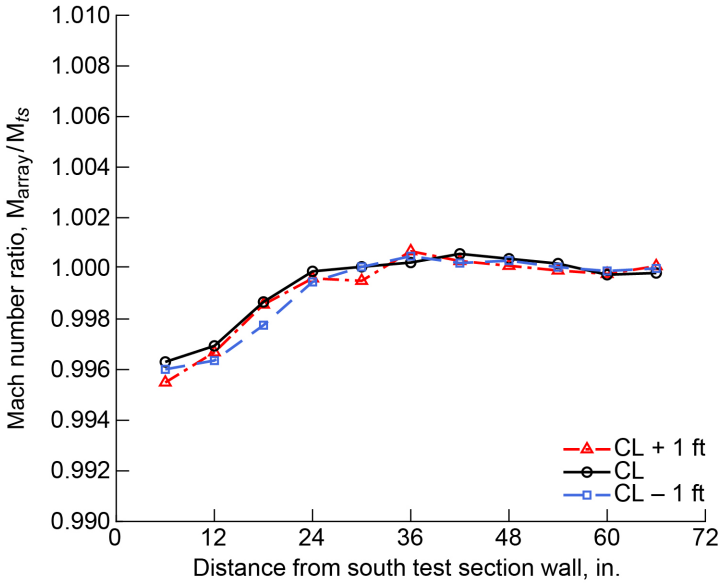

Figure 59.—Mach number ratio distributions in 8- by 6-ft supersonic test section near test section station 44.25 at centerline (CL) and 1 ft above and below CL. Data acquired during supersonic test section characterization (2020 test) at flexwall setting of Mach 1.44; 0.002 = ΔM of 0.0028.

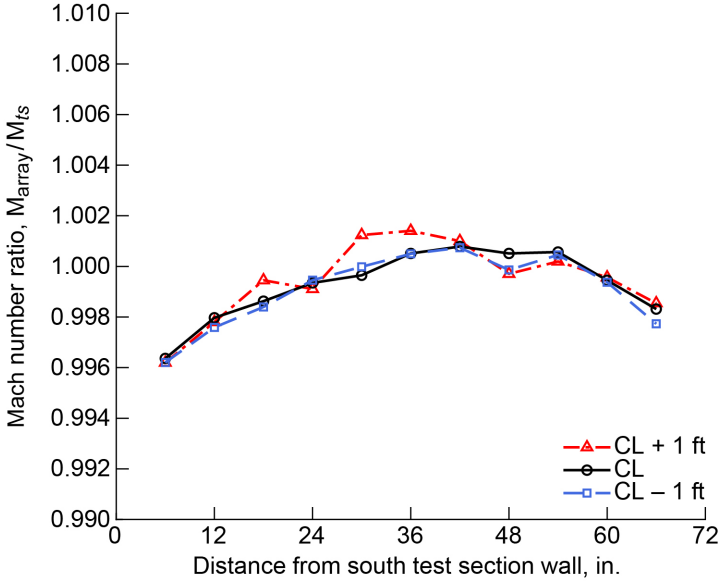

Figure 60.—Mach number ratio distributions in 8- by 6-ft supersonic test section near test section station 44.25 at centerline (CL) and 1 ft above and below CL. Data acquired during supersonic test section characterization (2020 test) at flexwall setting of Mach 1.50; 0.002 = ΔM of 0.0029.

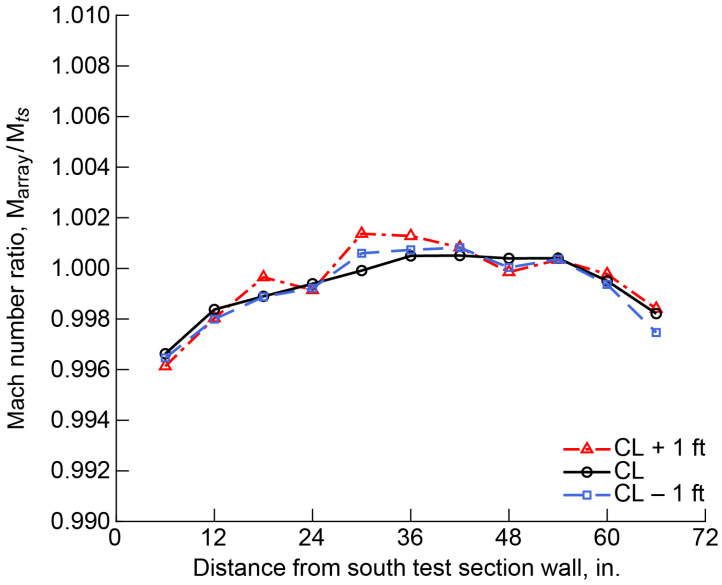

Figure 61.—Mach number ratio distributions in 8- by 6-ft supersonic test section near test section station 44.25 at centerline (CL) and 1 ft above and below CL. Data acquired during supersonic test section characterization (2020 test) at flexwall setting of Mach 1.52; 0.002 = ΔM of 0.0030.

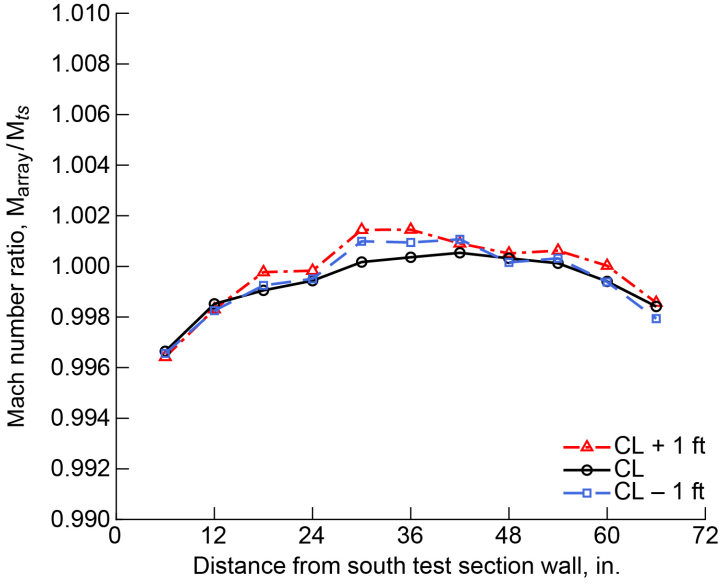

Figure 62.—Mach number ratio distributions in 8- by 6-ft supersonic test section near test section station 44.25 at centerline (CL) and 1 ft above and below CL. Data acquired during supersonic test section characterization (2020 test) at flexwall setting of Mach 1.53; 0.002 = ΔM of 0.0030.

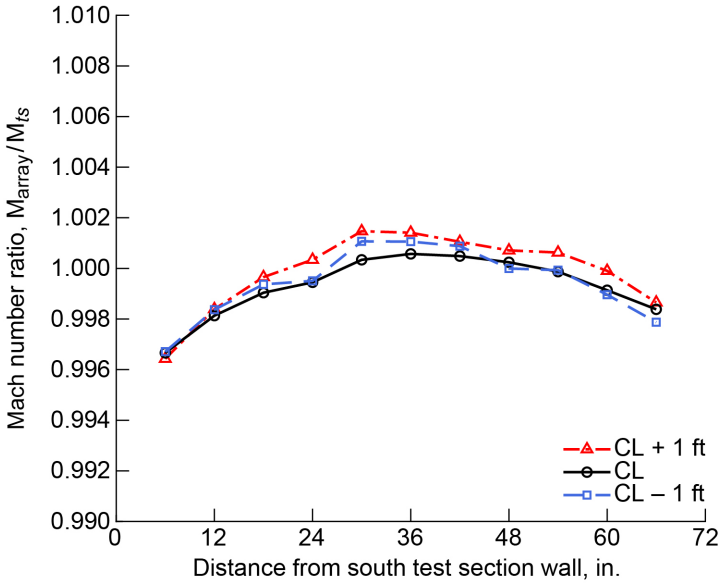

Figure 63.—Mach number ratio distributions in 8- by 6-ft supersonic test section near test section station 44.25 at centerline (CL) and 1 ft above and below CL. Data acquired during supersonic test section characterization (2020 test) at flexwall setting of Mach 1.54; 0.002 = ΔM of 0.0030.

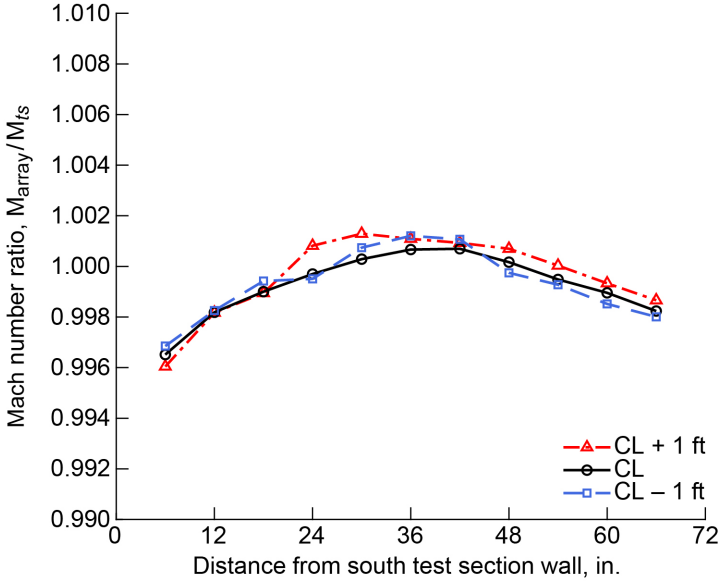

Figure 64.—Mach number ratio distributions in 8- by 6-ft supersonic test section near test section station 44.25 at centerline (CL) and 1 ft above and below CL. Data acquired during supersonic test section characterization (2020 test) at flexwall setting of Mach 1.55; 0.002 = ΔM of 0.0030.

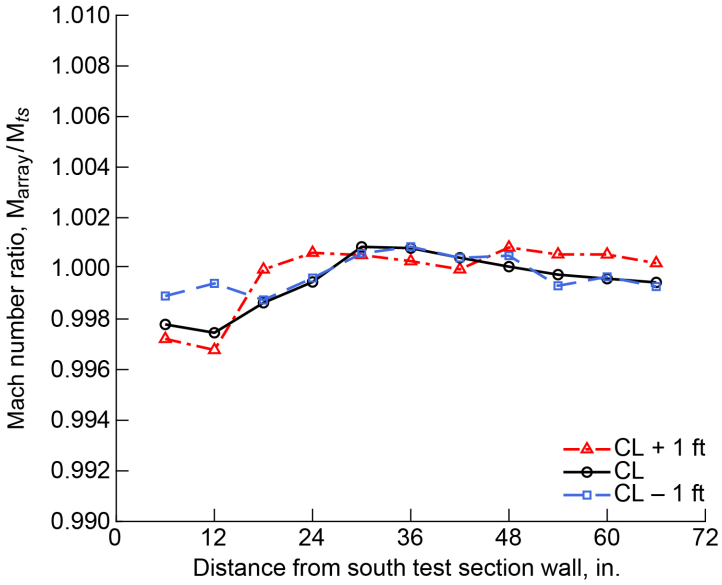

Figure 65.—Mach number ratio distributions in 8- by 6-ft supersonic test section near test section station 44.25 at centerline (CL) and 1 ft above and below CL. Data acquired during supersonic test section characterization (2020 test) at flexwall setting of Mach 1.60; 0.002 = ΔM of 0.0031.

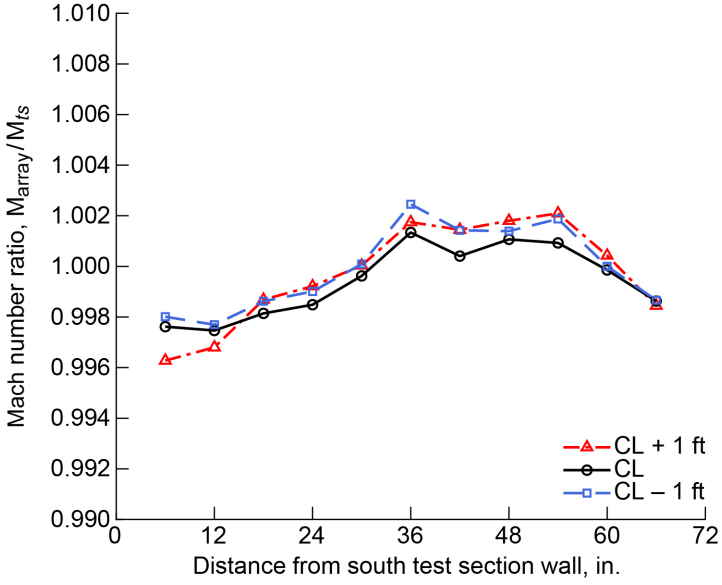

Figure 66.—Mach number ratio distributions in 8- by 6-ft supersonic test section near test section station 44.25 at centerline (CL) and 1 ft above and below CL. Data acquired during supersonic test section characterization (2020 test) at flexwall setting of Mach 1.70; 0.002 = ΔM of 0.0033.

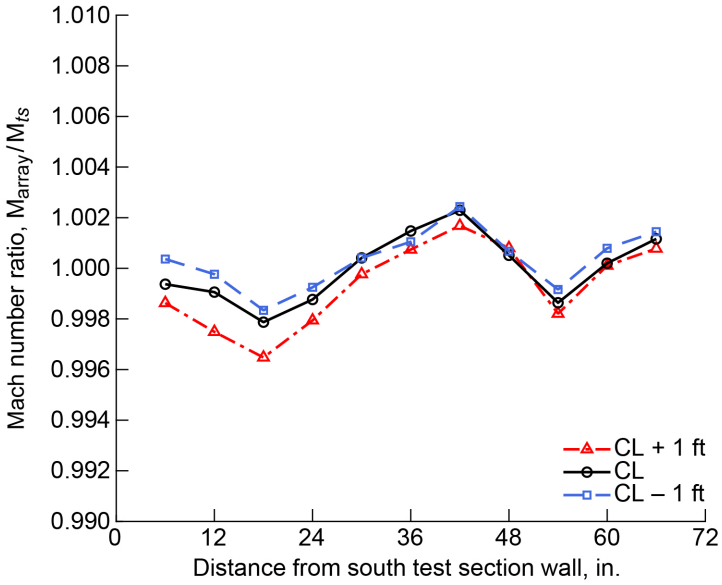

Figure 67.—Mach number ratio distributions in 8- by 6-ft supersonic test section near test section station 44.25 at centerline (CL) and 1 ft above and below CL. Data acquired during supersonic test section characterization (2020 test) at flexwall setting of Mach 1.80; 0.002 = ΔM of 0.0035.

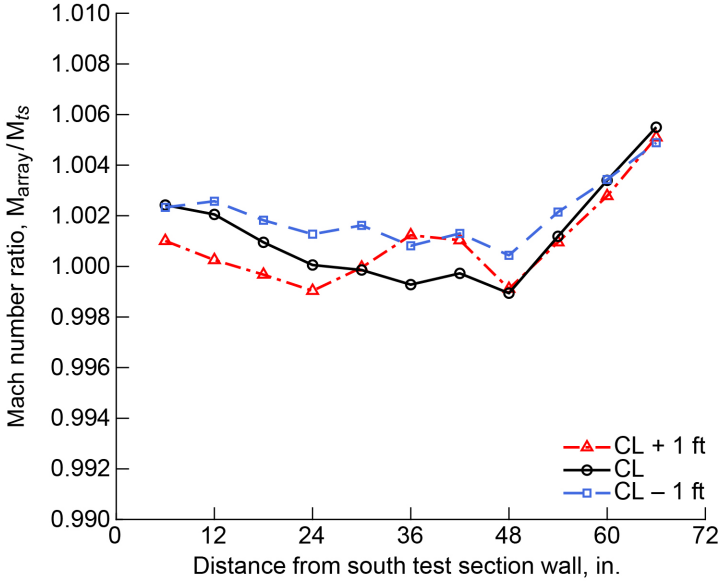

Figure 68.—Mach number ratio distributions in 8- by 6-ft supersonic test section near test section station 44.25 at centerline (CL) and 1 ft above and below CL. Data acquired during supersonic test section characterization (2020 test) at flexwall setting of Mach 1.90; 0.002 = ΔM of 0.0037.

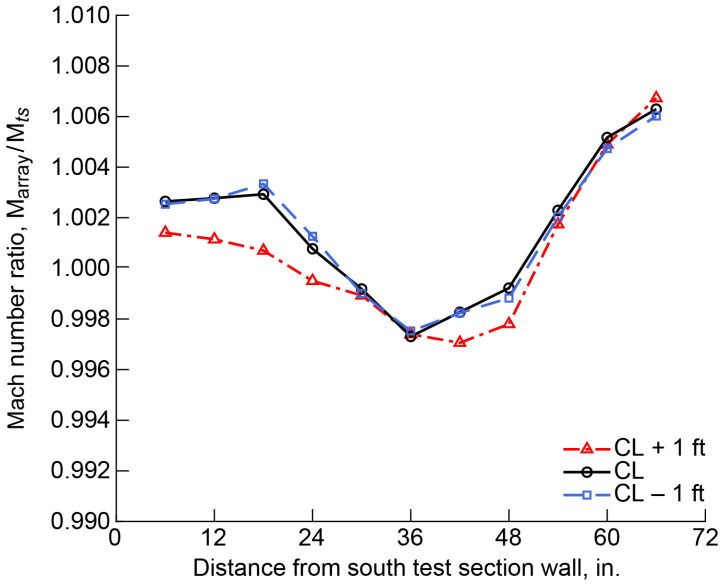

Figure 69.—Mach number ratio distributions in 8- by 6-ft supersonic test section near test section station 44.25 at centerline (CL) and 1 ft above and below CL. Data acquired during supersonic test section characterization (2020 test) at flexwall setting of Mach 2.00; 0.002 = ΔM of 0.0039.

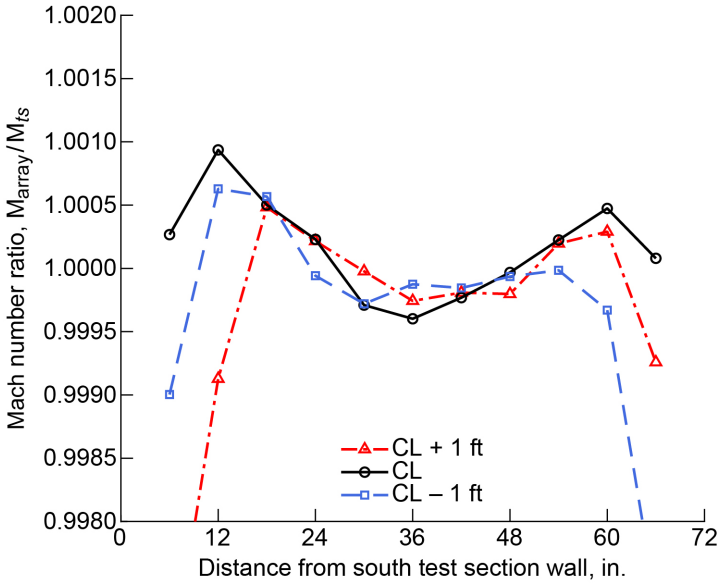

Figure 70.—Mach number ratio distributions in 8- by 6-ft supersonic test section near test section station 44.25 at centerline (CL) and 1 ft above and below CL. Data acquired during supersonic test section characterization (2020 test) at transonic array Mach number of 0.842; 0.0005 = ΔM of 0.0004.

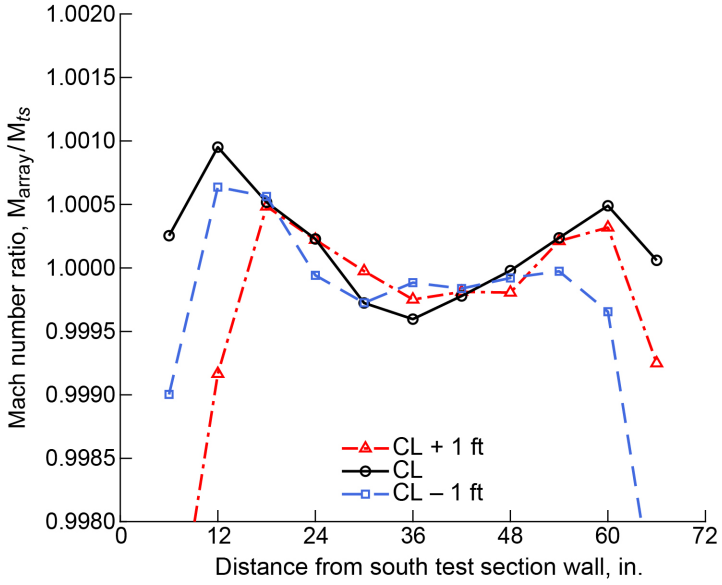

Figure 71.—Mach number ratio distributions in 8- by 6-ft supersonic test section near test section station 44.25 at centerline (CL) and 1 ft above and below CL. Data acquired during supersonic test section characterization (2020 test) at transonic array Mach number of 0.831; 0.0005 = ΔM of 0.0004.

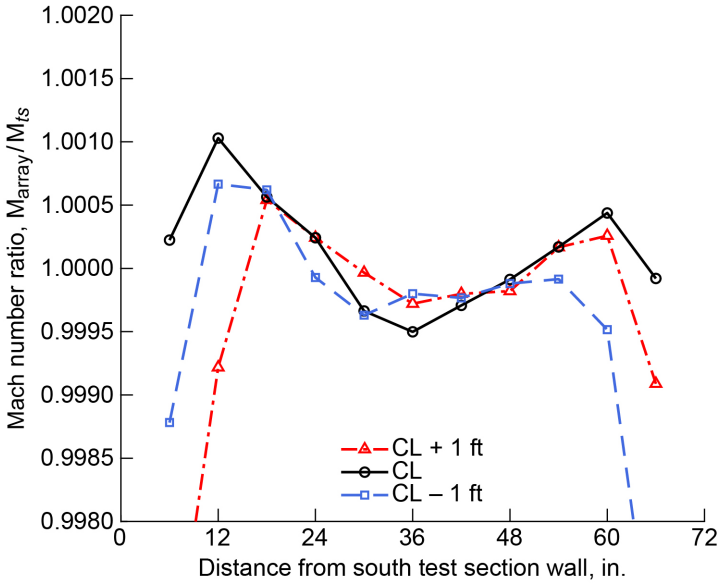

Figure 72.—Mach number ratio distributions in 8- by 6-ft supersonic test section near test section station 44.25 at centerline (CL) and 1 ft above and below CL. Data acquired during supersonic test section characterization (2020 test) at transonic array Mach number of 0.769; 0.0005 = ΔM of 0.0004.

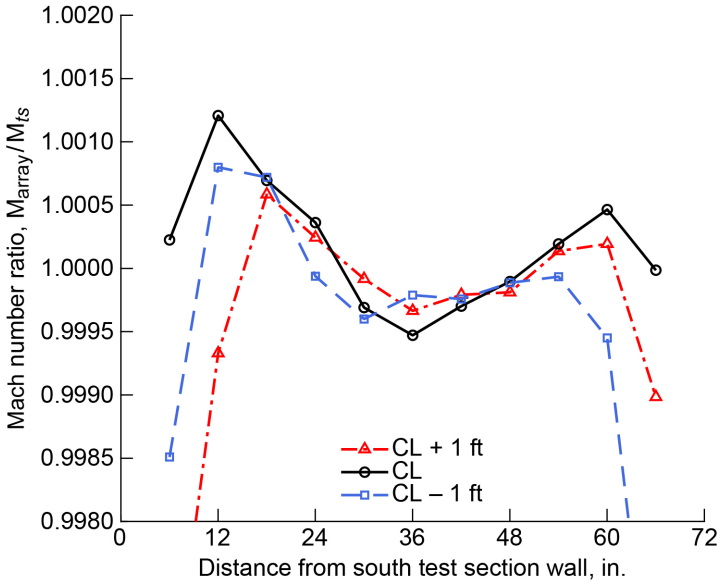

Figure 73.—Mach number ratio distributions in 8- by 6-ft supersonic test section near test section station 44.25 at centerline (CL) and 1 ft above and below CL. Data acquired during supersonic test section characterization (2020 test) at transonic array Mach number of 0.683; 0.0005 = ΔM of 0.0003.

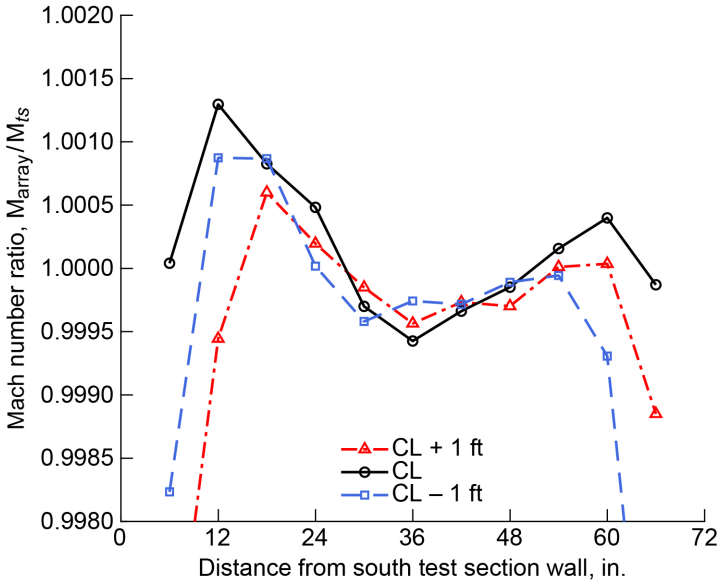

Figure 74.—Mach number ratio distributions in 8- by 6-ft supersonic test section near test section station 44.25 at centerline (CL) and 1 ft above and below CL. Data acquired during supersonic test section characterization (2020 test) at transonic array Mach number of 0.586; 0.0005 = ΔM of 0.0003.

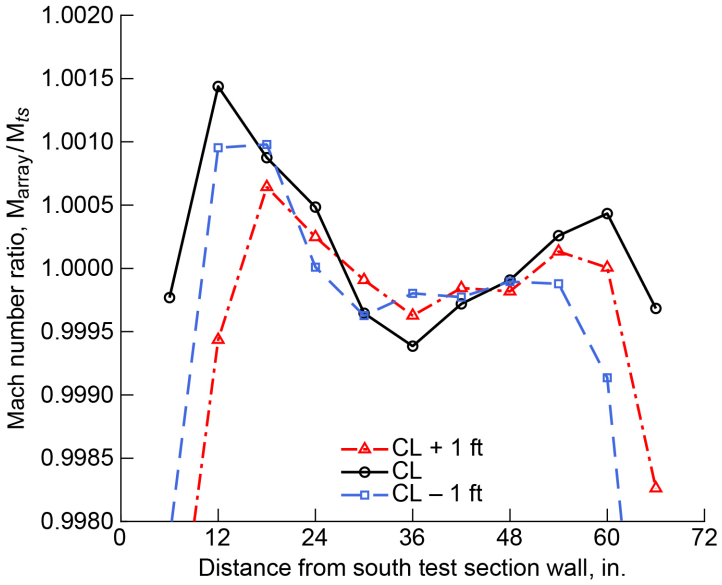

Figure 75.—Mach number ratio distributions in 8- by 6-ft supersonic test section near test section station 44.25 at centerline (CL) and 1 ft above and below CL. Data acquired during supersonic test section characterization (2020 test) at transonic array Mach number of 0.492; 0.0005 = ΔM of 0.0002.

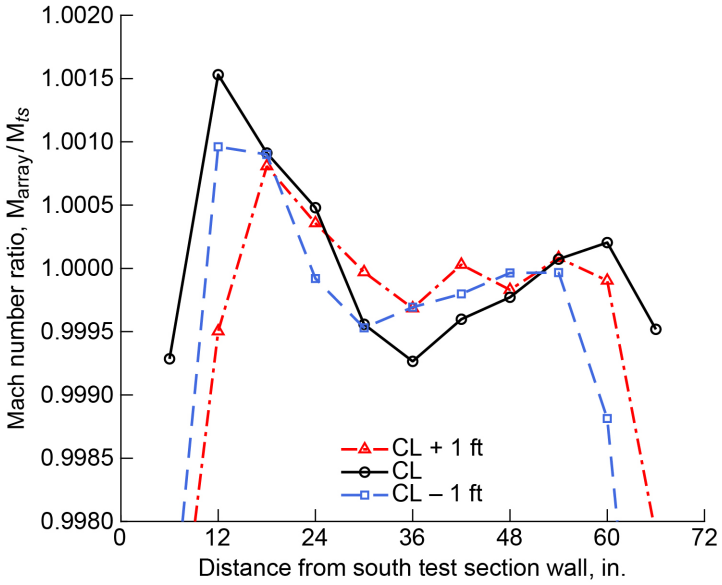

Figure 76.—Mach number ratio distributions in 8- by 6-ft supersonic test section near test section station 44.25 at centerline (CL) and 1 ft above and below CL. Data acquired during supersonic test section characterization (2020 test) at transonic array Mach number of 0.395; 0.0005 = ΔM of 0.0002.

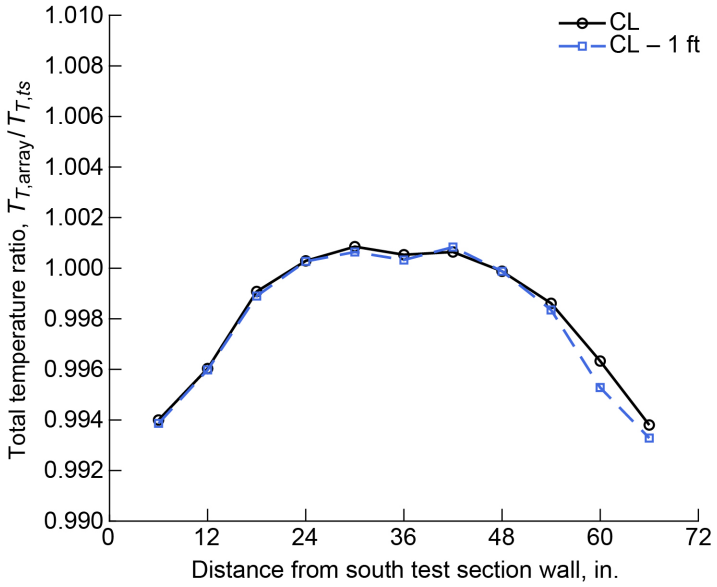

Figure 77.—Total temperature ratio distributions in 8- by 6-ft supersonic test section near test section station 44.25 at centerline (CL) and 1 ft below CL. Data acquired during supersonic test section characterization (2020 test) at flexwall setting of Mach 1.30; 0.002 = ΔT_T of 1.20 R.

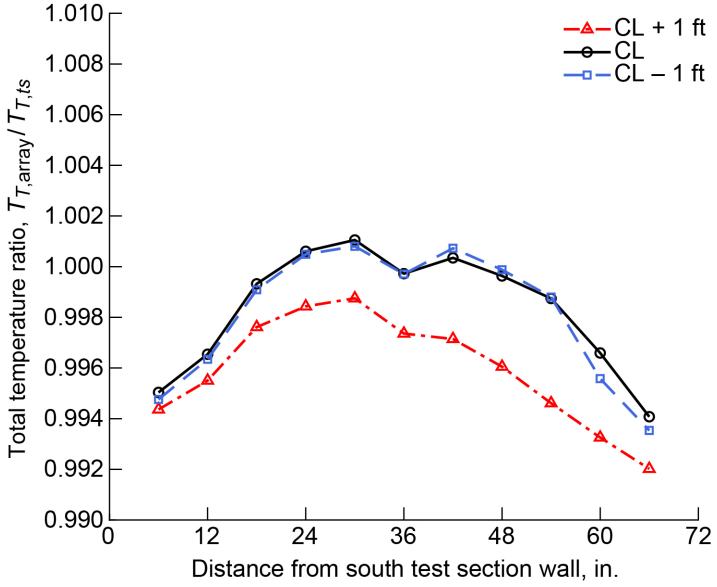

Figure 78.—Total temperature ratio distributions in 8- by 6-ft supersonic test section near test section station 44.25 at centerline (CL) and 1 ft above and below CL. Data acquired during supersonic test section characterization (2020 test) at flexwall setting of Mach 1.40; 0.002 = ΔT_T of 1.22 R.

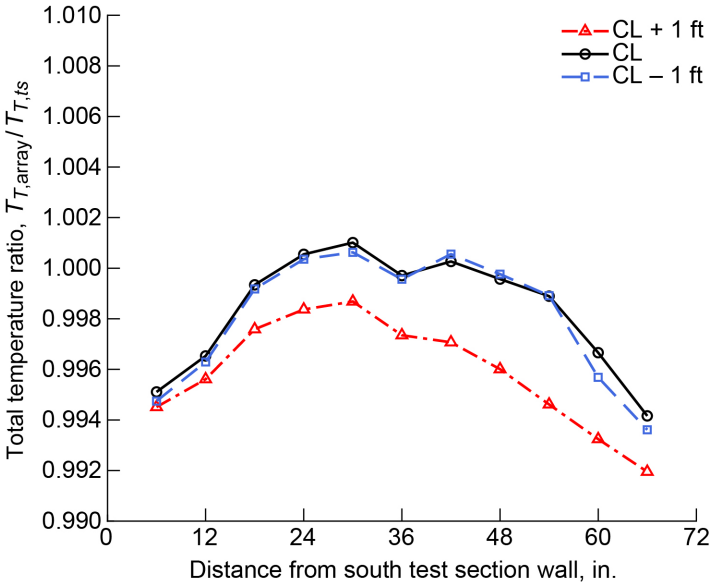

Figure 79.—Total temperature ratio distributions in 8- by 6-ft supersonic test section near test section station 44.25 at centerline (CL) and 1 ft above and below CL. Data acquired during supersonic test section characterization (2020 test) at flexwall setting of Mach 1.42; 0.002 = ΔT_T of 1.22 R.

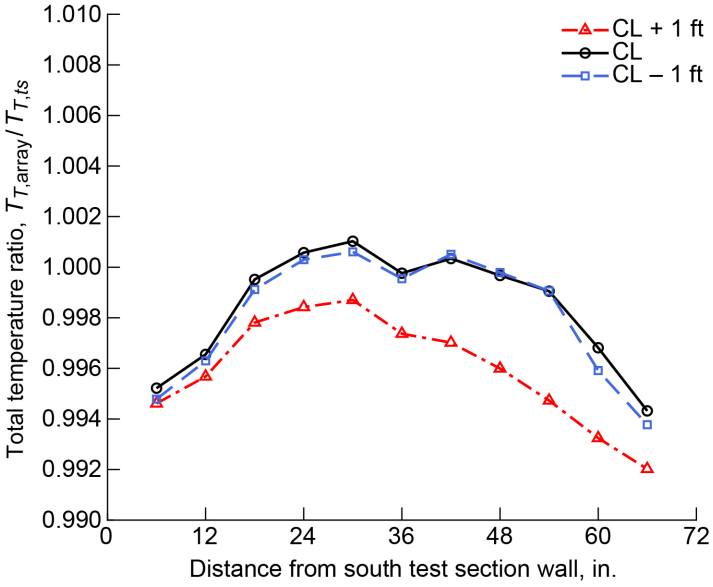

Figure 80.—Total temperature ratio distributions in 8- by 6-ft supersonic test section near test section station 44.25 at centerline (CL) and 1 ft above and below CL. Data acquired during supersonic test section characterization (2020 test) at flexwall setting of Mach 1.43; 0.002 = ΔT_T of 1.22 R.

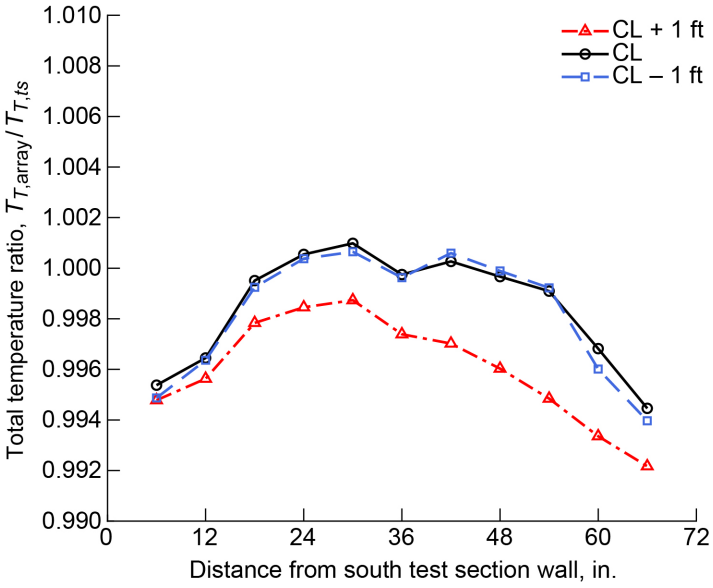

Figure 81.—Total temperature ratio distributions in 8- by 6-ft supersonic test section near test section station 44.25 at centerline (CL) and 1 ft above and below CL. Data acquired during supersonic test section characterization (2020 test) at flexwall setting of Mach 1.44; 0.002 = ΔT_T of 1.22 R.

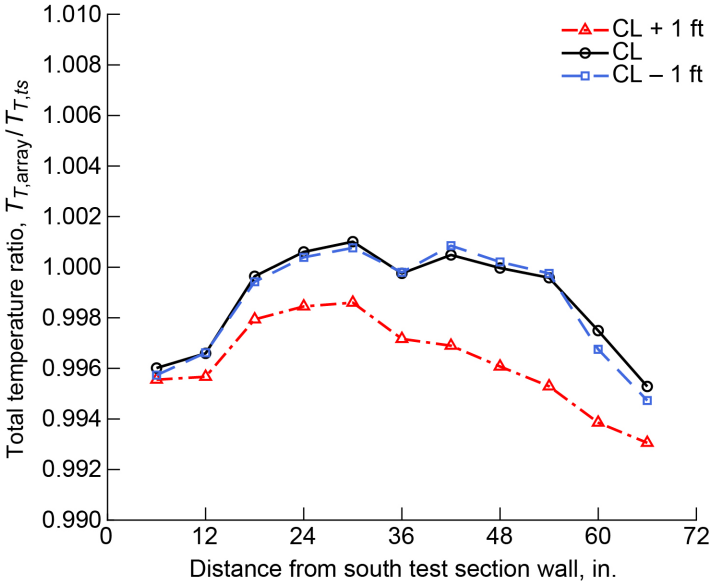

Figure 82.—Total temperature ratio distributions in 8- by 6-ft supersonic test section near test section station 44.25 at centerline (CL) and 1 ft above and below CL. Data acquired during supersonic test section characterization (2020 test) at flexwall setting of Mach 1.50; 0.002 = ΔT_T of 1.23 R.

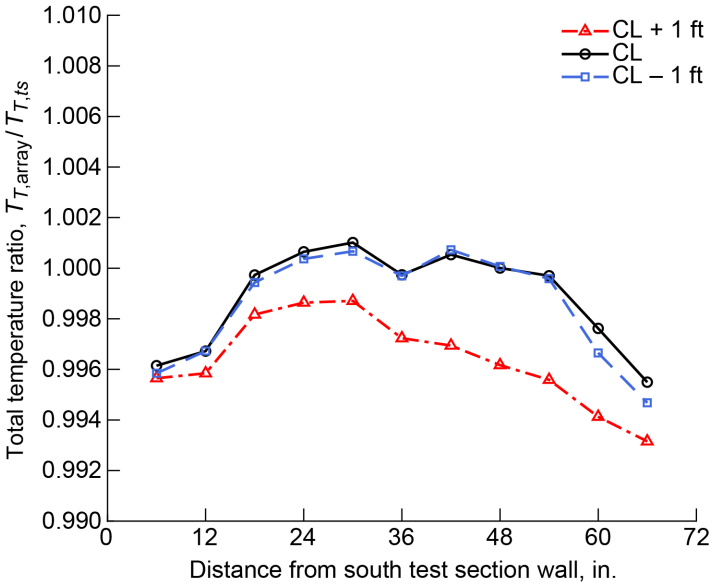

Figure 83.—Total temperature ratio distributions in 8- by 6-ft supersonic test section near test section station 44.25 at centerline (CL) and 1 ft above and below CL. Data acquired during supersonic test section characterization (2020 test) at flexwall setting of Mach 1.52; 0.002 = ΔT_T of 1.24 R.

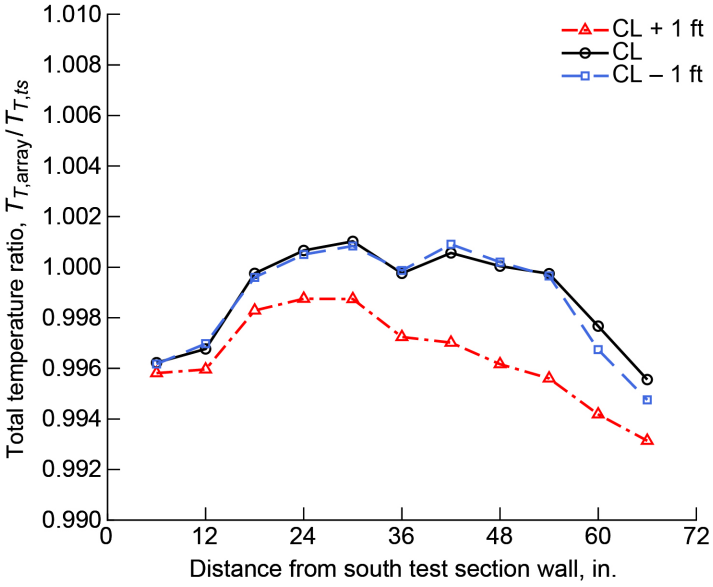

Figure 84.—Total temperature ratio distributions in 8- by 6-ft supersonic test section near test section station 44.25 at centerline (CL) and 1 ft above and below CL. Data acquired during supersonic test section characterization (2020 test) at flexwall setting of Mach 1.53; 0.002 = ΔT_T of 1.24 R.

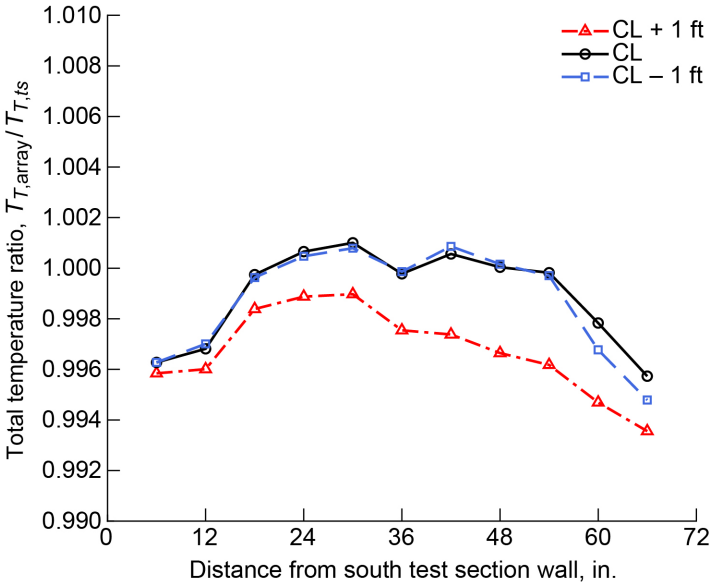

Figure 85.—Total temperature ratio distributions in 8- by 6-ft supersonic test section near test section station 44.25 at centerline (CL) and 1 ft above and below CL. Data acquired during supersonic test section characterization (2020 test) at flexwall setting of Mach 1.54; 0.002 = ΔT_T of 1.24 R.

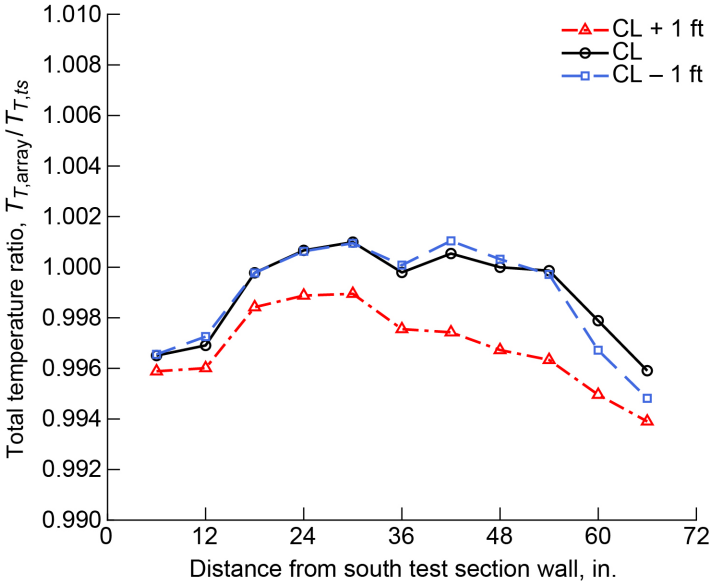

Figure 86.—Total temperature ratio distributions in 8- by 6-ft supersonic test section near test section station 44.25 at centerline (CL) and 1 ft above and below CL. Data acquired during supersonic test section characterization (2020 test) at flexwall setting of Mach 1.55; 0.002 = ΔT_T of 1.24 R.

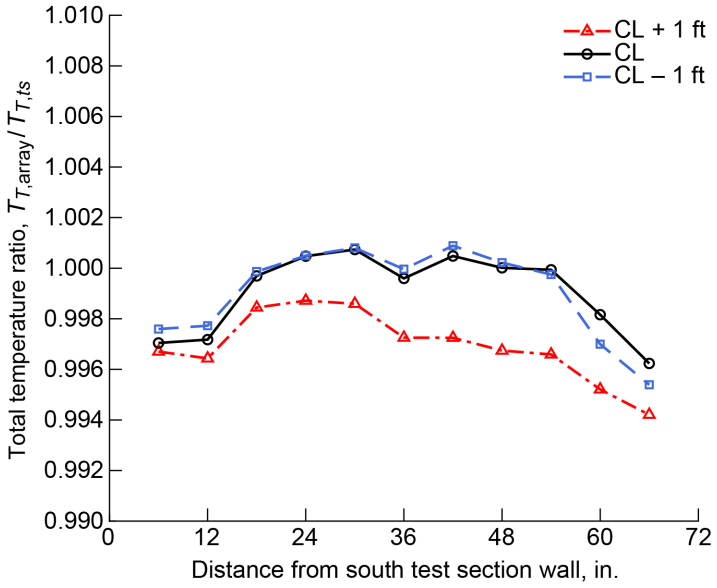

Figure 87.—Total temperature ratio distributions in 8- by 6-ft supersonic test section near test section station 44.25 at centerline (CL) and 1 ft above and below CL. Data acquired during supersonic test section characterization (2020 test) at flexwall setting of Mach 1.60; 0.002 = ΔT_T of 1.25 R.

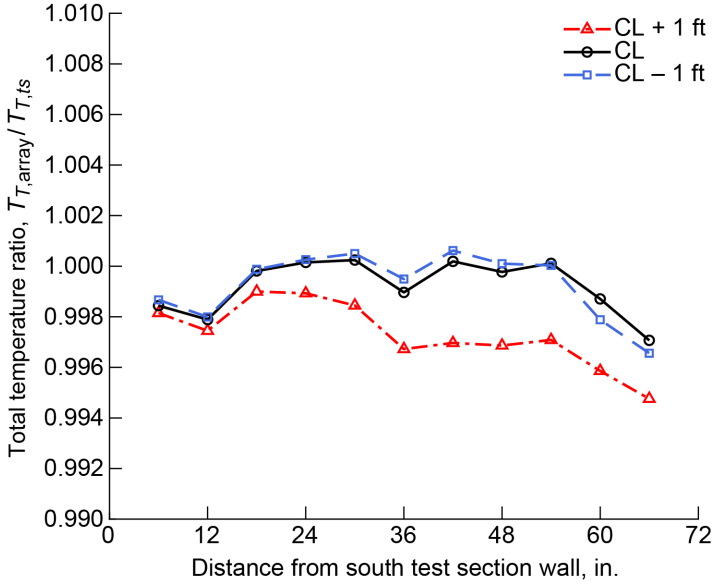

Figure 88.—Total temperature ratio distributions in 8- by 6-ft supersonic test section near test section station 44.25 at centerline (CL) and 1 ft above and below CL. Data acquired during supersonic test section characterization (2020 test) at flexwall setting of Mach 1.70; 0.002 = ΔT_T of 1.27 R.

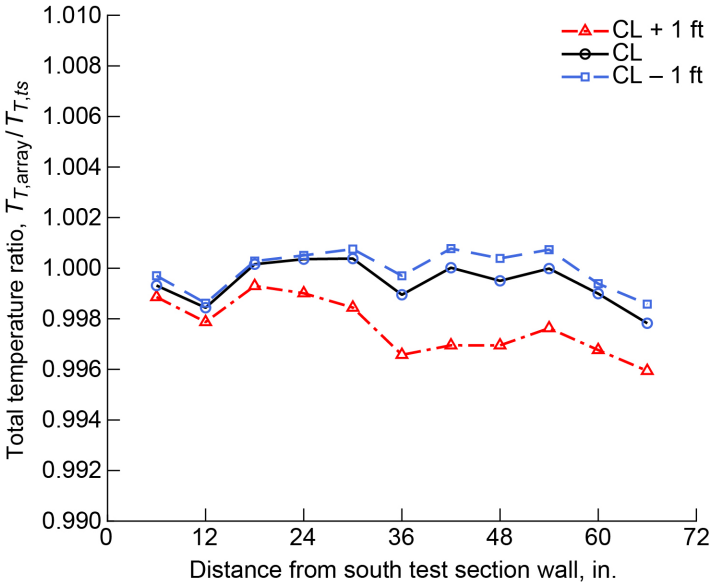

Figure 89.—Total temperature ratio distributions in 8- by 6-ft supersonic test section near test section station 44.25 at centerline (CL) and 1 ft above and below CL. Data acquired during supersonic test section characterization (2020 test) at flexwall setting of Mach 1.80; 0.002 = ΔT_T of 1.28 R.

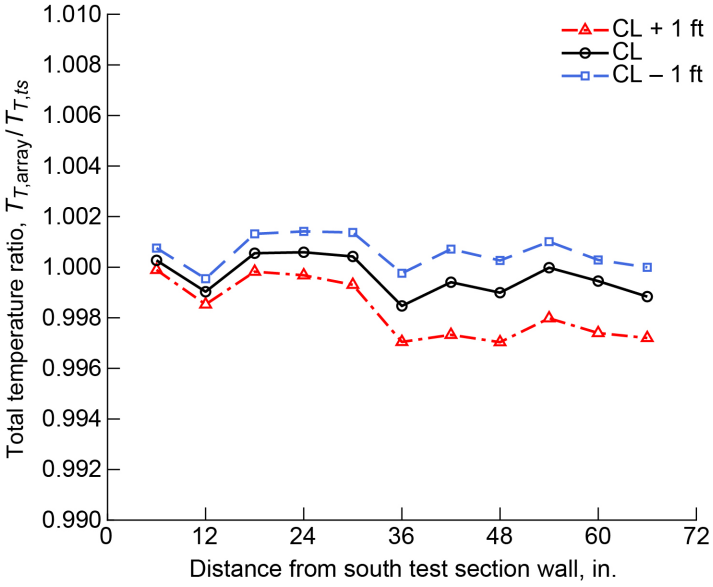

Figure 90.—Total temperature ratio distributions in 8- by 6-ft supersonic test section near test section station 44.25 at centerline (CL) and 1 ft above and below CL. Data acquired during supersonic test section characterization (2020 test) at flexwall setting of Mach 1.90; 0.002 = ΔT_T of 1.29 R.

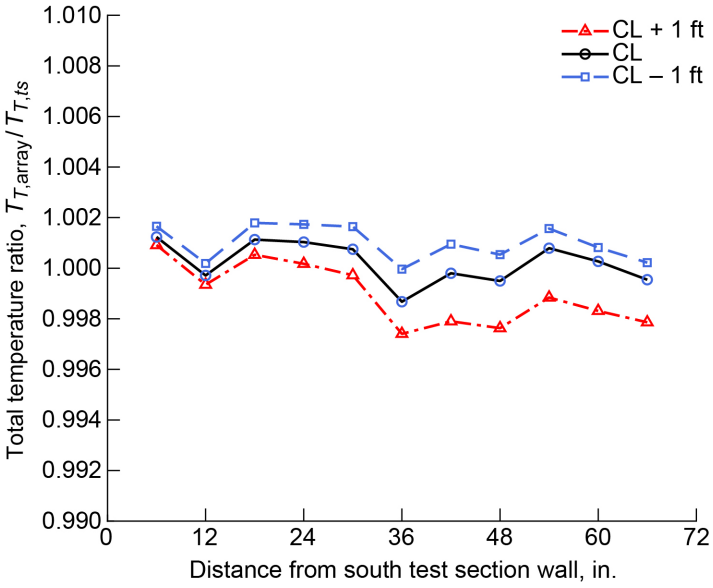

Figure 91.—Total temperature ratio distributions in 8- by 6-ft supersonic test section near test section station 44.25 at centerline (CL) and 1 ft above and below CL. Data acquired during supersonic test section characterization (2020 test) at flexwall setting of Mach 2.00; 0.002 = ΔT_T of 1.29 R.

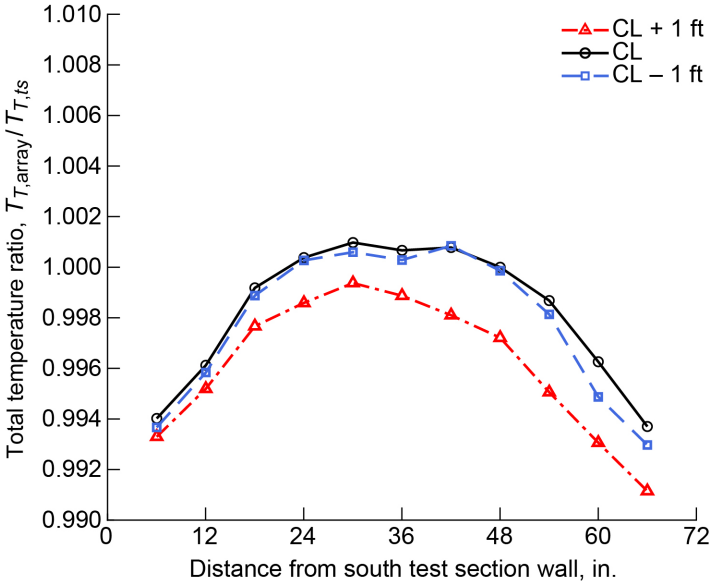

Figure 92.—Total temperature ratio distributions in 8- by 6-ft supersonic test section near test section station 44.25 at centerline (CL) and 1 ft above and below CL. Data acquired during supersonic test section characterization (2020 test) at transonic array Mach number of 0.842; 0.002 = ΔT_T of 1.19 R.

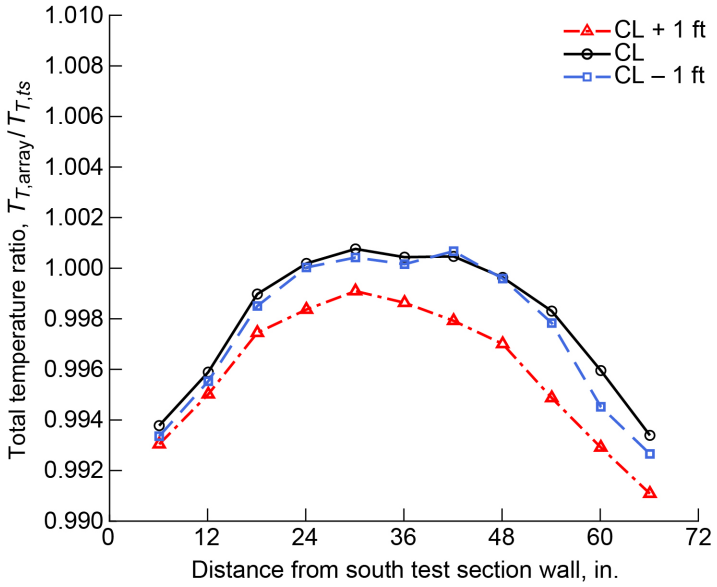

Figure 93.—Total temperature ratio distributions in 8- by 6-ft supersonic test section near test section station 44.25 at centerline (CL) and 1 ft above and below CL. Data acquired during supersonic test section characterization (2020 test) at transonic array Mach number of 0.831; 0.002 = ΔT_T of 1.19 R.

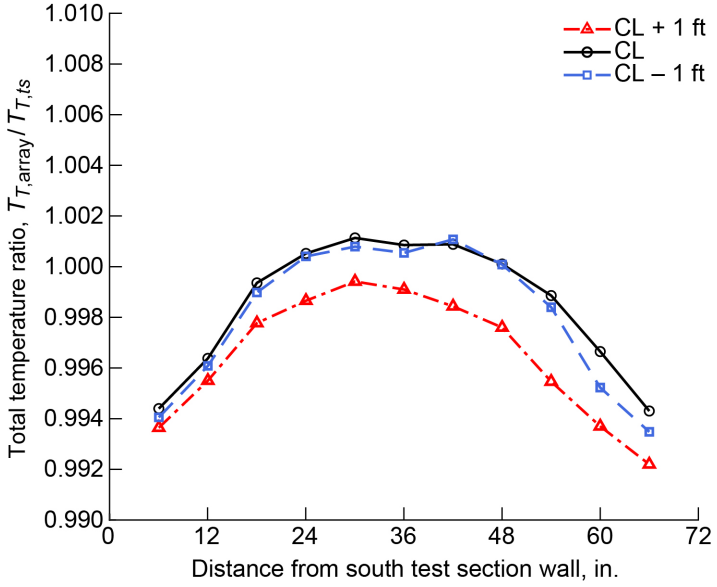

Figure 94.—Total temperature ratio distributions in 8- by 6-ft supersonic test section near test section station 44.25 at centerline (CL) and 1 ft above and below CL. Data acquired during supersonic test section characterization (2020 test) at transonic array Mach number of 0.769; 0.002 = ΔT_T of 1.20 R.

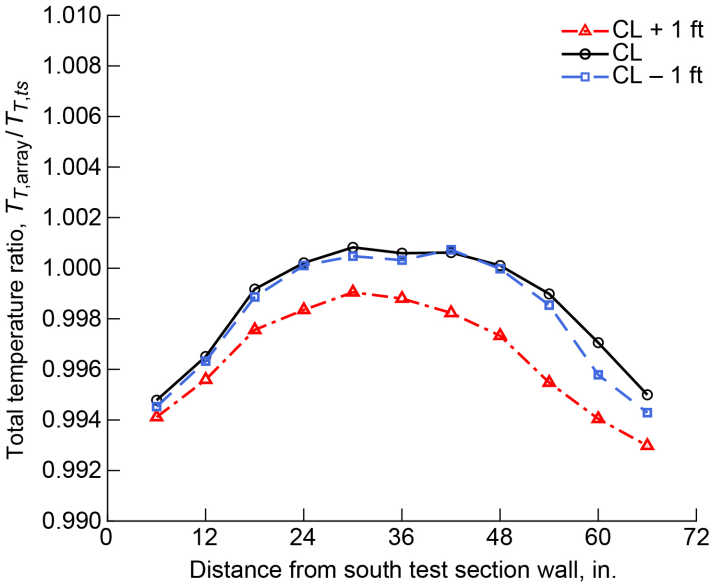

Figure 95.—Total temperature ratio distributions in 8- by 6-ft supersonic test section near test section station 44.25 at centerline (CL) and 1 ft above and below CL. Data acquired during supersonic test section characterization (2020 test) at transonic array Mach number of 0.683; 0.002 = ΔT_T of 1.19 R.

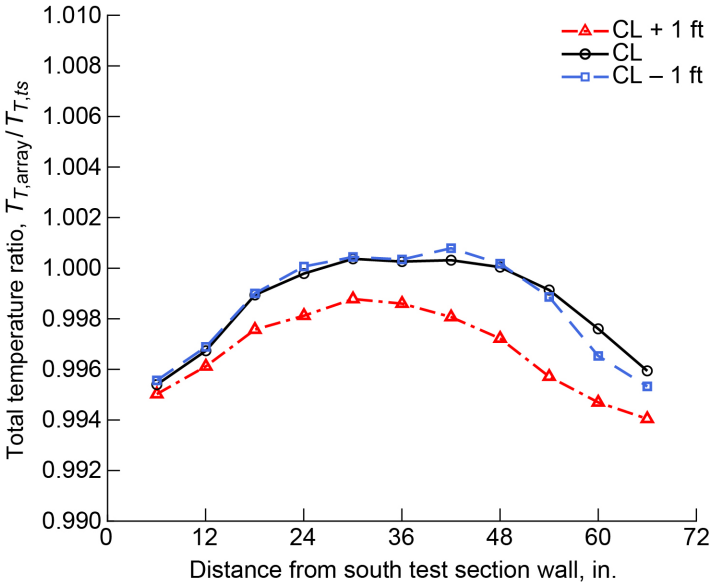

Figure 96.—Total temperature ratio distributions in 8- by 6-ft supersonic test section near test section station 44.25 at centerline (CL) and 1 ft above and below CL. Data acquired during supersonic test section characterization (2020 test) at transonic array Mach number of 0.586; 0.002 = ΔT_T of 1.19 R.

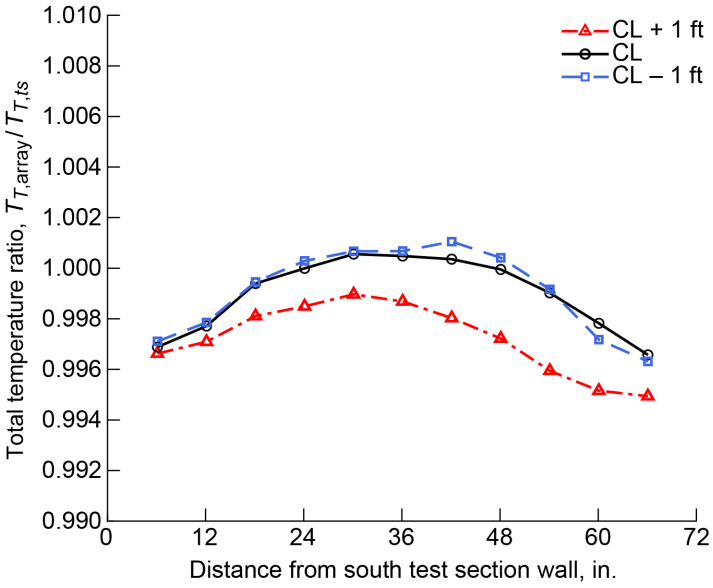

Figure 97.—Total temperature ratio distributions in 8- by 6-ft supersonic test section near test section station 44.25 at centerline (CL) and 1 ft above and below CL. Data acquired during supersonic test section characterization (2020 test) at transonic array Mach number of 0.492; 0.002 = ΔT_T of 1.15 R.

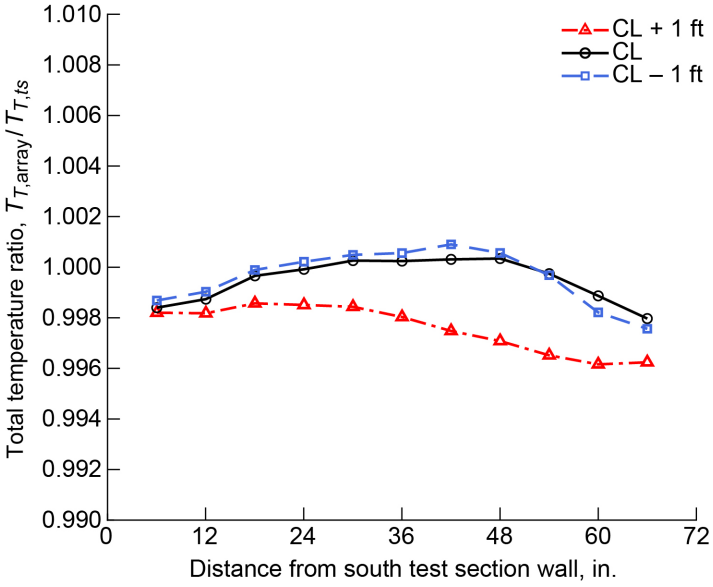

Figure 98.—Total temperature ratio distributions in 8- by 6-ft supersonic test section near test section station 44.25 at centerline (CL) and 1 ft above and below CL. Data acquired during supersonic test section characterization (2020 test) at transonic array Mach number of 0.395; 0.002 = ΔT_T of 1.15 R.

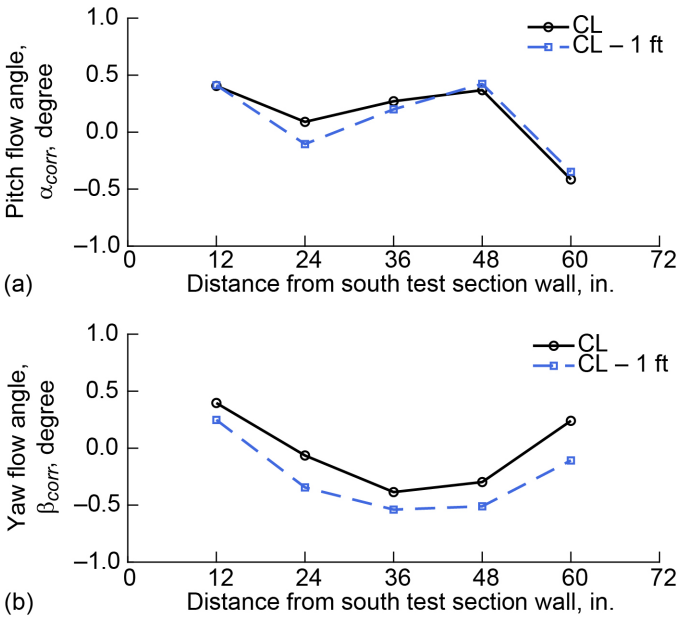

Figure 99.—Pitch and yaw flow angles in 8- by 6-ft supersonic test section near test section station 44.25 at centerline (CL) and 1 ft below CL. Positive pitch, α, is from floor to ceiling and positive yaw, β, is from left to right when upstream looking aft. Data acquired during supersonic test section characterization (2020 test) at flexwall setting of Mach 1.30. (a) Pitch. (b) Yaw.

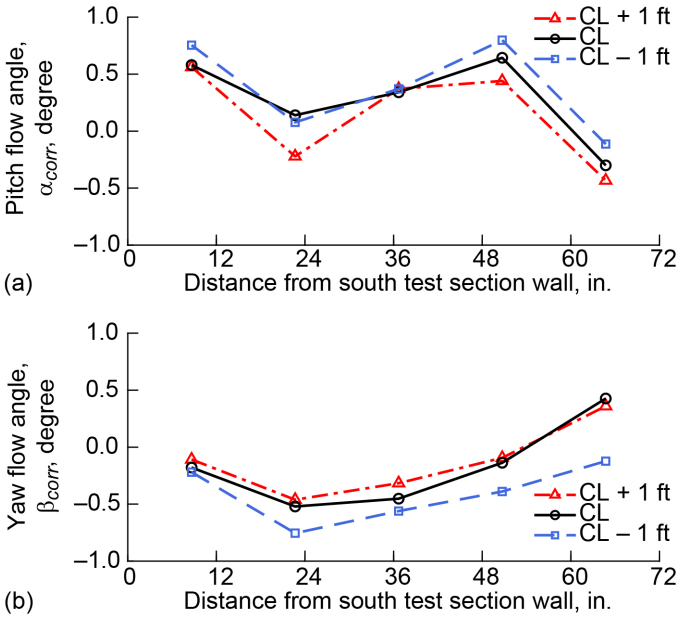

Figure 100.—Pitch and yaw flow angles in 8- by 6-ft supersonic test section near test section station 44.25 at centerline (CL) and 1 ft above and below CL. Positive pitch, α, is from floor to ceiling and positive yaw, β, is from left to right when upstream looking aft. Data acquired during supersonic test section characterization (2020 test) at flexwall setting of Mach 1.40. (a) Pitch. (b) Yaw.

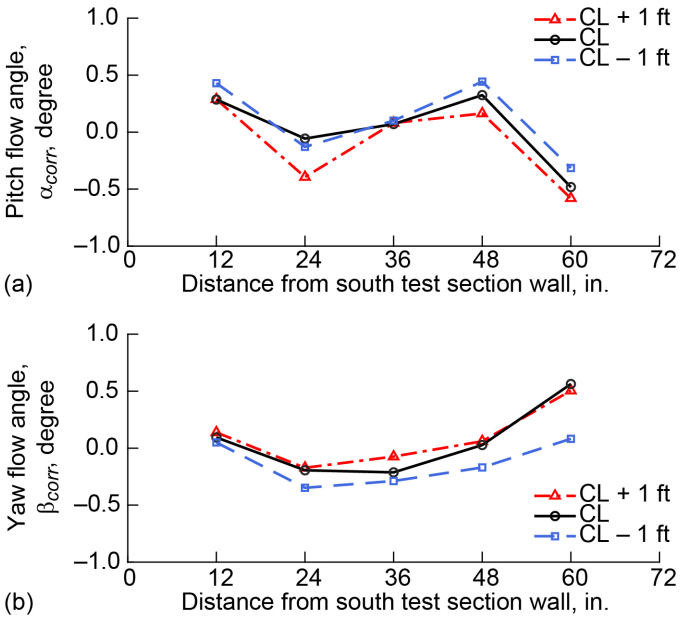

Figure 101.—Pitch and yaw flow angles in 8- by 6-ft supersonic test section near test section station 44.25 at centerline (CL) and 1 ft above and below CL. Positive pitch, α, is from floor to ceiling and positive yaw, β, is from left to right when upstream looking aft. Data acquired during supersonic test section characterization (2020 test) at flexwall setting of Mach 1.42. (a) Pitch. (b) Yaw.

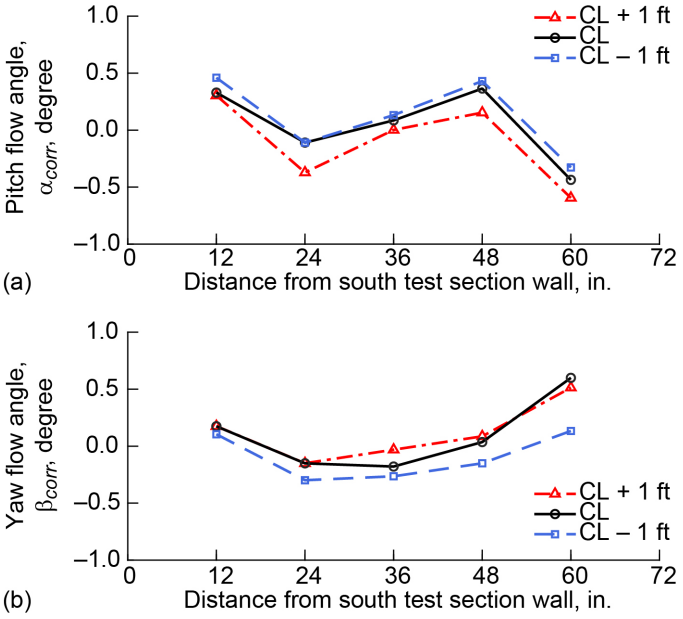

Figure 102.—Pitch and yaw flow angles in 8- by 6-ft supersonic test section near test section station 44.25 at centerline (CL) and 1 ft above and below CL. Positive pitch, α, is from floor to ceiling and positive yaw, β, is from left to right when upstream looking aft. Data acquired during supersonic test section characterization (2020 test) at flexwall setting of Mach 1.43. (a) Pitch. (b) Yaw.

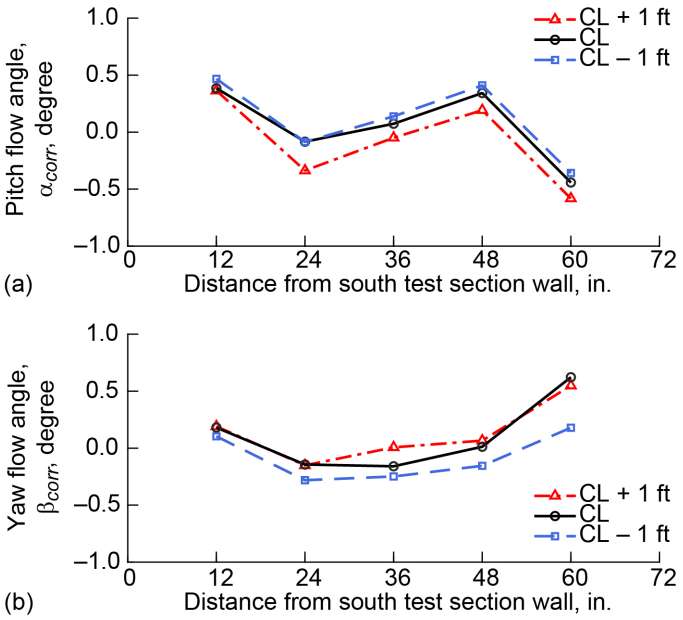

Figure 103.—Pitch and yaw flow angles in 8- by 6-ft supersonic test section near test section station 44.25 at centerline (CL) and 1 ft above and below CL. Positive pitch, α, is from floor to ceiling and positive yaw, β, is from left to right when upstream looking aft. Data acquired during supersonic test section characterization (2020 test) at flexwall setting of Mach 1.44. (a) Pitch. (b) Yaw.

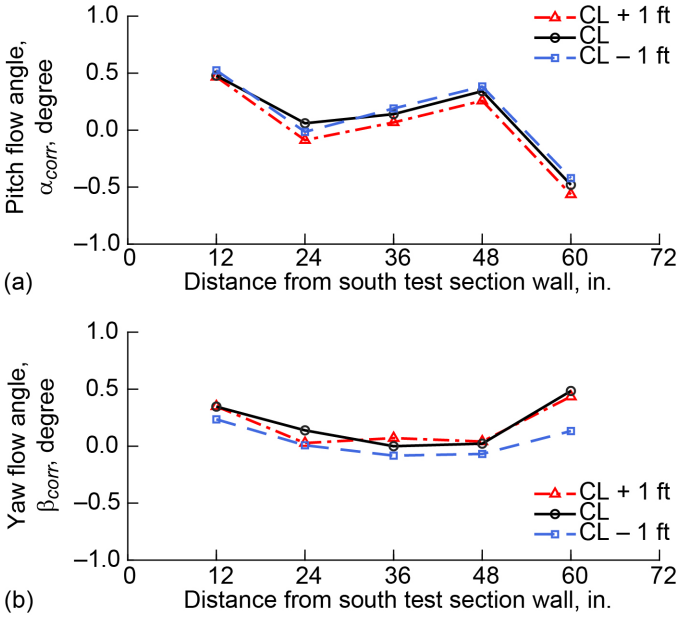

Figure 104.—Pitch and yaw flow angles in 8- by 6-ft supersonic test section near test section station 44.25 at centerline (CL) and 1 ft above and below CL. Positive pitch, α, is from floor to ceiling and positive yaw, β, is from left to right when upstream looking aft. Data acquired during supersonic test section characterization (2020 test) at flexwall setting of Mach 1.50. (a) Pitch. (b) Yaw.

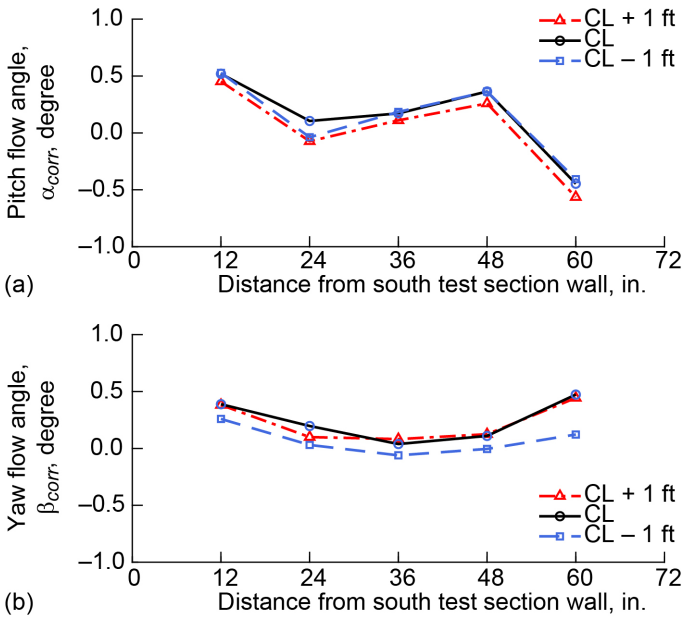

Figure 105.—Pitch and yaw flow angles in 8- by 6-ft supersonic test section near test section station 44.25 at centerline (CL) and 1 ft above and below CL. Positive pitch, α, is from floor to ceiling and positive yaw, β, is from left to right when upstream looking aft. Data acquired during supersonic test section characterization (2020 test) at flexwall setting of Mach 1.52. (a) Pitch. (b) Yaw.

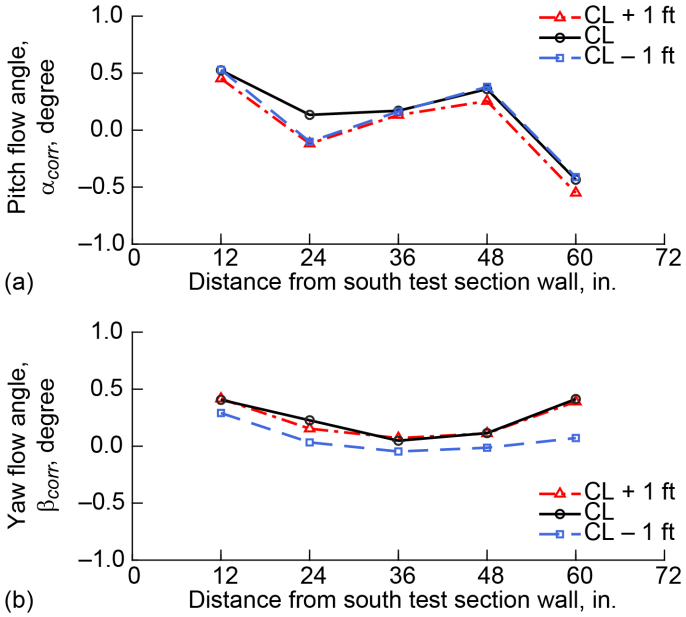

Figure 106.—Pitch and yaw flow angles in 8- by 6-ft supersonic test section near test section station 44.25 at centerline (CL) and 1 ft above and below CL. Positive pitch, α, is from floor to ceiling and positive yaw, β, is from left to right when upstream looking aft. Data acquired during supersonic test section characterization (2020 test) at flexwall setting of Mach 1.53. (a) Pitch. (b) Yaw.

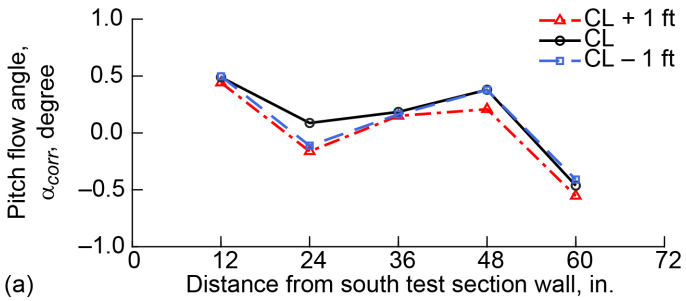

(a)

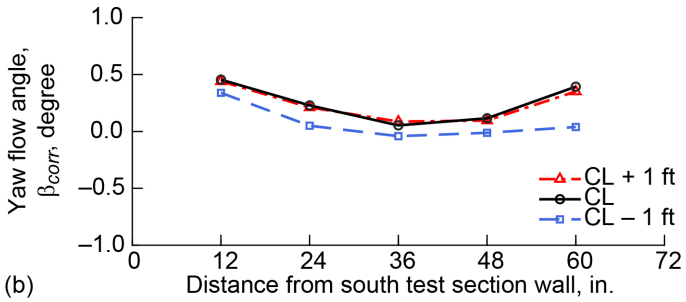

(b)

Figure 107.—Pitch and yaw flow angles in 8- by 6-ft supersonic test section near test section station 44.25 at centerline (CL) and 1 ft above and below CL. Positive pitch, α, is from floor to ceiling and positive yaw, β, is from left to right when upstream looking aft. Data acquired during supersonic test section characterization (2020 test) at flexwall setting of Mach 1.54. (a) Pitch. (b) Yaw.

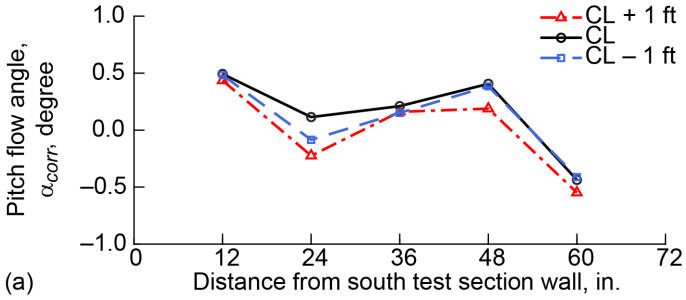

(a)

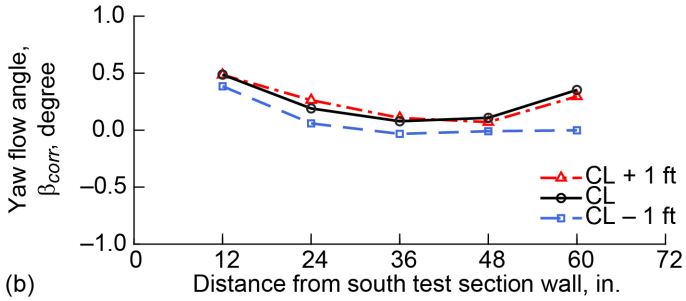

(b)

Figure 108.—Pitch and yaw flow angles in 8- by 6-ft supersonic test section near test section station 44.25 at centerline (CL) and 1 ft above and below CL. Positive pitch, α, is from floor to ceiling and positive yaw, β, is from left to right when upstream looking aft. Data acquired during supersonic test section characterization (2020 test) at flexwall setting of Mach 1.55. (a) Pitch. (b) Yaw.

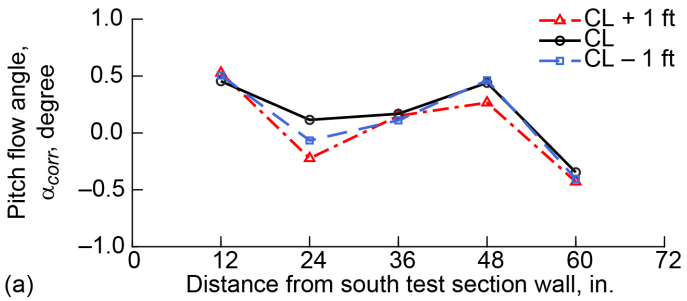

(a)

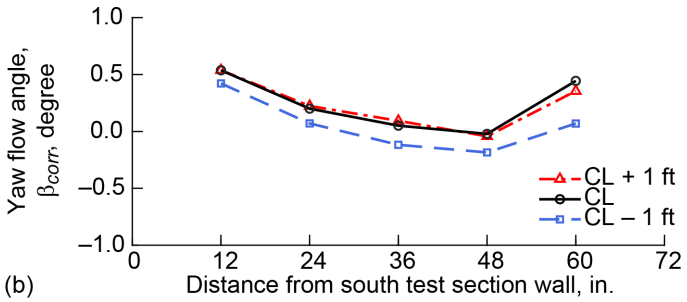

(b)

Figure 109.—Pitch and yaw flow angles in 8- by 6-ft supersonic test section near test section station 44.25 at centerline (CL) and 1 ft above and below CL. Positive pitch, α, is from floor to ceiling and positive yaw, β, is from left to right when upstream looking aft. Data acquired during supersonic test section characterization (2020 test) at flexwall setting of Mach 1.60. (a) Pitch. (b) Yaw.

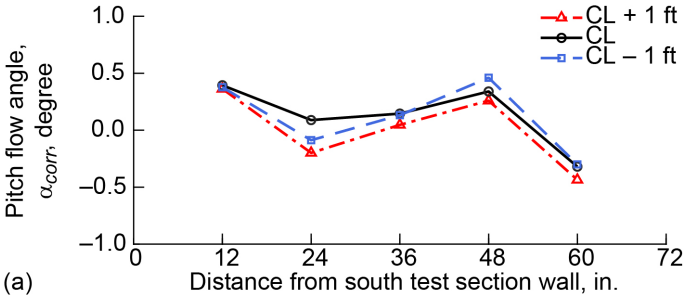

(a)

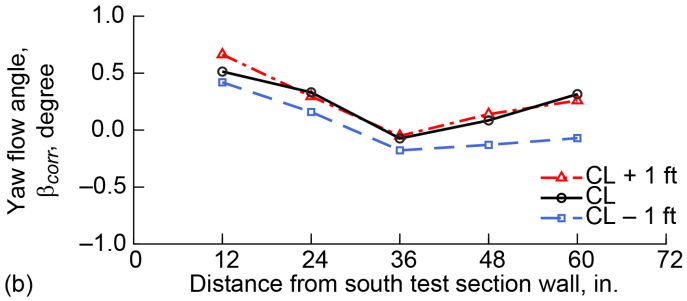

(b)

Figure 110.—Pitch and yaw flow angles in 8- by 6-ft supersonic test section near test section station 44.25 at centerline (CL) and 1 ft above and below CL. Positive pitch, α, is from floor to ceiling and positive yaw, β, is from left to right when upstream looking aft. Data acquired during supersonic test section characterization (2020 test) at flexwall setting of Mach 1.70. (a) Pitch. (b) Yaw.

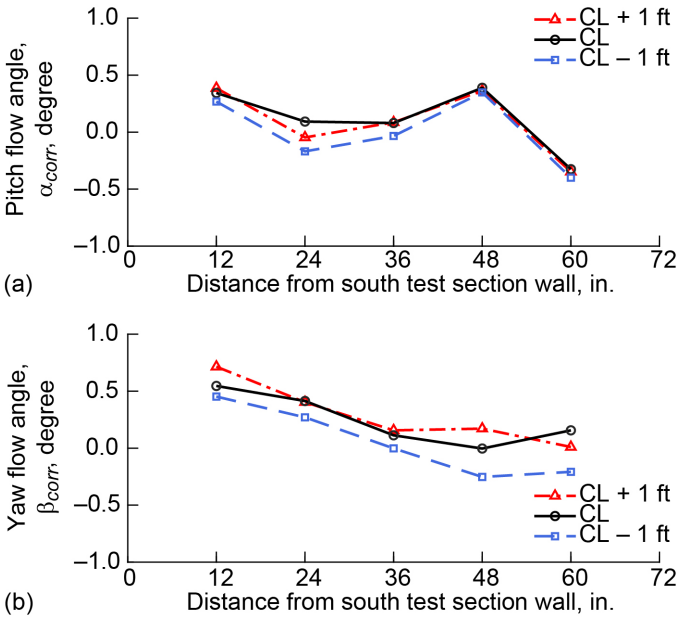

Figure 111.—Pitch and yaw flow angles in 8- by 6-ft supersonic test section near test section station 44.25 at centerline (CL) and 1 ft above and below CL. Positive pitch, α, is from floor to ceiling and positive yaw, β, is from left to right when upstream looking aft. Data acquired during supersonic test section characterization (2020 test) at flexwall setting of Mach 1.80. (a) Pitch. (b) Yaw.

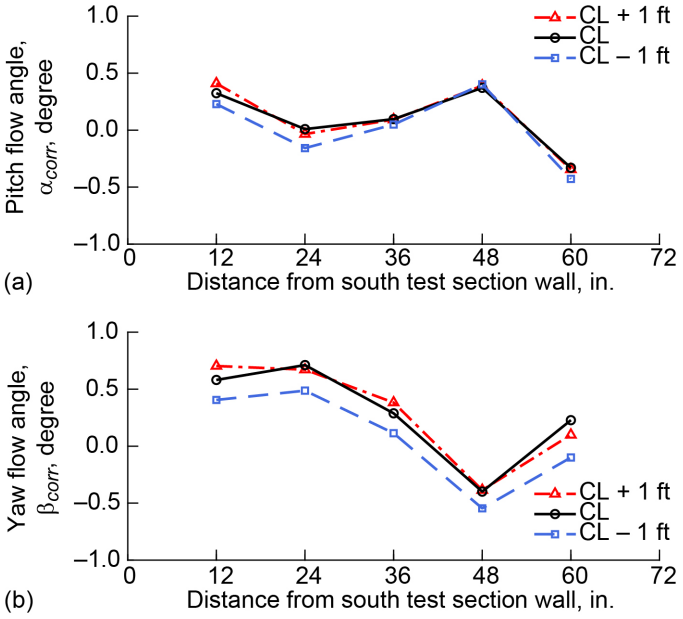

Figure 112.—Pitch and yaw flow angles in 8- by 6-ft supersonic test section near test section station 44.25 at centerline (CL) and 1 ft above and below CL. Positive pitch, α, is from floor to ceiling and positive yaw, β, is from left to right when upstream looking aft. Data acquired during supersonic test section characterization (2020 test) at flexwall setting of Mach 1.90. (a) Pitch. (b) Yaw.

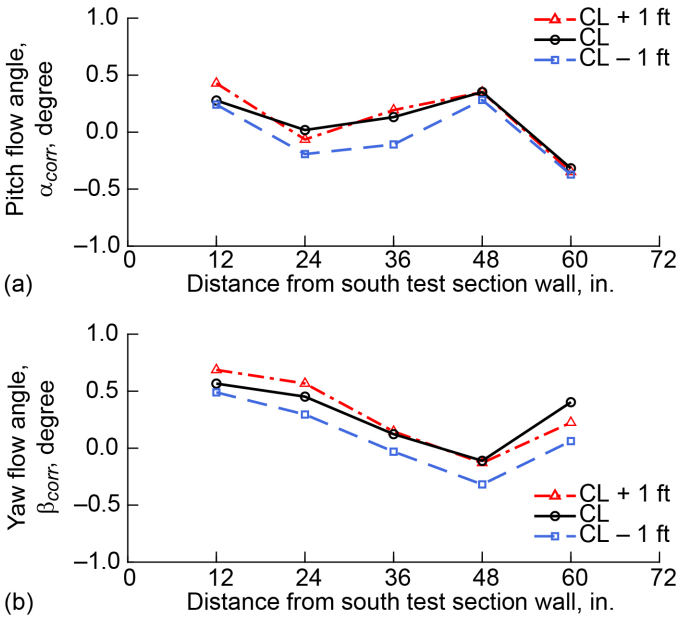

Figure 113.—Pitch and yaw flow angles in 8- by 6-ft supersonic test section near test section station 44.25 at centerline (CL) and 1 ft above and below CL. Positive pitch, α, is from floor to ceiling and positive yaw, β, is from left to right when upstream looking aft. Data acquired during supersonic test section characterization (2020 test) at flexwall setting of Mach 2.00. (a) Pitch. (b) Yaw.

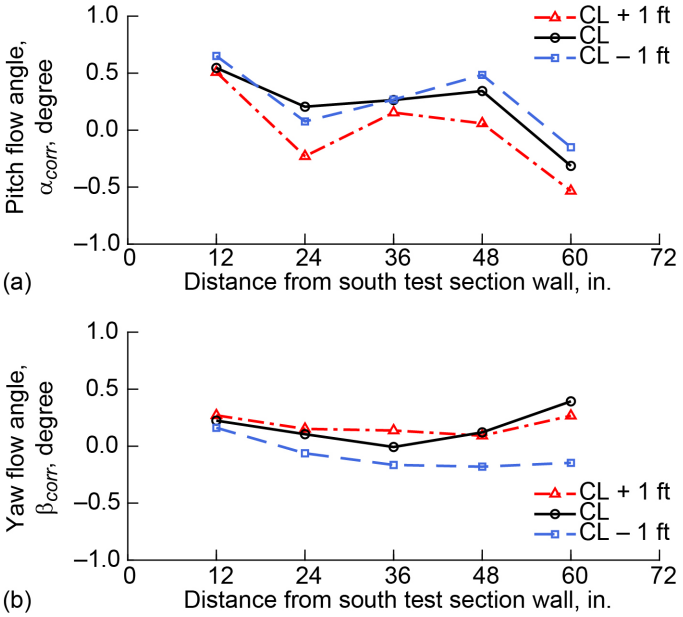

Figure 114.—Pitch and yaw flow angles in 8- by 6-ft supersonic test section near test section station 44.25 at centerline (CL) and 1 ft above and below CL. Positive pitch, α, is from floor to ceiling and positive yaw, β, is from left to right when upstream looking aft. Data acquired during supersonic test section characterization (2020 test) at transonic array Mach number of 0.842. (a) Pitch. (b) Yaw.

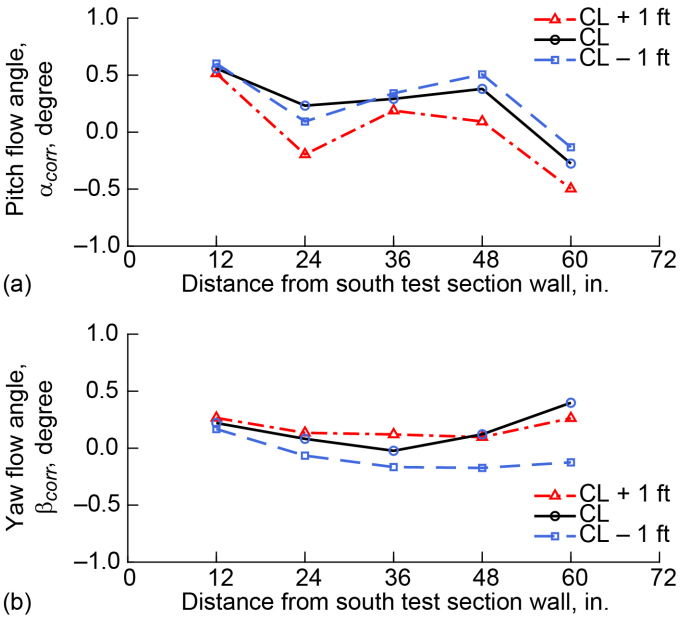

Figure 115.—Pitch and yaw flow angles in 8- by 6-ft supersonic test section near test section station 44.25 at centerline (CL) and 1 ft above and below CL. Positive pitch, α, is from floor to ceiling and positive yaw, β, is from left to right when upstream looking aft. Data acquired during supersonic test section characterization (2020 test) at transonic array Mach number of 0.831. (a) Pitch. (b) Yaw.

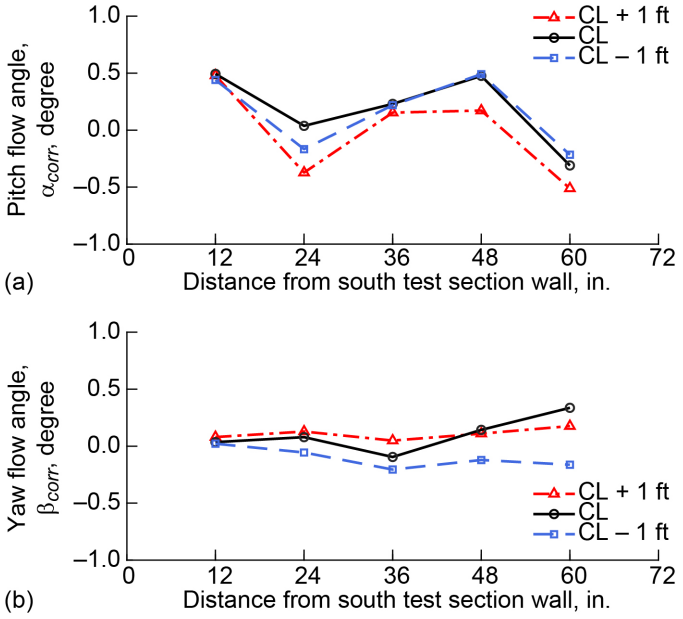

Figure 116.—Pitch and yaw flow angles in 8- by 6-ft supersonic test section near test section station 44.25 at centerline (CL) and 1 ft above and below CL. Positive pitch, α, is from floor to ceiling and positive yaw, β, is from left to right when upstream looking aft. Data acquired during supersonic test section characterization (2020 test) at transonic array Mach number of 0.769. (a) Pitch. (b) Yaw.

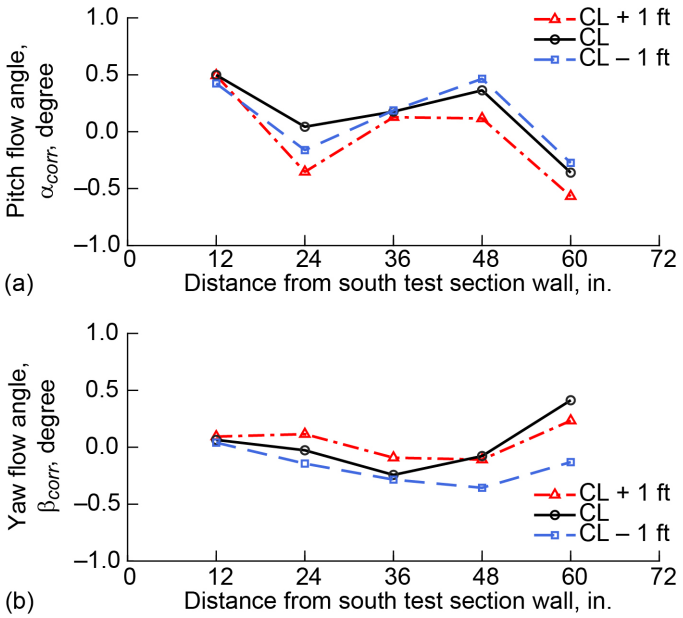

Figure 117.—Pitch and yaw flow angles in 8- by 6-ft supersonic test section near test section station 44.25 at centerline (CL) and 1 ft above and below CL. Positive pitch, α, is from floor to ceiling and positive yaw, β, is from left to right when upstream looking aft. Data acquired during supersonic test section characterization (2020 test) at transonic array Mach number of 0.683. (a) Pitch. (b) Yaw.

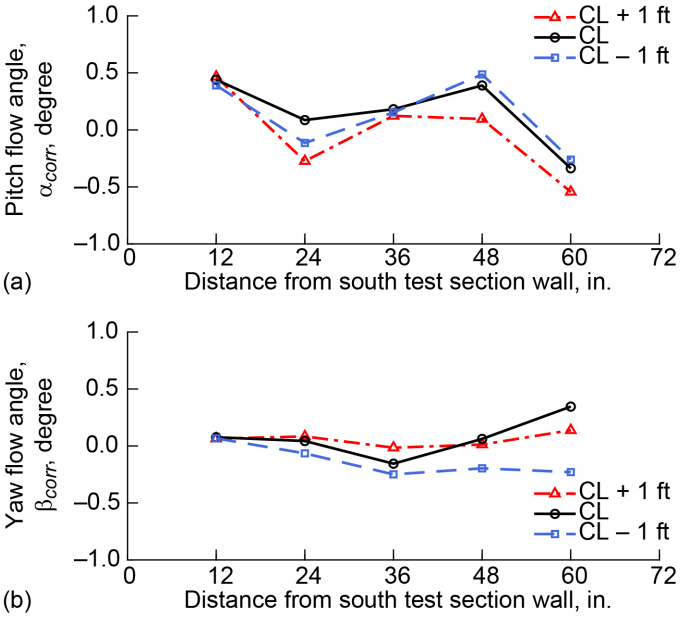

Figure 118.—Pitch and yaw flow angles in 8- by 6-ft supersonic test section near test section station 44.25 at centerline (CL) and 1 ft above and below CL. Positive pitch, α, is from floor to ceiling and positive yaw, β, is from left to right when upstream looking aft. Data acquired during supersonic test section characterization (2020 test) at transonic array Mach number of 0.586. (a) Pitch. (b) Yaw.

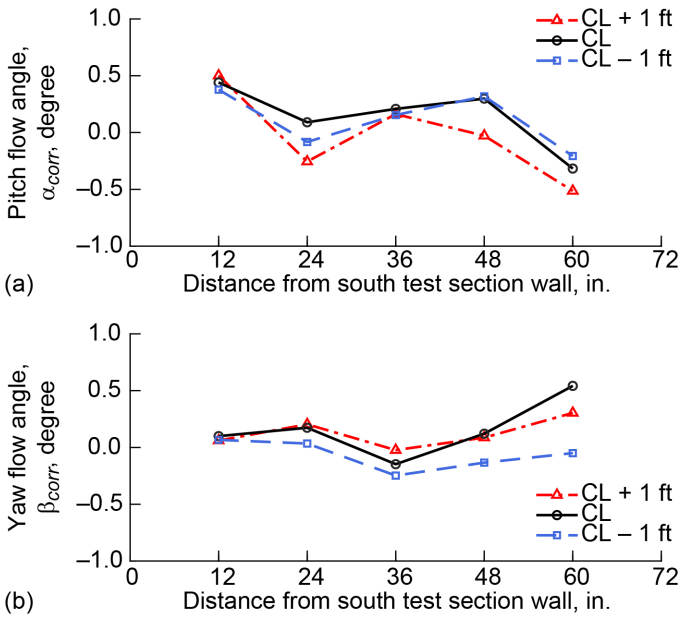

Figure 119.—Pitch and yaw flow angles in 8- by 6-ft supersonic test section near test section station 44.25 at centerline (CL) and 1 ft above and below CL. Positive pitch, α, is from floor to ceiling and positive yaw, β, is from left to right when upstream looking aft. Data acquired during supersonic test section characterization (2020 test) at transonic array Mach number of 0.492. (a) Pitch. (b) Yaw.

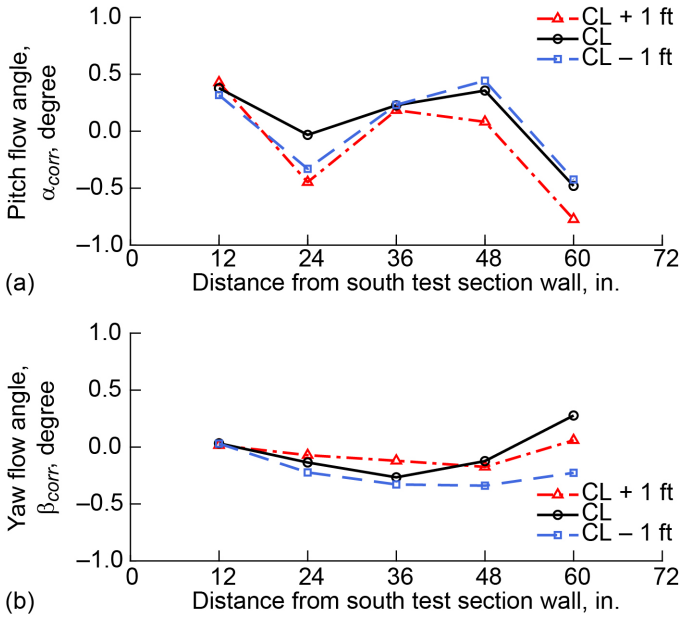

Figure 120.—Pitch and yaw flow angles in 8- by 6-ft supersonic test section near test section station 44.25 at centerline (CL) and 1 ft above and below CL. Positive pitch, α, is from floor to ceiling and positive yaw, β, is from left to right when upstream looking aft. Data acquired during supersonic test section characterization (2020 test) at transonic array Mach number of 0.395. (a) Pitch. (b) Yaw.

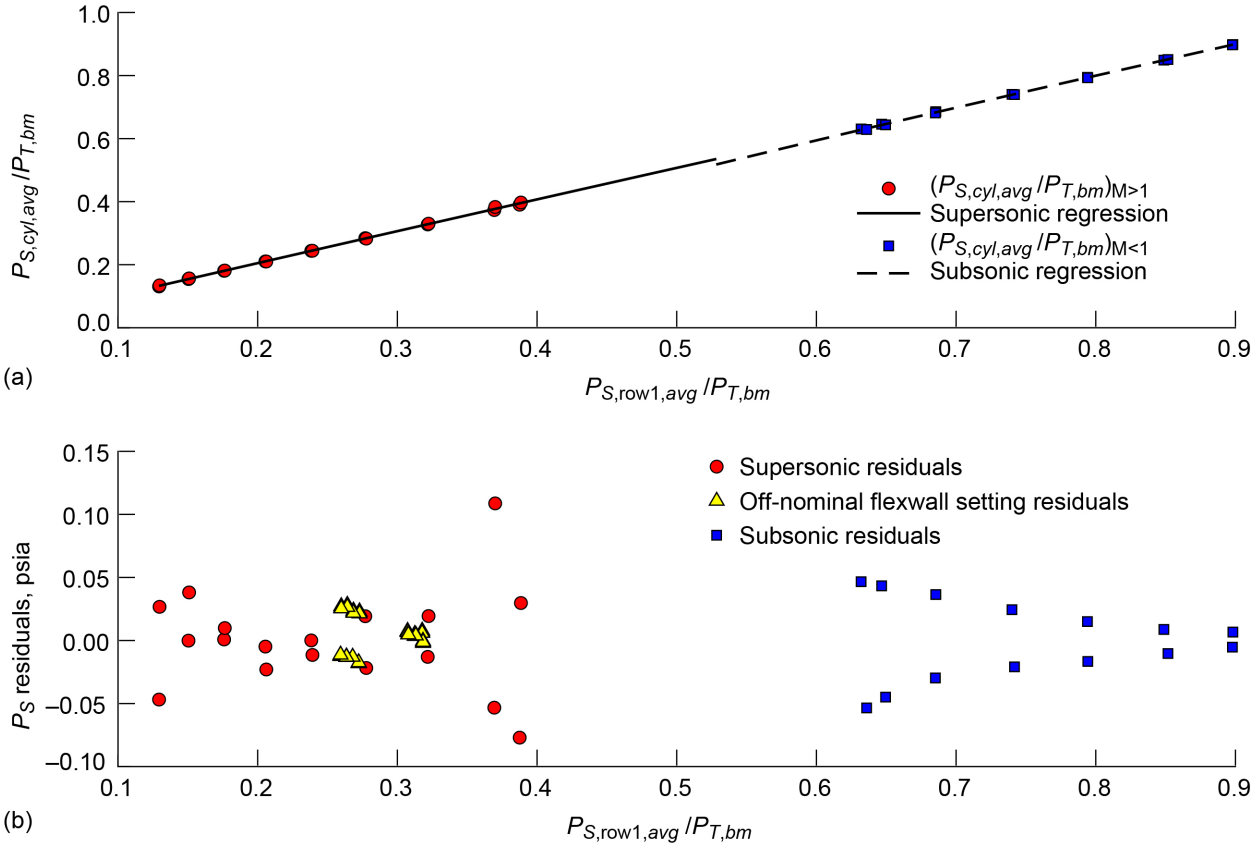

Figure 121.—Supersonic test section static pressure regression models and their associated residuals. Test section static pressure is represented by data acquired on the cylinder of the 4-inch-diameter cone cylinder at two axial positions in the supersonic test section. Regression model residuals were multiplied by measured bellmouth total pressure, $P_{T,bm}$, at each condition to put them in engineering units. (a) Regression models. (b) Residuals.

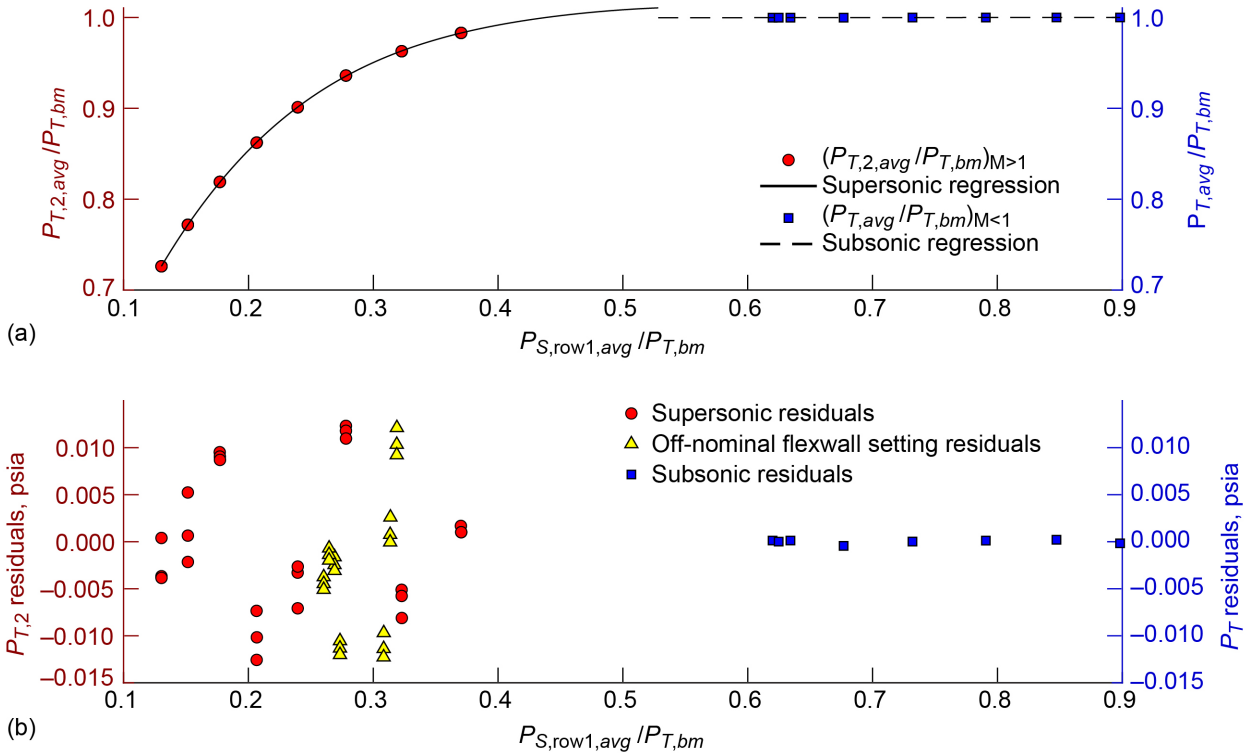

Figure 122.—Supersonic test section total pressure regression models and their associated residuals. Test section total pressure behind a normal shock, $P_{T,2}$, is shown on left y-axis for supersonic conditions and total pressure for subsonic conditions is shown on right y-axis. Data for these regression models were acquired by transonic array pressure probes at test section centerline. Regression model residuals were multiplied by measured bellmouth total pressure, $P_{T,bm}$, at each condition to put them in engineering units. (a) Regression models. (b) Residuals.

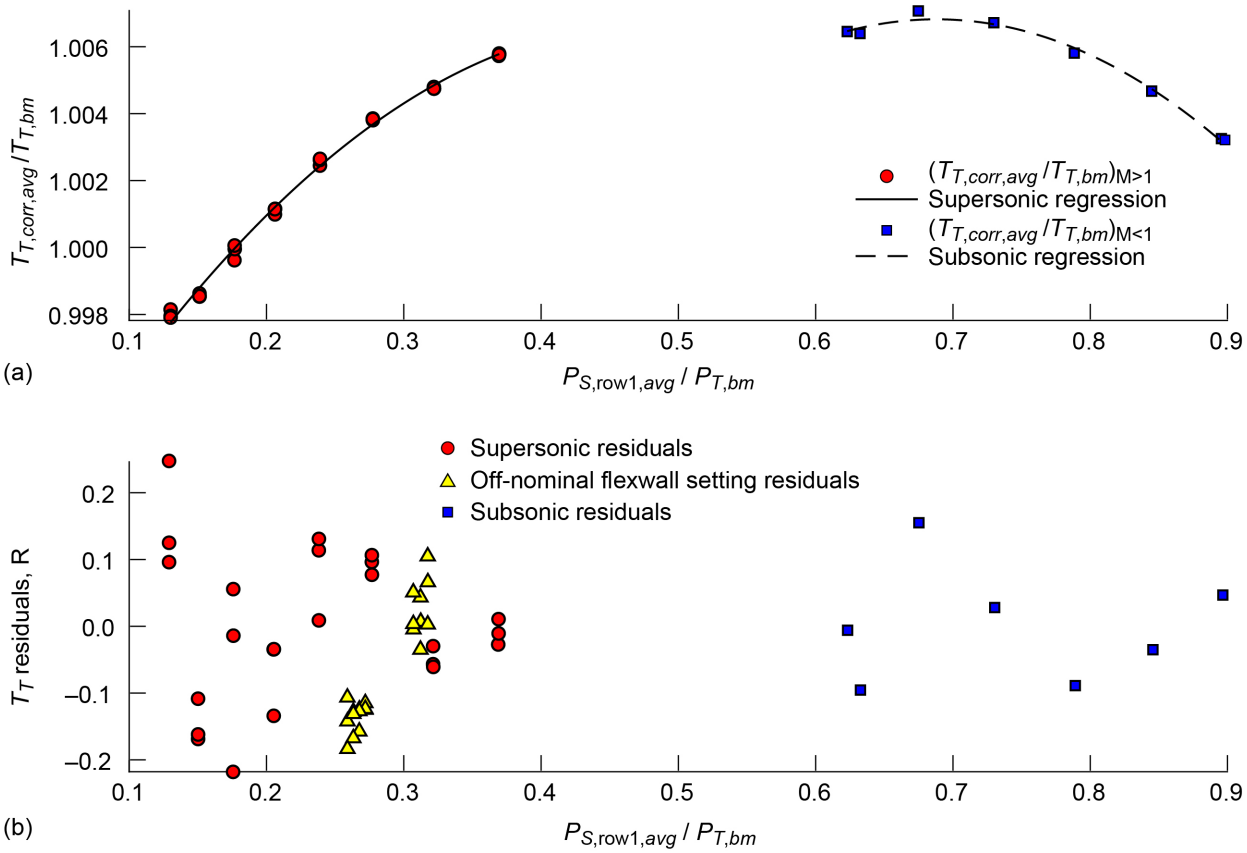

Figure 123.—Supersonic test section total temperature regression models and their associated residuals. Data for these regression models were acquired by transonic array thermocouple probes at test section centerline. Regression model residuals were multiplied by measured bellmouth total temperature, $T_{T,bm}$, at each condition to put them in engineering units. (a) Regression models. (b) Residuals.